A MATHEMATICAL STUDY ON BIOMECHANICS MODELS ON HUMAN BODY

Thesis Submitted for the Award of the Degree of

DOCTOR OF PHILOSOPHY

in

Mathematics

By

Harpreet Kaur

Registration Number: 41900742

Supervised By

Prof. (Dr.) A. K. Awasthi (25155)

Professor, Department of Mathematics

School of Chemical Engineering and Physical Sciences

LOVELY PROFESSIONAL UNIVERSITY, PUNJAB

2023

DECLARATION

I, hereby declared that the presented work in the thesis entitled "**A Mathematical Study On Biomechanics Models On Human Body**" in fulfillment of degree of **Doctor of Philosophy (Ph.D.)** is outcome of research work carried out by me under the supervision of **Prof. (Dr.) A. K. Awasthi**, working as a **Professor**, in the **Department of Mathematics, School of Engineering and Physical Sciences**, of Lovely Professional University, Punjab, India. In keeping with general practice of reporting scientific observations, due acknowledgements have been made whenever work described here has been based on findings of other investigator. This work has not been submitted in part or full to any other University or Institute for the award of any degree.

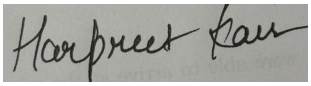

(Signature of Scholar)

Name of the scholar: **Harpreet Kaur**

Registration No.: **41900742**

Department/School: **Department of Mathematics, School of Engineering and Physical Sciences, of Lovely Professional University, Punjab, India**

CERTIFICATE

This is to certify that the work reported in the Ph. D. thesis entitled "**A Mathematical Study on Biomechanics Models On Human Body**" submitted in fulfillment of the requirement for the reward of degree of **Doctor of Philosophy (Ph.D.)** in the **Department of Mathematics, School of Engineering and Physical Sciences**, is a research work carried out by **Harpreet Kaur, 41900742**, is bonafide record of his/her original work carried out under my supervision and that no part of thesis has been submitted for any other degree, diploma or equivalent course.

(Signature of Supervisor)

Name of Supervisor: **Prof. (Dr.) A. K. Awasthi**

Designation: **Professor**

Department/School: **Department of Mathematics, School of Engineering and Physical Sciences**

University: **Lovely Professional University, Punjab**

Abstract

Engineering and biological sciences have lately intertwined to form the area of bio-engineering. A complete exploitation of the current knowledge in these two domains and the integration of engineering and biological sciences might be of enormous advantage to men, because of the potential for improved knowledge of the phenomena that continue to occur in the human body due to this interaction. Biomechanics research has progressed from basic topical applications of elementary mechanics to whole fields of study. Biomechanics studies and research currently outnumber those in fundamental mechanics, indicating the growing relevance of this field of study. The current state of the art in biomechanical modelling is evaluated, with special emphasis on physical and mathematical identifications of the human body. Due to this, several distinct fields of applied theoretical physics and mathematics, including biomechanics, mathematical biology, and thermodynamics, have recently developed. It concerns the mechanical characteristics of heat transmission, diffusion through stenosis, and the mechanobiology of fracture issues. Biomechanical modelling is focused on the rapidly expanding field of biomechanical models and modelling techniques to enhance our comprehension of bodily functions. The hemodynamic properties of the blood flow might vary significantly as a result of this unwanted growth, which could be harmful to general health. For the velocity distribution, pressure, wall shearing stress, and other distinct phenomena, theoretical conclusions obtained for various geometrics are provided. The physical, chemical, and flow characteristics of blood must be well understood in order to describe capillary transport mechanisms and the dynamics of the circulatory system in the body. According to this study, the consistent state heat balance equation, integral equation, and the model representing the movement of species owing to facilitated and

molecular diffusion were created using the finite difference approach. Finally, the effects of radiation, blood flow convection, tissue metabolism in the body, and concentration of oxygen and carbon dioxide are discussed. The results of various flow circumstances are illustrated with some plausible data.

Last but not least, The mathematical theory of elasticity helps in the study of physical quantities in the problem of structures. The structures face the problem of crack's presence, which makes the problem difficult but not impossible to deal with. Mathematically the structure with cracks is treated as a mixed boundary value problem. integral equations are useful in a variety of problems. Integral equations are utilized to address fracture mechanics and fracture design concerns. In fracture design criteria, stress and crack opening displacement components play a vital role. When considering the joining of two longitudinally propagating cracks at the interface of an isotropic and an orthotropic half-space in the human body, one can obtain an exact form of stress and displacement components. Near the fracture tips, the expression was derived using a Fourier transform method, however, these components were then assessed using Fredholm integral equations before being reduced to coupled Fredholm integral equations. We employ the Lowengrub and Sneddon problem in this research and reduce it to triple integral equations. The Srivastava and Lowengrub method reduces the solution of these equations to a coupled Fredholm integral equation. A decoupled Fredholm integral equation of the second kind is the result of further reduction of the issue. Triple integral equations are solved and the problem is reduced to a connected Fredholm integral equation. A decoupled Fredholm integral equation of the second sort is created by solving the Fredholm integral equation. Stress and crack opening displacement components drive interest in fracture design standards on a physical level. At last, Simple calculations in their precise form may be made for the stress and displacement components.

Acknowledgement

At the outset, I'd like to express my sincere gratitude to the almighty god and also express my deepest gratitude and appreciation to all those who have contributed to the completion of this thesis.

First and foremost, I am immensely grateful to my supervisor, Prof.(Dr.) A. K. Awasthi for his invaluable guidance, support, and encouragement throughout this research journey. His unwavering support and valuable suggestions have been of immense help in the successful completion of this project. Their expertise and insightful feedback have been instrumental in shaping this thesis. This research would not have been feasible without their tireless efforts.

I would also like to express my deepest gratitude to my parents. Their unconditional love, unwavering support, and sacrifices have been the cornerstone of my journey. They have been my pillars of strength, always believing in me and encouraging me to pursue my dreams. Their guidance, encouragement, and sacrifices throughout the years have made this achievement possible. I am forever indebted to them for their endless love and support.

My heartfelt thanks go to my friends for their unwavering belief in my abilities and for their unconditional support during the highs and lows of this academic pursuit. Their encouragement and understanding have been a constant source of motivation.

Additionally, I would like to acknowledge the contribution of Lovely Professional University for providing the necessary resources, facilities, and research opportunities that have greatly enhanced the quality and depth of this study.

Last but not least, I am grateful to all the colleagues who willingly participated in this research, as their involvement and cooperation have played a crucial role in

gathering the data necessary for this study.

Although it is impossible to name everyone who has contributed in some way to this thesis, please know that your support and encouragement have not gone unnoticed and are greatly appreciated.

Thank you all for your unwavering support, and belief in my abilities, and for being an integral part of this academic journey.

Once again, I thank God, my advisor, my family, and the university for their invaluable guidance and support.

Contents

List of Figures

List of Tables

Chapter 1

INTRODUCTION

Engineering and biological sciences have lately intertwined to form the area of bio-engineering. A complete exploitation of the current knowledge in these two domains and the integration of engineering and biological sciences might be of enormous advantage to men. Because of the potential for improved knowledge of the phenomena that continue to occur in the human body due to this interaction. The main subjects taught in bio-engineering education are (a) Applied biology, (b) Biomedical engineering, and (c) Biomechanics.

Applications of engineering principles to biological and medical problems have developed a new field of biomedical engineering. It has been acknowledged that accurate physiological, physical, and mathematical descriptions with sufficient consideration for experimental findings are required for useful mathematical modelling in biomedical engineering. The mathematical modelling of the issues in biomedical engineering has a very broad application. Each study poses a challenge in terms of fundamental issues including mass, momentum, and heat transfer as well as geometry, chemical kinetics, and thermodynamics are used to create functional connections that make sense. There is a great need to apply engineering principles and models of analysis

to systems of life sciences. An abstract, condensed construct that is connected to a section of reality and was created with a particular goal in mind is referred to as a mathematical model. The necessity for expensive or impossible real-world tests is diminished by modeling. Consequently, when framing mathematical problems, simplifying assumptions are applied

. It is evident that not every physiological process can be explained using mechanical tools and techniques. Investigations have focused on four areas: (a) the cardiovascular system, which includes the heart; the pulmonary system, which includes the airways; and (b) The lungs and the breathing muscles (c) muscle mechanics, including an analysis of the materials in the skeletal, cardiac, and smooth muscles, and (d) a wide term used to refer to the body's connective tissues, which also include structures like bone, cartilage, tendon, and skin. It also contains proteins like collagen and elastin as well as complex polysaccharides. The unsteady flow of a non-Newtonian, viscous, incompressible, non-homogeneous anisotropic suspension through a challenging branching network of elastic tubes with a decreasing cross-sectional area with distance from the source is typically the scenario that applied mathematicians must consider when analyzing circulatory systems.

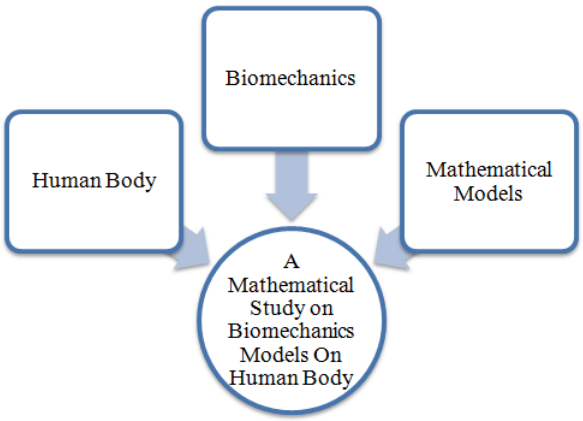

Figure 1.1: Title of Thesis

1.1 BIOMECHANICS

Biomechanics is the study of the biological mechanics of movement and forces applied to the human body. It looks at the forces and movements that act on the body and how they affect the body's structure and function. It is the application of mechanical principles to living organisms, such as the analysis of the forces that act on a body and the effects of those forces on the body's structure and function. Biomechanics covers topics such as the effects of gravity and momentum, the effects of muscle and joint forces, the impact of external forces, the effects of body shape or size on movement and function, and the effects of body position and posture on performance. Biomechanics is the application of mechanical principles to the study of biological systems. It is a field of study that uses mathematical modeling to understand biological processes, such as the mechanics of muscles, bones, and joints, as well as the forces that act on them. By understanding the forces that act on these systems, researchers can develop better treatments for injuries, diseases, and other conditions.

Biomechanics involves many different branches of mathematics, such as calculus, linear algebra, and differential equations. Calculus is used to examine the motion of objects and the forces that act on them. Linear algebra can be used to model the interactions between different structures and forces, while differential equations are used to describe the behavior of systems over time. By applying mathematical principles to biomechanical systems, researchers can better understand how forces interact with tissue and how they affect the body's overall structure and function.

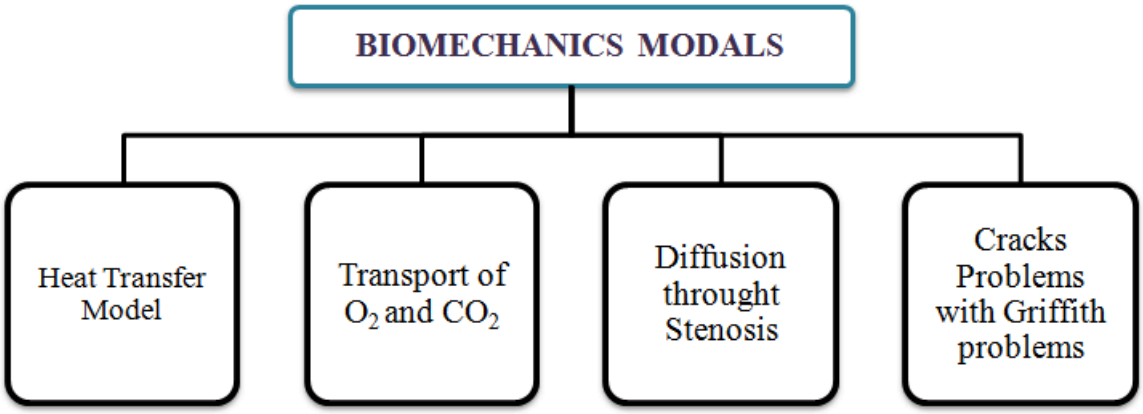

Figure 1.2: Biomechanics Models

1.2 HUMAN BODY

The most complicated organism on the earth, the human body is without a doubt. Imagine a universe made up of billions of minute components, each with its own identity and functioning in harmony to serve the whole. The preservation of life depends on a huge variety of physiological and biochemical functions, making humans a particularly complex multicellular creature. The human body is one structure, yet it's composed of billions of smaller structures. All of these activities together allow people to survive in their circumstances, make use of them, and perpetuate the species through procreation. A functional organism is made up of a multitude of organs, tissues, and cells that make up the human body. The body is divided into several systems, each with its own unique function.

1.3 BLOOD

Blood is a unique physiological fluid that transfers waste materials away from cells as well as important chemicals like nutrition and oxygen to the body's cells. In

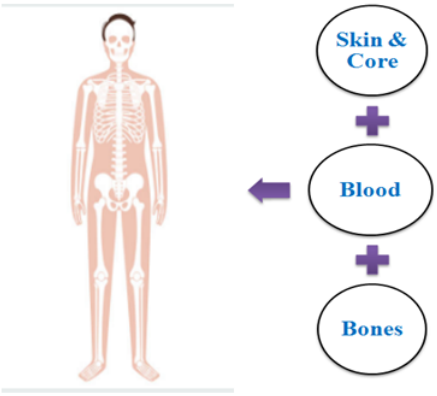

Figure 1.3: Human Body

a complicated, continuous aqueous phase, human blood is a particle suspension. There are both organic and inorganic salts as well as tiny organic molecules in this continuous phase known as plasma. The primary means of transportation is blood. One milliliter of human blood contains roughly $5x10^9$ cells. About 4 .9% of these cells are plate cells, 13% are white cells and most of the cells in the blood are red cells.

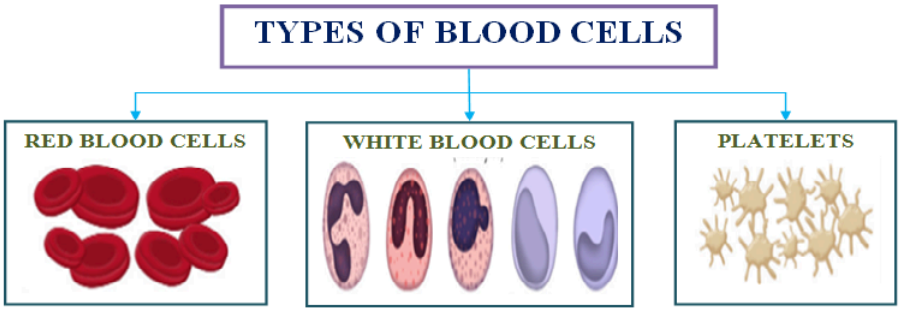

Figure 1.4: Types of Blood.

1.3.1 RBC

Red blood cells, also known as erythrocytes, are the most common type of blood cells and are in charge of transferring oxygen from the lungs and carbon dioxide

out of the body's tissues. The protein hemoglobin, which also contains the iron-rich substance heme that binds to oxygen, is what gives them their red colour. The red cell is not shaped like a spherical. In motionless blood, the red cell has a biconcave discard shape with an 8.1-micron main diameter. It can be as thick as 2 microns. Hematocrit, also known as the volume fraction occupied by red cells in a suspension, is a common way to express the concentration of most red blood cells in a suspension. Red blood cells congregate face-to-face in normal blood. A main aggregation like this is known as a rouleau and has 6–10 red cells in a stack. Proteins, which are large molecules with molecular weights ranging from 44,000 to over 1,000,000, make up around 7% of the blood's total weight. Albumin, which has a molecular weight of 69,000, makes up around half of the protein mass. At sea level, the average human hematocrit is between 42 and 45 percent. Essentially, blood plasma protein is a diluted (0.15N) electrolyte solution with around 8% protein by weight. Compared to plasma, RBCs are heavier. White blood cells are of several types but are generally round and somewhat larger than R.B.C. Lymphocytes, monocytes, eosinophils, neutrophils, and basophils are the major W.B.C. The W.B.C.s are important in combating infections by the production of antibodies or by the direct engulfment and digestion of bacteria.

About 97 percent of the blood's total volume is made up of red cells. The functionally important constituent, of blood, is the red cell. Its primary functions include transferring oxygen from the lungs to every cell in the body and eliminating carbon dioxide produced during metabolic activities. Around 70% of a red blood cell is made up of water, and 25% of it is hemoglobin (by volume). The rest of the cell consists of protein, each molecule contains four heme groups, complex organic molecules to yield oxyhemoglobin (Hb_4O_8). The capacity of hemoglobin for oxygen bounds as oxyhemoglobin is 40 times greater than the solubility of oxygen in the blood and this accounts for the great efficiency of blood as an oxygen transfer.

The core of the red cells, also known as erythrocytes, is filled with a complicated aqueous solution that is virtually saturated hemoglobin solution. The outside of the red cells is made up of a thin, flexible, but practically unstretchable envelope or membrane. Moreover, the protein molecules and red blood cells all have a negative charge. Blood clotting is the collective result of various irreversible mechanical and chemical changes that happen when blood is removed from its native environment. Due to the difficulties in doing repeatable rheological measurements in the limited time between blood collection and the onset of blood clotting, it is difficult to determine the exact effects of different anticoagulants on the rheological characteristics of blood.

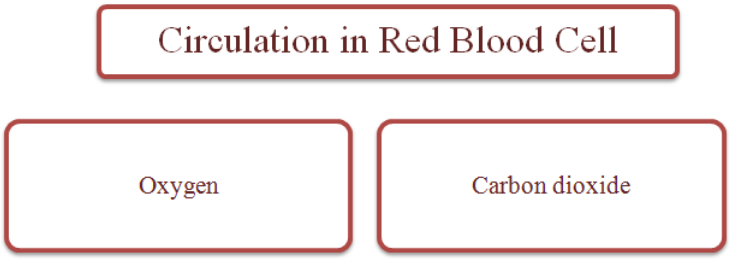

Figure 1.5: Circulation in Red Blood Cell.

1.3.2 WBC

Leukocytes, or white blood cells, are a component of the body's immune system and aid in the defense against infections. They have a nucleus and are bigger than red blood cells, which helps them to differentiate between foreign substances and normal body cells.

1.3.3 PLATELETS

Platelets, or thrombocytes, are small cell fragments that help the blood to clot. They are important in preventing excessive bleeding when a blood vessel is damaged.

1.4 CIRCULATION

The circulatory system of the human body is made up of an intricate web of blood vessels that serve vital purposes such as respiration, nutrition, excretion, protection, and regulation. The internal diameter of blood vessels ranges from 2.5 cm to 4 microns circulation may be classified into two main categories Macrocirculation and Microcirculation. Most of the effects in physiological flows have been directed toward the problems related to the circulatory and respiratory systems. These vessels are tapered and branched in the flow direction. Blood flow in the circulatory and airflow in the respiratory system takes place in distensible vessels and is unsteady.

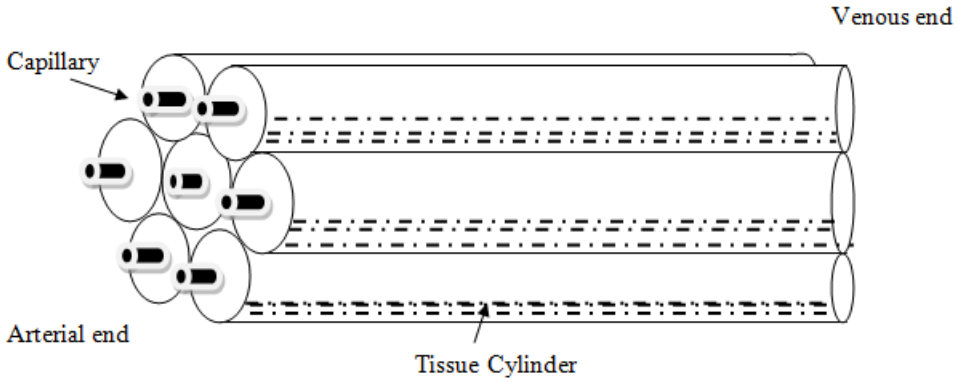

Figure 1.6: Krogh cylinder arrangement.

In the lungs, blood is oxygenated after being decreased in the tissue. To perform opposing tasks at these two locations, it must alternately flow through the lungs and tissues. Broadly, the circulation system is divided into two functionally opposite points. (i) The systemic circulation

(ii) pulmonary circulation.

Thousands of these tiny channels are traversed by the blood as it travels from the arterioles to the veins. The capillaries in the tissues' capillaries release blood, which

the veins then transport to the heart. This is called systemic circulation. Systemic circulation is characterized as a highly controlled high-pressure, high-resistance system serving a wide variety of tissues dispersed over a long distance from the heart. The heart pumps out roughly 5.5 liters of blood each minute, of which the brain receives about 0.75 liters, the kidneys 1.1 liters, the liver 1.1 liters, the heart muscles 0.25 liters, and so on [1]. The cardiac output is the amount of blood the heart pumps into the arteries in a minute. A cardiac cycle is a collective name for the succession of distinct activities that the heart does. It begins with any one of the individual actions or movements that the heart makes, and it is made up of a series of changes that occur until that specific activity starts to repeat itself. Systole and diastole are terms used to describe the contraction and relaxation of the heart, respectively[2]. The other circulation is called pulmonary circulation which is distributed only to the lungs. The quantity of blood passing through the lungs is precisely equal to the quantity passing through the remainder of the body. In pulmonary circulation, the left half of the heart pumps purified blood from the lungs to the various regions of the body whereas the right side of the heart sends impure blood from various sections of the body to the lungs for cleansing.

1.4.1 MICROCIRCULATION

At the level of the terminal arteries, the Womersley number and Reynolds number tend to be 1. In the capillaries, venules, and arteries farther downstream. The Reynolds number and Wormersley number both drop below 1. In these vessels, the influence of inertial forces decreases, and the interplay of viscous stress and pressure gradient regulates the flow. The true meaning of microcirculation is this.
Microcirculation is not simply characterized by a low Reynolds number (1). Other features include at least three others. It's important to acknowledge each blood

cell's uniqueness. The blood and tissue around the blood vessel exchange fluids and other substances.

Local flow regulation is carried out by the smooth muscle of the microvasculature. Capillary circulation's capacity for thought is demonstrated by the blood flow's continuous change. The number of capillaries undergoing active circulation as well as the flow's direction and velocity all fluctuate. While the majority of capillaries experience intermittent circulation, other channels maintain a constant flow during the ebb and flow of the blood. Via two or three different pathways, the bloodstream travels from the arteriole to the venule at once. In a later stage, the blood overflows into several side branches, arising from a single arteriole and capable of actively supplying circulation to up to 15-20 capillary capillaries.

A single layer of endothelial cells makes up the wall of a capillary blood artery, which is encircled by a basement membrane that splits to confine sometimes occurring cells known as pericytes. The pericytes may develop into smooth muscle cells, according to theory. The endothelial cells contain a significant number of vesicles. It is thought that these vessels are material carriers. Endothelial cells that line the capillary wall are in close proximity to one another. With electron microscopy, the neighboring cytoplasm and opposing cell membrane both seem darker. As a result of the close opposition or fusion of the exterior leaflets of the plasma lemma at these locations, tight functions, or muscular occludes, fully obliterate the intercellular space and block the intercellular clefts. Where applicable (in the brain). These junctions, known as Zonulae, are part of an uninterrupted seal and block the flow of molecules with a radius of 2.5 mm or more. Similar to industrial metal construction's spot welding (maculae) and seam welding (zonular), these light functions. To create a continuous barrier, they join the endothelial cells. They are crucial in influencing the endothelium molecules' permeability to water and other substances.

Blood artery endothelial cell lining can vary in appearance depending on the organ.

The endothelial cells in the first continuous type are closely bonded. The cells in the vessels of striated muscle can be relatively thin and flat. They may be cuboidal and come from thick layers in older capillary venules. The endothelial cells of the second fenestrated type are so thin that the membrane's opposing sides are very near to one another. This kind also has diaphragms with fenestrated openings that are only around 25 mm thick and 100 mm broad. Endothelial cells next to one another are still closely bound. Three groups or organs have been described for this sort of vessel.

(1) endocrine gland

(2) organs that produce or absorb fluids, such as the ciliary body of the eye, the intestinal villus

(3) retia mirabilia, such as the renal medulla froid plexus of the brain

The third kind of endothelium is known as the discontinuous type, which features a discontinuous basement membrane as well as observable intercellular spaces. They develop in the veins known as sinusoids. They are common in organs like the liver, spleen, and bone bones, whose main jobs are to add to or remove from the blood-stream big chemicals, entire cells, and foreign particles. The distribution of blood flow velocity and hematocrit must be correlated since every microcirculation circuit originates from bifurcating blood vessels. The downstream branch of a row capillary that separates into two equal daughters will produce more red blood cells, raising its hematocrit Biomechanical [3]

Experimental studies to establish the configuration of blood arteries in tissue sparked the earliest interest in the mathematical modeling of microcirculation. These tests were carried out because researchers were curious about the method by which oxygen was delivered from blood to tissue and how this transfer might be regulated. While [Ranvier[4]] and [Spaltecholz[5]] determined the geometric arrangement of blood vessels in striated muscle, [Krogh [6, 7]] is credited for inspiring and setting the

foundation for the first conceptual model of microcirculation. Krong hypothesized that the rate of oxygen transfer was proportional to the quantity and distribution of capillaries in the tissue, as well as the permeability of the capillary wall and surrounding tissues to oxygen. Krongh's research revealed that open capillaries were distributed relatively equally in a cross-section of striated muscle. Based on these observations, he concluded that each capillary might be seen as running parallel to the muscle tissues, feeding a concentric circle of tissue surrounding the capillary and that this tissue region was distinct from the other parallel capillaries and the tissues they provided. By counting capillaries in each cross-section and dividing the cross-sectional area by the total number of capillaries found, he was able to determine the average radius of a hypothetical tissue cylinder. Krong realized that such an ideal physical geometric arrangement Fig. 1.1 could be mathematically described. Despite not being a mathematician, Krogh persuaded a colleague, Danish mathematician Erlang, to explain his conceptual model mathematically. Krogh's tissue cylinder model, although a fairly simplified model, was a significant step forward in the research of substrate supply to live tissue. He not only launched the analysis but also charted its trajectory from 1929 to the present.

In his studies, Roughton[8] proposed that oxygen is mixed with material in the tissue via a reversible mechanism. Numerous particular examples of his model were considered, but solutions to entirely generic equations were not discovered. Kelly appears to have been the first to attempt to incorporate intra-capillary circumstances[9]. The microcirculation is an extensive network of microvessels that distributes blood flow throughout living tissues[257]. Kelly suggested that, in specific circumstances, To ensure a linear decrease in the oxygen content of capillary blood from the arterial to the venous end, the researcher incorporated the concept of a non-linear oxygen hemoglobin dissociation curve. This innovative approach led to the development of the first model that encompassed oxygen distribution within both the capillary and

the Krogh tissue cylinder.

1.4.2 MACROCIRCUATION

The class of blood flow issues in major blood vessels having an internal diameter of more than 500, such as the aorta, arteries, and veins, are dealt with in macrocirculation. Major characteristics of the flow include a high Reynolds number Blood arteries can experience turbulent flow at Reynolds numbers higher than 2300. Such flow circumstances should be analyzed using governing equations that take into account inertial effects, blood vessel curvature effects, pulsatile flow, and blood vessel wall distensibility. If the vessel width is greater than the size of the red blood cell, blood may be thought of as a homogenous and continuous fluid. The most extensively researched issues in macrocirculation are the propagation of pressure waves and the pulsatile flow impact [10, 3, 11]. Additionally, there has been much research done on flow disruptions at bifurcations, bends, and other similar locations, as well as their consequences on pathological states [12, 13].

1.5 BLOOD VESSELS

Viscoelasticity in blood arteries is a well-known behavior. Following a rapid stretch, tension increases and declines towards a final value, leading to stress relaxation With an abrupt shift in tension, a persistent deformation (Creep) is seen. The simplest model forecasts a reaction that might be resolved into one or more exponentials, although this is seldom if ever observed. For the most part, it has been essential to assume that the material reaction is equivalent to that of any collection of relaxing components with a range of time constants.

The fact that blood arteries are always under significant longitudinal stress in vivo is a key finding. They can shrink by up to 40% when they are taken out of the

body, and as they do so, their diameter grows. This retraction phenomenon is quite intriguing; it occurs in veins and arteries and decreases in quantity with aging [14]. The arteries of an ancient subject are too lengthy for their location. It is unclear how the forces causing refraction form; it's possible that the initial polymerization process is to blame and that longitudinal tension is "built-in" at this point. Moreover, it will be demonstrated that vessel diameters, even at very modest pressures, exhibit significant fluctuation, particularly when smooth muscle activity increases. A clear definition of strain based on unstressed dimensions is impossible given all of the above information. Studying subsequent deformations with subsequent load increments and defining an incremental strain as the relationship between the deformation and the initial dimensions measured seems to be the most suitable response. A fundamental pattern of three concentric layers may be found in the construction of blood arteries. The innermost tunica in the time is made up of a thin (0.5–1μm) layer of endothelial cells that are normally spaced apart from one another by narrow oblique lefts (10–20μm) in "continuous" capillaries that frequently exhibit one or more sites of narrowing Karnofsky (1968). In these capillaries, the whole vessel wall's endothelial cells and basement membrane are present. The degree of fit between neighboring cells in different capillary types varies significantly, and this has a substantial impact on how well they operate.

Underneath the thin layer of connective tissue that forms the border of the thick tunica media, there is the endothelium. Internal elastic lamina, which is a fenestrated membrane fully surrounding the vascular lumen, is a notable layer of elastic tissue that separates this from the intima. Together with elastin, the media also includes collagen and smooth muscle fiber. The adventitia, the outermost layer, connects outwardly with surrounding tissue and has a significant amount of collagen. The walls of blood arteries, except capillaries, never cease, and the bigger vessels also transmit nutrients via the adventitia and external media.

The biggest arteries are now known as elastic arteries because they have relatively thick walls made of elastic tissue. Based on histological appearance, it is assumed that the aorta and its main branches are included in the word "elastic," as well. According to chemically established elastin collagen ratios, [15] demonstrated that the intrathoracic aorta and all other arteries, including the pulmonary arteries, differed very sharply from one another. The ratio was two for the thoracic aorta whereas it was inverted in other places, or 0.5. Beyond these channels, blood is gathered into veins that gradually get bigger until leaving the capillaries, where just the endothelium is left. Generally speaking, veins surround arteries, and their cross-sectional areas are bigger than those of arteries at any given location, with a correspondingly reduced blood flow velocity. Collagen is found in veins in quite high concentrations; the collagen-to-elastin ratio is around 3.1 [16]. While the pulmonary and systemic arteries share a lot of the same structural characteristics, elastic and muscular vessels can be separated. In pulmonary veins, there are no figures for the relative wall thickness, which is often less than in systemic arteries with a comparable configuration. According to research by Reid, the relative wall thickness of the smallest muscle branches of the pulmonary artery grows relatively abruptly. It is generally accepted that the same is true in the systemic bed. notwithstanding the fact that no measurements on appropriately pressurized vessels at their normal length are available.

With the exception of the tiniest blood channels, whose cells are relatively close to blood, perhaps $25\mu m$, the walls of blood vessels are supplied with blood flow. The blood vessels that supply bigger blood vessel walls are known as vasa vasorum, and a material's mechanical qualities are influenced by both its structure and ultrastructure in addition to its composition. The characteristics of an artery rely on both the amount of collagen present and how the collagen fibers are distributed throughout the tissue. Throughout the arterial tree, there are differences in blood

artery structure. Chemically measured elastin/collagen ratios demonstrated that the pulmonary artery and the internal thoracic aorta are clearly unique from all other arteries in the body[15].

In large arteries, the number of lamellae layers grows with wall thickness, which is a constant percentage of arterial diameter in and of itself. Smaller arteries, like the femoral or carotid, have a little thicker relative wall, less elastin in the media, and finally, when the artery is further away from the aorta, just the inner and outer elastic lamina are visible. The number of muscle fibers rises, they are arranged in roughly concentric layers with noticeable muscle attachments, and they are arranged in a helical pattern with a higher pitch in the vessels that are farther away from the center. Yet, in the capillaries, just the endothelium is left as one moves further out from the center.

1.6 VISCOSITY OF BLOOD

Understanding blood viscosity and the elements that determine blood viscosity is significant for a variety of reasons. Viscosity is the property of a fluid that determines its resistance to flow. Viscosity is not the lone determinant, since local control can also be exercised by variations of vessel diameter that accompany physical or chemical stimuli. The viscosity has a significant role in defining the regional pressure changes through the cardiovascular systems, which in turn affects the indigenous inflow rates through each member of the vascular network. Blood viscosity's sensitivity to minute compositional changes is what gives it therapeutic significance. One can of ten diagnose Pathological states by detecting a change of blood viscosity due to an alteration in blood composition. It has been suggested that cell flexibility influences blood viscosity, particularly at high hematocrit values. Hardened cells display shear thickening behavior at high shear rates of around (50/Sec), whereas normal cells

exhibit shear thinning behavior [17, 18]. Apart from the temperature viscosity relationship, it is observed that the osmotic pressure difference also influences the blood viscosity. This determines to a large extent the shape, size, and elasticity of the red cells. The effect of globins on Viscosity is illustrated in the disease macroglobulinemia [19]. The blood viscosity is influenced by a number of rheological parameters, such as plasma blood cells. With an increase in protein content, the plasma becomes more viscous. Yet, depending on their size and form, various proteins have varying effects on plasma viscosity. Serum usually has a viscosity that is 20% less than that of Plasma. Fibrinogen is the largest of the Proteins in Plasma. Its influence on Plasma Viscosity can be seen in the difference between plasma and serum viscosity. Albumin, the smallest plasma protein molecule present in the largest concentration changes in albumin structure has the least effect of the three proteins on plasma viscosity, but the substance makes an important contribution to plasma viscosity through its high concentration in plasma. On the basis of several experiments made by [20, 21], it is observed that temperature may affect the viscosity of blood through changes in plasma, Viscosity, red cell wall elasticity viscosity of cell contents, and cell shape. Many empirical equations have been suggested to expense blood viscosity as a function of cell concentration and Plasma viscosity. The influence of viscosity on mass and heat transfer has been studied extensively with various fluids and systems. However, there have been very few studies of heat transfer and most none of mass transfer with respect to the influence of Plasma and blood viscosity [22, 23]. In the usual study of cardiovascular diseases, doctors commonly are concerned with cholesterol levels, the abnormalities of blood pressure, the formation of atherosclerotic Plaques, and so forth. Most of these measures are to fight heart disease, the number one killer is of a remedial nature, that is once it occurs, how to cure it. Even after all these efforts, the killer is still at large- even now 55% of all annual deaths from all causes are due to these diseases. To fame the killer, perhaps, the strategy

has to be changed. We have to adopt preventive measures, that is diagnose these diseases much before their clinical symptoms appear and interpret the cause of the disease. Platelets and white cells in general have little influence on blood viscosity because they are present in a very minute quantity when compared with red cells. However, if the red and white cells are removed from the blood, there is a strong attraction of platelets for one another.

1.7 STENOSIS

Stenosis refers to the abnormal growth in the artery's lumen. This unwelcome development has the potential to significantly alter the hemodynamic properties of blood flow, which might be harmful to normal health. It is fairly typical to observe narrowings in the circulatory system of mammals, some of which are at least somewhat axisymmetric or collar-like. These enlargements may be brought on by intravascular plaque, ligament impingements, or vessel wall dispersion [24, 25]. Atherosclerosis is the principal cause of myocardial and cerebral fraction several hypotheses for the development of the diseases have been proposed in the literature. Chemical reactions and hemodynamic forces play a major role in the development of atherosclerosis and thrombosis. Atherosclerotic lesions are frequently discovered at the points where two arterial segments abruptly diverge, in curved arterial segments, or generally anywhere there are abrupt changes in geometry (and therefore in flow characteristics). Deposits and blockages are discovered in the bends and bifurcations of the human circulatory system, and if they form in the arteries supplying the essential organs, they may cause unexpected deaths. In addition to these, the femoral, popliteal, and Kidney arteries experience atheromatous and thrombosis. Numerous investigations have demonstrated the significance of biofluid processes in atheromatous is [26, 27]. The development of arterial diseases has been shown to be influenced by factors

such as geometry, flow rate ratio, pulsatility and elasticity of the wall, and non-Newtonian flow behavior. However, while ongoing research into blood flow patterns has produced valuable information, the precise relationship between hemodynamics and potential causal mechanisms is still unknown. The role of hemorheological abnormalities is predominant in the development of various diseases. Due to the presence of stenosis in the lumen, higher resistance to flow is caused and this effect becomes more severe as the size of the stenosis increases [28, 29]. Further, the effect of stenosis is to increase shear stress at the wall and cause flow separation which has important implications in cardiovascular diseases such as atherosclerosis [30, 31, 32, 33, 34, 244]. Many studies have looked at the characteristics of blood flow in arteries with modest stenosis in recent years. A thorough analysis of this issue was done by [34], who offered a mathematical model to theoretically examine the impact of time-dependent stenosis on blood flow characteristics. He determined that when stenosis size increases, the wall shear stress, and resistance to flow (independence) both rise. Obtaining numerical solutions to the Navier-Stokes equations for flow through a confined tube has allowed researchers to examine the impact of flow separation in such a situation [35, 36]. In two-dimensional [37, 38] or axisymmetric [39, 40, 41, and 42] conduct, a number of writers have thought about numerical treatments of symmetric constriction. Although axis-symmetric conduits may be more reflective of the invivo condition even if the vascular lesions themselves are typically not symmetric, two-dimensional studies provide numerous ways to pinpoint some of the key aspects of the issue. In these studies, no attempt has been made to study the effect of Viscosity variation of the blood though it varies across the artery [43, 44, 45, 46, 47, 48] Considering the radial variation of Viscosity, [49, 50, 51]discussed the two-fluid model of blood (Newtonian fluids with different viscosity) flow through an artery with mild stenosis. effect of the peripheral layer on resistance to flow and wall shear stress has been analyzed. They came to the conclusion that, for a certain

stenosis size, the resistance to flow and the wall shear stress decrease with a drop in the peripheral layer viscosity (while maintaining a constant come viscosity).

1.8 DISEASES

As compared to mechanical systems, physiological systems operate trouble-free for a very long period unless and until they suffer some external or internal disorders that result in diseases. Atherosclerosis is the principal cause of myocardial and cerebral infarction. Several hypotheses of the development of the diseases have been proposed in literature chemical reactions and hemodynamic forces play major roles in the development of atherosclerosis and thrombosis. In the human circulatory system, bends and bifurcations are common sites where deposits and blockages can form. These can pose a significant risk, especially if they occur in arteries that supply vital organs, potentially leading to sudden deaths. Several studies have shown the importance of biofluid mechanisms in atherosclerosis [26, 27]. It has been demonstrated that in addition to geometry, flow rate ratio, the pulsatility and elasticity of the wall and Non-Newtonian flow behavior contribute to the development of arterial diseases. it has been found that the isosorbide dinitrate (IDSN) causes a decrease in arterial stiffness and a significant rise in the pulsatility index as a result of an increase in both the size and duration of reverse flow. Because cigarette smoking causes a rise in heart rate and arterial blood pressure [51, 52]. The smoking of two cigarettes per day causes an increase in arterial wall stiffness and a diminution of the pulsatility index due to a decrease in reverse flow. The role of hemorheological abnormalities is very predominant in the development of various diseases. Identification of any changes in blood viscosity is the most straightforward use of blood rheology in clinical practice. [53, 54] Dintenfass has presented the data gathered for this proposal. Higher viscosity is present in ill patients. The blood's coagulation

properties are the second crucial rheological element used in therapeutic settings. Hemophiliac individuals are an apparent example of this since they have trouble with blood coagulation. On the other hand, hypertension and artery sclerosis appear to be associated with an increase in the flexibility of thrombi. The erythrocyte sedimentation rate is a third variable that is used in clinical settings. Red blood cells still have the potential to aggregate and induce sedimentation in anti-coagulated blood. Several studies have now shown that decreased blood filter ability and increased Viscosity may be the primary lead to essential hypertension. When none of the traditional causes of hypertension can be shown, essential hypertension is diagnosed in otherwise healthy persons. While a healthy heart would only be able to maintain a normal cardiac output when confronted with abnormally viscous blood by raising its output pressure, a rise in the viscosity of these patients' blood may very well be the fundamental mechanism. Microangiopathy illustrates the complex interaction between hemorheological bio-chemical pathological and another hematological process [55, 56]. Several studies have shown a link between increased blood viscosity, reduced blood cell filtering ability, and clinical severity of microangiopathy, Diabetic subjects have generally higher blood Viscosity than normal and they are more susceptible to cardiovascular diseases[57]. Ischemia of the legs is invariably associated with significant stenosis or occlusion of major arteries. A number of studies have shown that whole blood viscosity and more particularly blood cell filter ability are not abnormal in patients with intermittent claudication but are of Prognostic significance [58]. This has important implications for both surgeons and internists dealing with patients with peripheral Ischaemia. Several workers' haemo-rheological have changes documented associated with principal myocardial infractions such as haemoconcentration, increased plasma, fibrinogen, and decreased blood filter ability [59]. There is clinical evidence that the changes in the flow properties of the blood do relate to the subsequent progress of the patient. this is probably an example of

the micro-circulatory vicious spiral.

1.9 WARM BLOOD ANIMALS AND COLD-BLOODED ANIMAL

According to their preferred body temperatures, the animal kingdom may be divided into basically two categories. Warm-blooded animals, also known as homeotherms, are those whose body temperature remains mostly constant in the face of significant variations in the ambient temperature, whereas cold-blooded creatures, also known as poikilotherms, have body temperatures that vary in response to such changes. Another species called hibernates has evolved along with homeotherms from Pio Kilotherms, and they go into hibernation in the winter while otherwise acting as warm-blooded creatures the rest of the year. Animals in hibernation don't need an external source of heat to get their body temperatures back to normal; they can accomplish it on their own, perhaps by igniting their massive reserves of brown fat.

1.10 REGULATION OF BODY TEMPERATURE

The fact that the body generates a sizable amount of heat internally and loses heat almost continuously while maintaining a constant temperature within a narrow range suggests the existence of a reliable mechanism that precisely balances heat gain and loss to maintain body temperature. Thermogenesis is the term used to describe the physiological process through which the body generates heat. Thermolysis is the term used to describe the process of releasing bodily heat by radiation, evaporation, etc. In the biological thermal system [60, 61, 63] discussed how much heat is produced by the body and where it comes from, how it is moved internally from one part of the body to another, and how it is lost to the environment through a vari-

ety of channels. The skin contains peripheral thermoreceptors that detect surface temperatures, whereas central thermoreceptors in the viscera, spinal cord, and hypothalamus detect core temperatures [256]. According to Guytona [64], the primary cause of heat generation in the body is metabolism, which is the chemical activity that enables cells to continue to function. Making the energy in meals available to the numerous Physiological systems of the cell is a major challenge for chemical processes occurring within the cells. Carbohydrates, proteins, and lipids from all energy meals may be oxidized in the cells, which releases a significant quantity of energy. In addition to heat, energy is also required for the physiological functions of the cells. In the case of a glandular solution,

(i) concentrating solute;

(ii) causing mechanical action;

(iii) affecting other bodily activities.

The physiological systems that control the chemical processes must be linked in order to produce this energy. Energy Transfer System and a unique biological enzyme work together to achieve this connection. Several studies [65, 66, 67, 68, 245, 169] have analytically forecasted temperature profiles from a few recorded temperatures, highlighting the need and difficulty of accurately measuring temperature profiles in cancer hyperthermia therapy. To determine temperature profiles in tissue subjected to non-uniform blood flow, Elokowitz [69] used numerical approaches for bio-heat transport equations. The mathematical formulation and modelling of bio-heat transfer applications are becoming more prevalent. A lot of emphases has been paid to the research and modelling of the bio-heat transfer process, which covers a variety of topics [60, 70, 166, 71, 72, 73]. A variety of simplifying assumptions must be made to aid analysis since the tissue is complex, non-homogenous, and non-isotropic. However, additional knowledge about the mechanisms behind thermal balance and their interactions is gained via studying models as well as the impacts of different

geometrical factors and boundary conditions. Consuming hot meals or beverages causes the liver to produce the most heat, with other organs producing far less heat. Heat generation is aided by the actions of several internal secretions and enzymes, such as thyroxine and epinephrine.

If the body temperature is greater than normal, metabolism will be sped up as a result of the increased temperature, much like other chemical processes. The unique presence of several minerals in the tissue causes them to speed up metabolism. More carbs are broken down when insulin is secreted too much, which results in more energy being released. The production of metabolic heat in the human body's periphery is correlated with the ambient temperature. The body's rate of heat production fluctuates quickly with the change in external temperature in developing children and those with very little fat deposition. It indicates The increased pace of metabolic heat generation can be attributed to a few aberrant factors in addition to the regular process. Three pathways, including the skin, lungs, and excretion, are used to lose body heat. Radiation, conduction, convection, and evaporation are the basic mechanisms by which heat is lost by the skin.

1.10.1 RADIATION

Around 60% of all heat loss is caused by this mechanism. Due to the temperature difference between the body and the cooler surroundings, the body loses heat through radiation. The temperature difference between the radiating body and the items it is emitted from, for example, is one factor that affects how much radiation an object emits. The relationship between these two temperatures is inversely proportional to their absolute temperature differences, each to the fourth power. Heat exchange through radiation is described below by Stefan's law.

$$H_r \propto (U_s^4 - U_a^4)$$

H_r is the heat loss due to the radiation U_s and U_a are the body surface and the atmospheric temperatures respectively.

1.10.2 CONDUCTION AND CONVECTION

Conduction and convection mechanisms transfer heat from the skin to the air when the ambient temperature is low, which is dependent on the temperature of the surrounding atmosphere. When the air progressively warms up and moves away from the skin, colder air from a higher layer replaces it. During these processes, the body loses around 15% of its heat.
It the heat loss by convection is H_c then we have.

$$H_c = h_c(U_s - U_a)$$

where h_c is a constant. Wind speed, air temperature, and relative air density all affect how much heat is lost by convection.

1.10.3 EVAPORATION

If H_c represents the heat lost due to evaporation then

$$H_c = LE$$

where L is the latent heat of sweat and E is the rate of evaporation E depends on

atmospheric vapor pressure, the amount of sweat and water available at the outer skin surface, the body loses over 22% of its heat through evaporation. Every time water evaporates from the skin of the body, heat is required to power the process, which is absorbed from the skin's surface and causes cooling. Diffusion via the skin, which is not entirely waterproof, causes water loss even when there is no sweating. Sweating plays an important role in heat regulation at high surrounding temperatures. it is a natural mechanism by which a person can control body temperature under high-stress conditions. At high temperatures or during great physical exertion the transfer of heat from the site of production to the skin, is aided by the secretion of sweat and diffusion of water from the skin surface and their evaporation.

Above 22.5°c and below 30°c or So the sweat is immediately evaporated in dry weather as soon as it reaches the skin's surface this phenomenon is called insensible perspiration. At low temperatures, up to 22.5°c evaporation from the body surface is very low and this process is called negligible insensible perspiration. The perspiration may go up to 1.5 liters per hour in the person maximally acclimatized to the heat. The population density and the activeness of the sweat glands differ from person to person.

1.11 FUNCTION OF THE SKIN

Skin envelopes the entire surface of the body and is smooth in some regions but rough and furrowed in others. It is glabrous in some areas, downy in others, and having in still others. It is thick, and horny in some regions, but thin, translucent, and pliable in others. Over bony regions it is firm, over soft parts it may glide easily and may be flaccid. In the human body, the skin is primarily in charge of regulating heat and temperature. [74, 75, 76, 105].

The skin defends the body against physical harm, bacterial infections, heat, cold,

moisture, drought, acid and alkali, and ultraviolet (UV) radiation from the sun. Skin is a sensitive organ to temperature and severe discomfort. This characteristic is connected to specific receptions in the area because perspiration evaporates, losing heat, while fat and hair retain heat. The skin is capable of easily absorbing some greasy substances. Chlorides are also stored in the extra water, salts, and waste that are expelled through perspiration and effort. The epidermis and dermis are two separate layers that make up the skin. The stratified squamous epithelium's surface and vascular layer are known as the epidermis. The ectodermal tissue is where the skin's appendages, such as hair, nails, sweat glands, and sebaceous glands, are formed. The deep, blood-filled layer of skin that forms from the mesoderm is called the dermis or corium. It is made up of the cornified zone, which is the superficial layer of the epidermis, and the germinative zone, which is the deep layer. It is made up of a combination of connective tissues, lymphatics, and nerves. A shallow papillary layer and a deep reticular layer separate the connective tissues. White fibrous tissue is the main component of the reticular layer, and it is mostly structured in parallel bundles. The dermis is the actual skin because it can be dried to create green hide and can be processed to create leather.

1.12 BLOOD CIRCULATION IN SKIN

The blood flow to the skin is around 25 C.C. per square meter of body surface area under typical cold circumstances. As opposed to that, the blood vessels contract more as the skin is heated until the maximum vasodilation has occurred, down to a temperature of around 13°C at which they achieve their greatest degree of constriction. The vascular structures responsible for heating the skin and the nutritive arteries, capillaries, and veins are the two main types of vessels that make up the skin's blood circulation system.

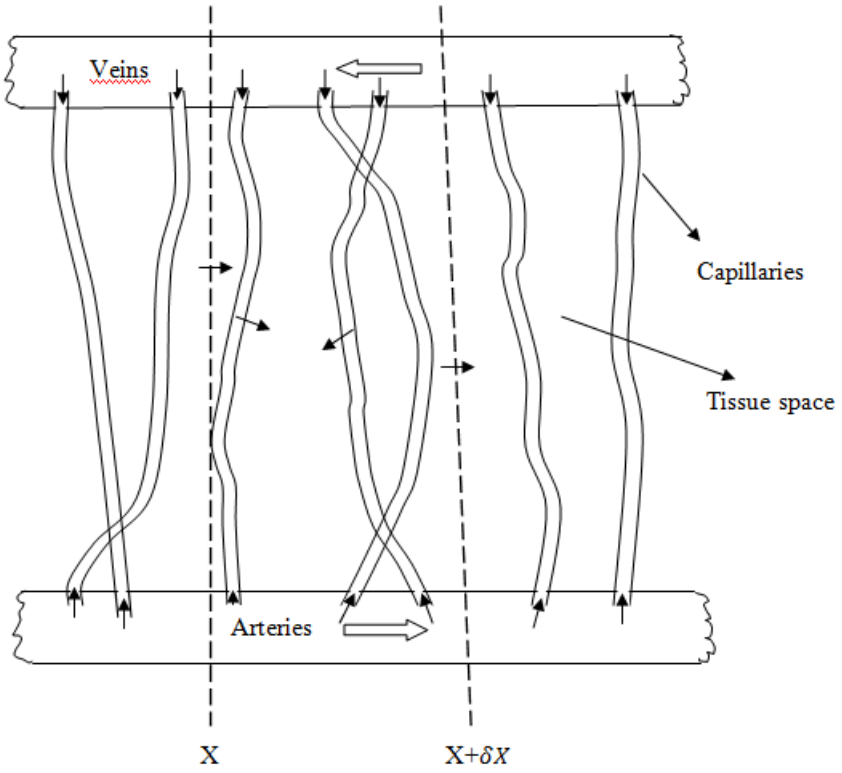

Figure 1.7: Schematic diagram of an element in the subcutaneous region.

Large blood vessels directly connecting arteries and veins, known as arteriovenous anastomoses, can be found in some skin locations as well as the enormous subcutaneous venous plexus, which holds a lot of blood and heats the skin's surface. The schematic diagram of an element in the subcutaneous region is shown in Figure 1.7.

1.13 DIFFUSION MECHENISMS

Using Krogh's theory to gauge the flow of oxygen to the brain's nerve cells. Because this application was in a tissue that differed significantly from striated muscle, their analytical modelling work needed to be complemented by extensive experimental research related to brain microcirculatory architecture and oxygen metabolism. In

addition to the previously considered radial components, axial diffusion must also be taken into consideration, extra factors that were based on their findings were added to the equations characterizing the Krongh tissue cylinder. Decker and Thews were able to come up with analytical answers for these extended equations, in a synopsis of the study, and later reported these solutions[77]. In addition to the tissue cylinder, Theews took oxygen gradients in capillaries into account. In the cardiovascular system, arteries, and veins serve primarily to carry blood to and from the microcirculation, Most of the work on capillary flow in microcirculation was based on Krogh's[78], Model and pioneering study of [79], which described the anomalous viscosity of the blood flowing in small diameter tubes of the order of 40 or so. Blood flow in this region transports gases and other dissolved substances to the arterial wall and supplies oxygen, and nutrition to the cells for their survival. Plasma soluble low molecular weight substances such as ions, and sugar amino acids pass more easily across the wall. Their further movement in the tissue to reach the cells follows more resistance due to the poroelastic nature of the tissues[80]. As regards, the two processes i.e. diffusion and flow, any capillary tissue exchange model involves two transport regions (capillary and enclosing tissue) within the capillary, the material is transported by convection and diffusion whereas in the tissue it is diffusion-dominated. Blum improved Krogh's cylinder with two more characteristics[81]. He considered a finitely permeable or semi-permeable capillary wall as well as a non-linear metabolic rate in the tissue space. Such findings would not apply to the substrate oxygen or the byproduct carbon dioxide since he did not take into account any blood substrate in the capillary blood. However, they would characterize the passive transport of any dissolved, flow-transported, and diffusible substrate, including glucose, bilirubin, and others. The mathematical study of a model for substrate concentration in tissue was examined by Salathe[82]. In their model, the substance diffuses into the surrounding tissue cylinder from a single cap-

illary. Blum developed the equations guiding this model. Earlier models identified single-phase rigid, elastic, or viscoelastic representation for the tissue[83, 84]. Recent observations conclude that these single-phase models are inadequate to incorporate all the important properties of such a complex multiphase interacting continuum in which they interact during flow and deformation. This study has further suggested developing the earlier models due to the introduction of the mixture theory of the interacting continua proposed by Green and Naghdi[85], and Chien et al. [86]. By the 1960s, as numerical approximation techniques advanced and electronic digital computers became more widely available, many researchers developed an interest in the mathematical description of substrate supply to tissue. The main goal of this interest was to provide a more comprehensive description of the Krogh cylinder and other model geometries. These expanded models explained how the substrate moved from the supplying arterioles to the capillaries via time-dependent flow, where a non-linear kinetic reaction took place in the capillary blood. The substrate then diffused within the capillaries, moved across a finitely permeable wall, and finally moved into the tissue space, where it diffused and was bound or consumed. The metabolic functional dependency on substrate level can be Michaelis Minten, first order (linear), or zero-order (constant) (non-linear) With some generalizations, Reneau et al. [87, 88, 89 90] explored the Krongh cylinder model. Several authors[91, 92, 93 94] investigated steady-state models in their subsequent research. More recently, [95, 82] examined capillary tissue diffusion in multi-capillary systems. Apelblat et al. [97] have conducted a thorough mathematical investigation of capillary tissue fluid exchange. In-depth research on the mathematical modeling of capillary tissue substrate exchange was conducted by Salthe[82]. They thought of a single capillary from which substrate would seep into the tissue cylinder around it.

1.14 GAS TRANPORT MECHANISMS

Beginning with a flat layer model of a cell, Nicholson and Roughten[98] have successfully modelled the first steps of O_2 absorption to red blood cells. A red blood cell's diameter is significantly greater than its thickness, such a representation neglects gas transfers through the ends and also neglects the curvature of the cell's surface. For species that do react with hemoglobin (CO, CO_2, O_2) the rate of diffusional and reactional uptake of the species by red blood cells can be measured conveniently in the rapid reaction apparatus, developed by Hartidge and Roughton[99]. There method for measuring the velocity of rapid chemical reactions, for the particular case of the reaction from Roughton[100].

$Hb + O_2 \rightarrow HbO_2$

CO_2 is also bound reversibly to hemoglobin, at different sites than those where O_2 is bound, and therefore is transported by this means. Since CO_2 has good solubility in aqueous solutions, a fair amount also is carried as dissolves gas CO_2 must first diffuse into a red blood cell and then react. The venous blood enters the lungs with 75% of the hemoglobin saturated with O_2 and leaves 97% saturated. CO_2 contents are considerably higher than O_2 contents., and very much less from the arterial to venous side. Finally, the major contributions of dissolved O_2 and CO_2 are apparent, Red blood cell hemoglobin interacts with oxygen and carbon dioxide, while serum albumin serves as a transporter for several tiny compounds. Stenosis A body is described as elastic if it can return to its original shape after being subjected to forces that cause deformations. It was Galileo who investigated the behavior of resistance of the solid- structure and gradually in 1978 Hooke's law came into existence. In the mathematical theory of elasticity, we deal with the calculation of the displacement field under an equilibrating system of forces. Navier gave the equations of equilibrium[141]. Cauchy[223], working from several presumptions, provided the

formulation of the linear theory of elasticity, which has remained the same up to this day. Green[85] rigorously deduced the equations of equilibrium while applying the concept of energy conservation. Some work was done and improved by authors[151, 238 239].

Numerous engineering structures are constructed by joining multiple materials that possess varying mechanical and elastic properties. Because loads are transferred from one material to the next across the interface, the system of heterogeneous materials must function as a single entity.

The development of fiber-reinforced composite materials has led to a growing utilization of laminated fiber-reinforced plates and various structural shapes in industries such as aerospace and electronics. The composite materials often combine a more dense, strong, and stiff reinforcing element in the form of fibers or whiskers with a binding material that is typically light, weak, and flexible. High strength-to-weight and stiffness-to-weight ratios are therefore easily attained. When there are more than six layers, these composite materials can be considered as orthotropic media.

Several efforts have been made over the past 20 years to create and demonstrate the characteristics of filament-reinforced composite materials. These efforts have only lately been focused on characterizing the fundamental materials and creating knowledge about their behavior.

There will also be instances where a variable skin thickness is preferred for an effective construction, such as in wing structures where the thickness of the wings decreases towards the tip. When a splash of air gush is passing over these blades, the fiber may be delaminated causing a fracture phenomenon to occur. The examination of these materials' mechanical behavior is required due to the laminated composite materials' steadily expanding utilization.

It is a very complex process to discuss the fracture phenomenon. We take a delaminated fiber from the matrix in some regions and for studying the phenomenon we

take up the join of two isotropic homogeneous dissimilar half spaces as the starting point.

1.15 BONES

Bone is the hardest tissue in the body. Human bones are the bones that make up the human skeleton. There are 206 bones in the adult human body. The bones provide structure, protect organs, and enable mobility. They also produce red and white blood cells, store minerals, and provide the body with structure. Bones are made of a combination of collagen, calcium, and other minerals. Many purposes are served by bones. They serve as the body's structure and enable movement of the entire body as well as individual body parts by producing joints that are propelled by muscles. The support that bones give the body enables us to move, stand up straight, and carry out daily tasks. Bones are living tissue that undergoes ongoing remodeling and renewal throughout a person's lifetime. Bones are classified into four categories .i.e long, short, flat, and irregular bones. All these types of Bones have an elastic property that allows them to absorb and dissipate energy when they are overloaded or stressed. This is known as the viscoelastic property of bones. This property allows bones to be flexible and deform to a certain extent before breaking. The ability of a bone to absorb energy helps protect the body from injuries. The elastic property of bones comes from the collagen fibers that make up the bone structure. These fibers are arranged in a specific way that allows them to stretch and bend, allowing the bone to absorb energy from impacts and other forces. The elastic property of bones also helps them to return to their original shape after the force is removed. This helps bones to maintain their structure and strength.

1. Long Bones: Long bones are found in the arms and legs and are longer than they are wide. They provide a structure for muscles to attach to and enable movement.

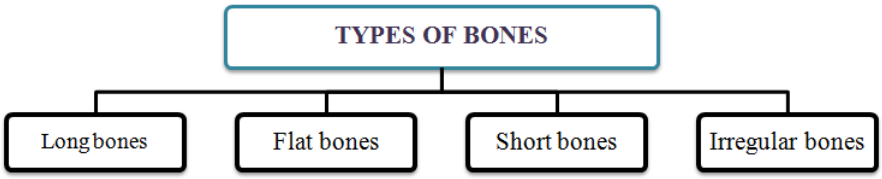

Figure 1.8: Types of Bones

The femur, tibia, and fibula are a few examples.

2. Short Bones: Short bones are the wrists and ankles, approximately cube-shaped bones. They provide stability and flexibility while also protecting the body's organs. The carpals and tarsals are two examples.

3. Flat Bones: Flat bones are found in the skull, ribs, and shoulder blades and are thin and curved. They protect internal organs and act as places where muscles can attach. The sternum, ribs, and scapula are among examples.

4. Irregular Bones: Irregular bones are found in the vertebrae and facial bones, and are asymmetrical in shape. They provide support and protection for the body's internal organs. The vertebrae and facial bones are two examples.

1.15.1 BODY FORCES

When a crack occurs, the body force acting on the crack is a tensile force. This is because the two sides of the crack are pulling away from each other, creating tension between them. This tension creates a force that acts on the crack, attempting to open it further. This force is known as a body force. These are the forces, which act from outside the structure, or like electrical or magnetic effects upon the structure. These forces may include electric and magnetic effects. It includes gravity effects too. But in practice, we generally see that when a body fractures, then we use the rivets just to make the structure workable.

In mathematical modeling, these rivets are simulated by concentrated body forces. We have discussed the effects of concentrated forces in the present thesis.

1.16 BRITTLE FRACTURE

The phenomenon of brittle fracture has affected social life. Prehistorical society used this phenomenon without knowing as it is today, in the shaping of stone tools. The essential processes of ancient construction were all dependent on the controlled manipulation of brittle fracture and it was known as the art of sculpture. Similarly, today many industrial manufacturing and construction processes involve brittle fracture at some stage. The sudden and catastrophic failure of structures occurring as a result of unexpected brittle fractures is not new.

The history of technology is full of such instances. During the latter half of the 19^{th} century and the first quarter of 20^{th} century, a great many similar disasters were recorded, involving bridge structures, naphtha conduits, gas tanks, water mains and water tanks, steam boilers, structural cranes, large and small guns, railroad tracks and other railways equipment, molasses tanks under both active and quiescent loads. These events led to independent investigations, which yielded some empirical information about "Crystallization", "Granulation" and "fatigue" as well as awareness that low temperatures may enhance the likelihood of brittle fracture.

These studies, however, did not produce a theoretically oriented body of scientific information related to brittle fracture. Griffith [101, 102] proposed an explanation of the fracture phenomenon in terms of the energy required for crack propagation. According to his hypothesis, the energy released during crack extension should be at least as much as the energy needed to generate the new fracture surfaces. Additionally, he made the claim that when the material at the crack's tip is strained

beyond the limit of its inherent strength, the fracture will become unstable.

Thus, the problem of equilibrium of elastic bodies with cracks is becoming an important tool in the hands of fracture design engineers. The following may be expressed using the linear fracture mechanics concept for an infinite plate with a centre crack:

(a). The fracture constantly moves in the direction of its initial length.

(b). Three alternative types of crack tip displacement exist, namely

(i) crack opening mode (Mode-I),

(ii) edge sliding mode (Mode-II),

(iii) crack tearing mode (Mode-III),

(c). crack tearing mode.

The fracture tip stress and displacement equations for the aforementioned modes may be expressed using Westergaard's equations.

The problems of the thesis can be extended further with the help of the following research papers: Lankford [103], Morozov [104], Nilsson and Brickstad [106], Russo [107], Yokobori, Kamei and Kounosu [108], Stahle [109], and Lemaitre [110]. Though in the studies we will not concentrate upon the origination of cracks, however, the following reasons can be described for the origination of cracks.

Accumulation of voids/flaws present in the medium. Lattice defects and pre-existing sub-micro cracks and their gathering to form a macro-crack. Welding defects or differential heat treatment.

These are some other following parameters, which accompany the initiation of a crack.

i). Material property

ii). The shape and dimension of the structure.

iii). Mode of applying load.

iv). Time

v). Temperature

vi). External loads/surface loads

vii). Strain rate and deformation history

The present thesis will consider only.

1.16.1 PHYSICAL ASPECT

In the theory of fracture of solids crack problems play an important role rather than primary of many of them. In crack problems, the separation between the crack's two opposing sides is always very short in comparison to its length. Therefore, the cracks are treated as discontinuities in the continuous. For the fracture process in materials to be a heterogeneous phenomenon in time and space, there is a strong dependence on both the homogeneities of the materials and the applied stress state. It is known that the formation, growth, and coalescence of voids control fracture in ductile materials [135, 234], whereas, in brittle materials, the primary causes of fracture are local cleavage factors and/or transgranular fractures [113].

In any event, a technique for evaluating the micro-cracks must be established in order to comprehend both the fracture process and the toughening mechanism. To study the crack opening mechanism the Griffith theory is enough. We know that solids contain surface tension, as do liquids when there is an external force in the medium, the work is done inside the medium. The work is stored as strain energy when the crack extends then the surface area increases which causes the surface tension to increase and this increase is balanced by the rate of release of strain energy. The crack will propagate when the applied stress Q exceeds the critical value Q_c given as

$$Q_c = \left[\frac{2ES}{\Pi c(1-\eta^2)}\right]^{\frac{1}{2}} \tag{1.1}$$

Where E, S, η, and c are Young's modulus, surface tension, Poisson ratio, and half

crack length respectively. The crack elastic energy of cracking is calculated through the formula.

$$W = 2\int_0^c p(x)u_Y(x,0)dx \tag{1.2}$$

Where p(x) is normally applied stress at crack faces, $u_Y(x,0)$ is crack opening displacement while crack occupies the space y = 0,

$-c < x < c$

Irwin gave an entirely different approach. He stated that the length of a Griffith crack would be increased from $2c$ to $2(c+\delta)$ then tensile stress $\sigma_{YY}(x,0)$ would try to close the crack which fits the original length. In doing so an amount of work $2G_c$ is called crack extension force. The relation

$$2\pi(1-\eta^2)K^2 = EG_c \tag{1.3}$$

exemplifies the relations between stress intensity factor K, defined as below

$$K = \lim_{x\to c_+} +\sqrt{X-c}d\xi\sigma_{YY}(x,0) \qquad c < x < \infty$$

1.16.2 THERMAL STRESS

The thermal stress set up in an elastic body containing cracks of different configurations has attracted the attention of many mathematicians physicists and engineers. For penny-shaped cracks, the thermal stress problems are done in [142, 143, 146, 147 149].

Following their investigation, Lal and Lal Pandey [114, 115] reduced the issue of axisymmetric penny-shaped crack issues to triple integral equations, which in turn

were reduced to an infinite set of simultaneous equations. Tweed and Melrose [116] have investigated the thermal stress problem of heat flow disturbed by two coplanar Griffith cracks by using the integral transform technique. Kushwaha and Chandra [117, 118, 119] have solved the problems of Griffith cracks in infinite solid and strip-whose edges are perpendicular by using Fourier transform methods.

1.16.3 BODY FORCE PROBLEMS

There are many problems in which body forces are acting symmetrically or unsymmetrically in an elastic body, see Dwivedi et al. [120, 121 122], Sneddon [123, 124], Sneddon and Tweed [125]. The problem in which the crack line is an axis of elastic symmetry has been discussed by Kushwaha [126]. As a special case, the research workers considered point body forces.

1.16.4 MODELS

To analyze the pattern and the mechanical response of elastic bodies where some force is applied we can use any one of the following methods.

1.16.5 EXPERIMENTAL MODELS

Though the results of these techniques are more reliable, nonetheless, the experiments performed over specimens may not hold well to the structures as such. And the elastic response of big structures cannot be obtained experimentally. So conducting these techniques is very sophisticated and costly, therefore, these cannot be popularized in a country like ours. Hence for more precessions in results, we shall follow other methods as known mathematical methods.

1.16.6 MATHEMATICAL MODELS

For analyzing the mechanical and the thermal response of a solid structure first, we solve the equations of equilibrium with compatibility relations the problems generated by the presence of crack lead to the dual, triple integral, and series relations. The solutions of these integral and series relations. The solutions of these integral or series equations may or may not lead to closed-form solutions.

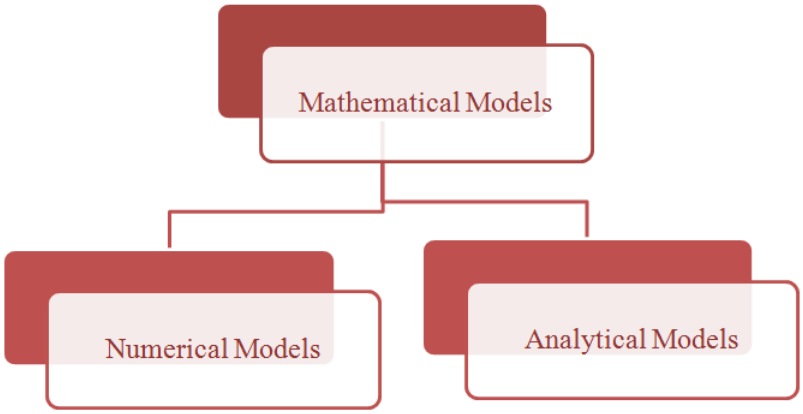

Figure 1.9: Mathematical Models

1.16.7 (a) NUMERICAL METHOD

In the vicinity of fracture tips, we resolve the equilibrium equations using compatibility relations and boundary conditions. There are mainly two methods:

Finite difference method [127]

Finite element method [128]

These methods can be applied to any type of geometrical configuration of the solid structure, however, an error is always involved. The stability and the convergence of the method always vary from problem to problem to problem therefore, the result can be used only as a starting point. The reliability of these results depends upon

experimental results. There are a few more methods. A superposition procedure for computing stress intensity factors in cracked elastic composites by Stief [129]. A constrained finite element procedure to compute S.I.F.S. for two-dimensional crack problems has been considered by Bowie [130]. Loakimidis [131, 132] investigates a novel class of approximation formulae for calculating stress intensity components based on numerical approaches of singular integral equations. Sections methods for the calculations of stress intensity factors by Wei and Wen [133]. The extrapolation technique to determine the S.I.F.S. is discussed by Carpenter [134]. Weiner-hopf technique is used by Georgiadis and Papadopoulos [144]. They mixed the use of the Fourier transform also. The hybrid finite element technique is developed by Byskov [127]

1.16.8 (b) ANALYTICAL METHOD

The basic philosophy of analytical methods is that the equations of equilibrium are reduced in terms of new functions. These functions are used to express the physical quantities. There are the following methods:

(a) Stress Function Method: Airy had given for the first time, this method for isotropic homogeneous elastic medium. It is called Airy's stress function. Only recently Kushwaha [145] has given this method for an orthotropic homogeneous medium. Maxwell extended this method of Airy's to three dimensions.

(b) Displacement Function Method: Finding a function that represents the displacement components reduces the boundary value problem to a simple problem. This method is divided into two parts:

(1). The solution is obtained that satisfies the boundary conditions. It is expressed in the form of an infinite series involving social functions, see Kushwaha [145] which is being elaborated in the Ph.D. thesis of Umesh Chandra [150].

(2). The quantities to be determined are expressed in terms of definite integrals. The integral represents the effect of singularity distributed over the surface throughout the volume [136].

(c) Potential Function Method: The equations of equilibrium and compatibility relations are satisfied by commonly known functions as potential functions. In two dimensions we can use Papkovitch-Bousinesque-Neuber potentials. For three dimensions we use Galerkin potentials. However, Sneddon and Berry [137] have modified the method of Pakovitch-Bousinesque potentials.

(d) Complex Variable Method: The theory of plane strain has been developed by Green [136], Kolosov-Mushkhelishvili [138], and Westergaard [139] and has modified the work of [130].

Bowier used the complex variable approach to determine the stress intensity parameters for fractures with equal spacing. The stress intensity variables for plates with equal and uneven parallel edge fractures have been studied by Raftopoulos and Farasmand [140].

1.17 OBJECTIVES OF THE PROPOSED RESEARCH WORK

1. Analysis of the essential role of biomechanics in the flow of transformation of the human body.

2. To find the vital role of biomechanics in musculoskeletal bone crack restoration. (Griffith crack problems)

3. Application of the principles of anatomy and physics to analysis of movement.

1.18 COMPOSITION OF THESIS

The plan of the thesis is as follows:

Chapter-1: It introduces the type of problems where they occur. It also relates to other physical phenomena and presents the necessity of the research work.

Chapter-2: Model on heat transfer between skin and core.

Chapter-3: Model on transport of O_2 and CO_2 in a red blood cell.

Chapter-4: Model for diffusion through Stenosis.

Chapter-5: Model on the transport of nutrients in pulsatile blood through time time-based stenotic tube.

Chapter-6: A model on finding the vital role of biomechanics in musculoskeletal bone crack restoration using Griffith crack. Deals with a Griffith- crack opened by the symmetrical system of body forces at the common interface. The closed form/exact expressions of stress intensity factors and crack opening displacement are presented in a general form. A special case of a point body force is considered.

The research work in fracture started in 1920 with the paper of Griffith [101]. But for 26 years it remained a rhetoric exercise only. It got an impulse when Sneddon [151] published a book. Additionally, the researcher incorporated Fourier transform techniques alongside the theory of dual integral equations. Sneddon and collaborators expanded Griffith's theory to three dimensions [152]. In the following lines, we discuss the physical aspect of crack(s) under mechanical, especially surface and body forces.

Chapter 2

MODEL ON HEAT TRANSFER BETWEEN SKIN AND CORE

Keywords: Skin, Core, Temperature, Steady-state, Transport, Heat transfer, Conduction, Radiation, Evaporation, Metabolic, Vascular, Thermal, Blood vessel, and venous Temperature.

2.1 INTRODUCTION

The recently developed field of Bio designing is a cross-preparation of the designing and organic sciences. The connection between designing and natural sciences and the full use of the current information on these two fields could be an extraordinary advantage to men. This interaction could lead to a better understanding of the phenomena that keep on occurring in the human body. The significant regions covered under the discipline of bio-designing are Applied science, Biomedical designing, and Biomechanics. Utilizations of designing standards for organic and medical issues have fostered another field of biomedical designing. It has been recognized that

meaningful mathematical modeling in biomedical engineering needs proper physiological, physical, and mathematical description with due regard to experimental findings. The scope of mathematical modeling of the problems in biomedical engineering is very large. A mathematical model is an abstract simplified construct related to a part of reality and created for a particular purpose. Modeling reduces the need for costly or impossible experiments with real life. Therefore, simplifying assumptions is introduced in formulating mathematical problems.

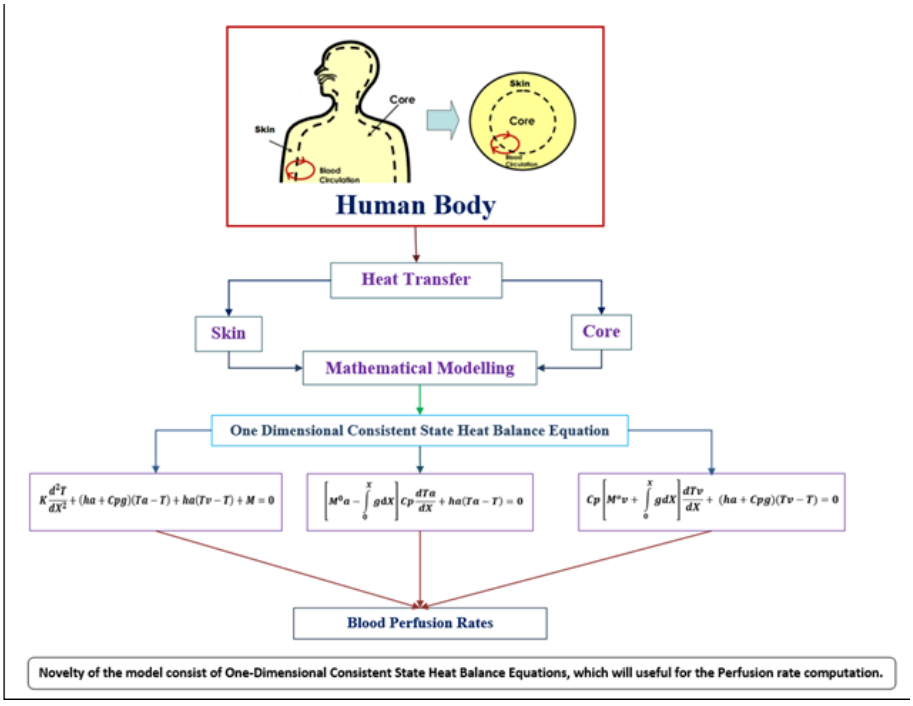

Figure 2.1: Heat transfer Model for Human Body

2.1.1 SKIN

The skin covers the entire body, some are slippery and some are rough and wrinkled. Some are shiny, some are smooth. Some regions are thick, while others are thin, transparent, and flexible. The bone part is hard and the soft part slides smoothly and is soft. The skin is mainly responsible for regulating body temperature and heat

in the human body. [Gray H Textbook Gray'sAnatony [74], Jarrett [105], Montagna [76]]. Protects the skin from mechanical damage, bacterial infection, heat and cold, moisture, dryness, acids, alkalis, and the sun. The skin is sensitive to severe pain and temperature. This property is associated with certain receptions situated in the region where heat is lost through the evaporation of sweat, and heat is conserved by fat and hair. Certain oily substances are freely absorbed by the skin. The excess of water salts and waste products re-excreted through sweat and skill also store chlorides. The skin is composed of two distinct layers, the epidermis, and dermis Epidermis is the super facial, vascular layer of stratified squamous epithelium. The skin is especially accountable for temperature control and heat reconciliation in the human body.

The temperature circulation in working muscles has been concentrated experimentally by numerous creators [Mensheh[153], Saltin, Jagge and Stolwijk [154], Stow and Shieve [155], Zavyalov [156]]. Hill [157] discovered that during the activity of separated muscles of warm and cold blood animals, their temperature elements showed a conventional similarity with that noticed for various interior organs. The examination and demonstration of bio-heat move measure cover different viewpoints and have gotten broad consideration [Shitzer[158], Stolwizk[159], Chato [111], Shitzer and Chato [161]] because of the way that the upkeep of a homeothermic state is of essential significance to homeotherms and is additionally perhaps the most convoluted issues.

The significant part that the skin of the homeotherm plays in the warm arrangement has for some time been recognized. Zhitomirskii and Kagna[162] considered temperature dispersion in a lone layered skeletal muscle going through rhythmical compressions. They showed that a smoother muscular movement couldn't cause the considerable temperature to ascend as the boundaries change to keep up the inner temperature of the muscle in the admissible reach. The thermal power balance for a

muscle of an animal involves thermal power provided by the bloodstream, the energy produced by metabolic interaction, the transport of warmth through the muscle by a temperature gradient, and energy moved to the climate by conduction, radiation, and evaporation. Because of the complex non-homogeneous, non-isotopic nature of tissues various improvements on suspicions have been made to work with the investigation. The evaluation of warmth moving across the skin will rely on the tissue formation and thickness of the skin and subcutaneous tissues. Numerous examinations have been embraced to elucidate the thermal conduct of organic tissues and the relationship that exists among the different components, viz, convection conduction, generation, evaporation, and radiation, overseeing the transport of fervor in the tissue.

Keller and Seller [163] have fostered an exceptionally basic model for heat moving between an isothermal core and ambiance. The furthest thickness of the skin was viewed as tiny and estimations were made without metabolic heat moving between either arteries or veins and tissue. One of the controls accessible to the body in the upkeep of a homoisothermic state is its capacity to change obstruction of its subcutaneous areas to heat flow [Trorell and Nilson [164], Steketee Vanderheek [165]].In prior models, an endeavor was made to represent the mix of conduction vasomotor action by a straightforward expansion impact [Hardy and Soder Storm [171] and Burton [167]]. Krogh [168] had recognized, a distinct vascular composition called rates which in specific species seem to work principally to preserve heat. In these designs conduits and veins are organized firmly pressed for counter-current movement Mitchell and Myers [169]. It has been seen that the evaluation of heat loss from the furthest point is identified with a nearby blood perfusion rate. [Burton and Edhalm [170], Hardy and Sodersterm [171], Lefever[172]]. K.E.Cooper, 0.G.Edholm, and R.F.Mottram [173] have discussed the blood flow in the skin and muscle of the human forearm. The evidence from the experiment in which the forearm was incised

strongly suggests that kin blood flow is zero in a blanched limb segment. Any small flow of blood through the skin after iontophoresis would give a slightly high figure for muscle blood flow and a consequent underestimate of the flow through the skin. This possibility cannot be excluded. Since direct observation of incised, was not made in each experiment. Pennes[174] imposed these models fundamentally by regarding tissue as a continuum of limited thickness and fostering the fitting heat preservation differential equation to depict the tissue temperature profile. Wissler[175] explains the abundant more convoluted problem of the overall heat balance by separating the body into an emblem of a cylindric zone thermally associated with the circulatory flow. His model additionally took conductive and conductive impacts yet he expects that blood vessel and venous blood temperatures are uniform in every zone so the impacts of nearby counter-current heat interchange are lost. lately, Gupta and Tandon [176] have refined a model for heat moving between core and skin. They consolidated the things of local factor perfusion rate notwithstanding convective heat move and metabolic heat generation contingent upon temperature.

Ming Fu et al. [177] have discussed a model of heat and moisture transfer through clothing and the impact of airspeed on the thermal and vapor obstruction of attire was contemplated. Xiaojiang Xu et al. [181] explain the Relationship between core temperature, skin temperature, and heat flux during exercise in heat. Salimpour and Shirani [182] investigated the effects of blood vessels on temperature distribution in skin tissue subjected to various thermal therapy conditions. Ichikawa and Ogino [183] measured energy transfer indicating that topical ice bag application absorbs insufficient energy to affect core temperature. Quantitative assessment of energy transfer was shown to inform the safe and appropriate use of thermotherapy. In prior models, an endeavor was made for either no metabolic heat generation rate or consistent blood vessel and venous temperature. The current part is a further conclusion of the prior work by consolidating the impact of temperature on arte-

rial and venous beds, notwithstanding metabolic heat generation contingent upon temperature and diverse environmental conditions.

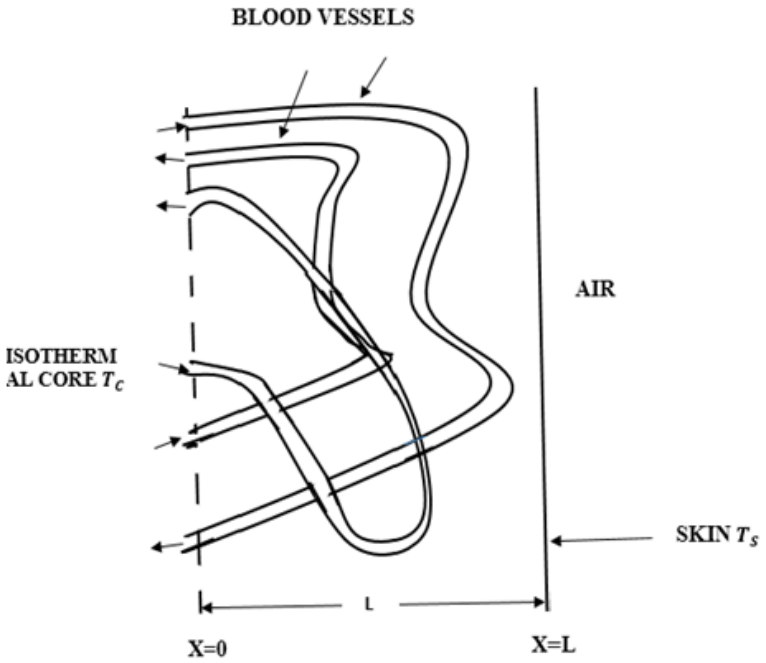

Figure 2.2: Schematic of subcutaneous region emphasizing its vascularization and temperature variation.

2.2 FORMULATION OF THE PROBLEM

The graphic diagram of the model is given below in Figure 2.2. Thermally, it is separated into two regions: an isothermal core and a peripheral zone with varying temperatures between the core and the skin discussed by Keller and Seller [163]. The peripheral layer thickness is small contrasted with the radius of the curve of the nearby surface. Since the region is small in this way were can be viewed as one-dimensional. The consistent state heat balance equation can be composed as follows:

$$K\frac{d^2T}{dX^2} + (ha + Cp \times g)(Ta - T) + ha(Tv - T) + M = 0 \tag{2.1}$$

$$\left[M^0 a - \int_x^0 g dX\right] Cp \frac{dTa}{dx} + ha(Ta - T) = 0 \tag{2.2}$$

$$Cp\left[M^o v + \int_X^0 g dX\right] \frac{dTv}{dX} + (ha + Cp \times g)(Tv - T) = 0 \tag{2.3}$$

Solve the equation (2.1) to find the value of T:

$K\frac{d^2T}{dX^2} + (ha + Cp \times g)(Ta - T) + ha(Tv - T) + M = 0$

$$\frac{d^2T}{dX^2} + \frac{(ha + Cp \times g)(Ta - T)}{K} + \frac{ha(Tv - T)}{K} + \frac{M}{K} = 0 \tag{2.4}$$

$$\frac{d^2T}{dX^2} + \frac{Ta(ha + Cp \times g)}{K} - \frac{T(ha + Cp \times g)}{K} + \frac{haTv}{K} - \frac{ha \times T}{K} + \frac{M}{K} = 0 \tag{2.5}$$

$$\frac{d^2T}{dX^2} + \left(\frac{Ta(ha + Cp \times g)}{K} + \frac{haTv}{K} + \frac{M}{K}\right) - \frac{Tha}{K} - \frac{Cp \times g \times T}{K} - \frac{ha \times T}{K} = 0 \tag{2.6}$$

Where

$$Ta(ha + Cp \times g) + \frac{haTv}{K} + \frac{M}{K} = 1$$

Equation (2.6) will become

$$\frac{d^2T}{dX^2} + 1 - \frac{2Tha}{K} - \frac{Cp \times g \times T}{K} = 0 \tag{2.7}$$

$$\frac{d^2T}{dX^2} + 1 - \frac{2T(ha - Cp \times g)}{K} = 0 \tag{2.8}$$

$$\left(\frac{d^2}{dX^2} - \frac{2(ha - Cp \times g)}{K}\right) T = -1 \tag{2.9}$$

$$\left(D^2 - \frac{2(ha - Cp \times g)}{K}\right) T = -1 \tag{2.10}$$

Auxiliary Equation

$D^2 - \lambda = 0$

$D^2 = \lambda$

$D = \pm\sqrt{\lambda}$

Where

$\lambda = \frac{2}{K(ha - Cp \times g)}$

Complementary solution

$$T = C_1 cos\sqrt{\lambda_1}X + C_2 sin\sqrt{\lambda_2}X - \frac{\lambda_1}{\lambda_2} \tag{2.11}$$

Using the boundary conditions X = 0 and X = L from fig. 2.2 having the value of C_1 and C_2.

$C_1 = T_c + \frac{\lambda_1}{\lambda_2}$

$C_2 = \frac{Ta - (Tc + \frac{\lambda_1}{\lambda_2})cos(\sqrt{\lambda_1}L) + \frac{\lambda_1}{\lambda_2}}{sin(\sqrt{\lambda_1}L)}$

$\lambda_1 = \frac{M^o ha - Cp \times g}{K}, \qquad \lambda_2 = \frac{Cp \times g \times Ta + M^o}{K}$

Solving equation (2.2), we get

$$\left[M^o a - \int_x^0 g dX\right] Cp \frac{dTa}{dX} + ha(Ta - T) = 0$$

$$\left[M^o a - gX\right] Cp \frac{dTa}{dX} + haTa - haT = 0 \tag{2.12}$$

$$\frac{dTa}{dX} + \frac{haTa}{[M^o a - gX]Cp} - \frac{haT}{[M^o a - gX]Cp} \tag{2.13}$$

Take, $\frac{ha}{Cp} \approx 1 \quad and \quad \frac{haT}{[M^o a - gX]Cp} \approx 0$

Now, equation (2.13) will become

$$\frac{dTa}{dX} = \frac{-Ta}{[M^o a - gX]} \tag{2.14}$$

$$\frac{dTa}{da} = \frac{-dX}{[M^o a - gX]} \tag{2.15}$$

Integrating the above equation, we get

$$log_{10}Ta = -log_{10}[M^o a - gX] - g + log_{10}C_3 \tag{2.16}$$

$$\frac{Ta[M^o a - gX]}{-g} = C_3 \tag{2.17}$$

Now, take the value Ta = constant.

Solving equation (2.3) find the value of Tv

$$Cp\left[M^0 v + \int_0^X gdX\right]\frac{dTv}{dx} + (ha + Cp \times g)(Tv - T) = 0$$

$$\left[M^o v + gX\right]Cp\frac{dTv}{dX} + Tv(ha + Cp \times g) - T(ha + Cp \times g) = 0 \tag{2.18}$$

$$\frac{dTv}{dX} + \frac{Tv(ha + Cp \times g)}{Cp[M^o v + gX]} - \frac{(haT + Cp \times g \times T)}{Cp[M^o v + gX]} = 0 \tag{2.19}$$

Where

$\frac{(ha+Cp\times g)}{Cp[M^o v+gX]} \approx 0$ *and* $\frac{ha+Cp\times g}{Cp} \approx 1$

Equation (2.19) will become

$$\frac{dTv}{dX} + \frac{Tv}{[M^o v + gX]} = 0 \tag{2.20}$$

$$\frac{dTv}{Tv} = -\frac{-dX}{[M^o v + gX]} \tag{2.21}$$

$$log_{10}Tv = -log_{10}[M^o v + gX].g + log_{10}C_4 \tag{2.22}$$

$$log_{10}Tv = log_{10}[M^o v + gX]^{-1}.g + log_{10}C_4 \tag{2.23}$$

$$log_{10}\frac{Tv[M^o v + gX]}{g} = log_{10}C_3 \tag{2.24}$$

$$Tv = \frac{g}{M^o v + gX} C_4 + C_5 \tag{2.25}$$

Where

$C_4 = C_1 \frac{sin\sqrt{\lambda_1 X}}{\sqrt{\lambda_1}} - C_2 \frac{cos\sqrt{\lambda_1 X}}{\sqrt{\lambda_1}} - \frac{\lambda_1}{\lambda_2} X$ and $C_5 = Ta - \frac{g}{[M^o v + gL]} \left[C_1 \frac{sin\sqrt{\lambda_1 L}}{\sqrt{\lambda_1}} - C_2 \frac{cos\sqrt{\lambda_1 L}}{\sqrt{\lambda_1}} - \frac{\lambda_1}{\lambda_2} L \right]$

Substituting the value of C_3 and C_4 in the equation (2.25), we get

$$T_v = \frac{g}{[M^o v + gX]} \left[C_1 \frac{sin\sqrt{\lambda_1 X}}{\sqrt{\lambda_1}} - \frac{cos\sqrt{\lambda_1 X}}{\sqrt{\lambda_1}} - \frac{\lambda_1}{\lambda_2} X \right] + Ta - \frac{g}{[M^o v + gL]} \left[C_1 \frac{sin\sqrt{\lambda_1 L}}{\sqrt{\lambda_1}} - \frac{cos\sqrt{\lambda_1 L}}{\sqrt{\lambda_1}} - \frac{\lambda_1}{\lambda_2} L \right]$$

Now, X=L then the above equation will become,

$$Tv = \frac{g}{M^o + gX} \left[\frac{C_1}{\sqrt{\lambda_1}} (sin\sqrt{\lambda_1 X} - sin\sqrt{\lambda_1 L}) - \frac{C_2}{\sqrt{\lambda_1}} (cos\sqrt{\lambda_1 X} - cos\sqrt{\lambda_1 L} - \frac{\lambda_1}{\lambda_2} (X - L) \right] + Ta \tag{2.26}$$

Using the non- dimensional scheme

$\theta_1 = \frac{T - Tc}{Ta - Tc}$, $\theta_2 = \frac{Tv - Tc}{Ta - Tc}$, $X = \frac{X}{L}$

We get,

$$\theta_1 = \left(\frac{C_1}{Ta - Tc} \right) cos(\sqrt{\lambda_1} LX) + \left(\frac{C_2}{Ta - Tc} \right) sin(\sqrt{\lambda_1} LX) - \frac{\lambda_2}{\lambda_1 (Ta - Tc)} - \frac{Tc}{Ta - Tc} \tag{2.27}$$

$$\theta_2 = \frac{g}{(M^o v + gXL)(Ta - Tc)} \left[\frac{C_1}{\lambda_1} \{ sin(\sqrt{\lambda_1} XL) - sin(\sqrt{\lambda_1} L) \} - \frac{C_2}{\lambda_1} \{ cos(\sqrt{\lambda_1} XL) - cos(\sqrt{\lambda_1} LX) - cos(\sqrt{\lambda_1} L) \} - \frac{\lambda_2 L}{\lambda_1} (X - 1) \right] + 1 \tag{2.28}$$

2.3 RESULTS AND DISCUSSIONS

The following values of physical and physiological parameters along with Table 2.1. are used for obtaining the temperature profile in the region under study.

K = 0.499 J/m Sec K

$C_p = 3799 J/KgK$

$Tc = 310K$

Te = 302 K

The blood perfusion rates are obtained from the expression

$$\lambda = \sqrt{\frac{Cp \times g}{K}}$$

Table 2.1: Blood perfusion rates for various types of tissue.

λ	Blood perfusion rate Kg/m Sec	Type of tissue
0.1	g(1) = 1.314 $\times 10^{-6}$	Negligible blood perfused tissue
0.1	g(2) = 1.314 $\times 10^{-4}$	Poorly perfused tissue
5.0	g(3) = 3.28595 $\times 10^{-3}$	Well perfused tissue
10.0	g(4) = 1.314 $\times 10^{-2}$	Highly perfused tissue

The temperature allocation in tissue and veins is introduced in Figures 2.3 to 2.6. The worth of M^o considered are 0, 0.17, and 0.25. The value of g is given in Table 2.1. No change among tissue and blood vessels or venous blood happens. The upsides considered are 0, 0.02, and 0.4. The values of Te considered are 278K, 302K, 303K, and 313K. For M^o= 0 and ha = 0, the outcomes are the same as those of Keller and Seller [163].

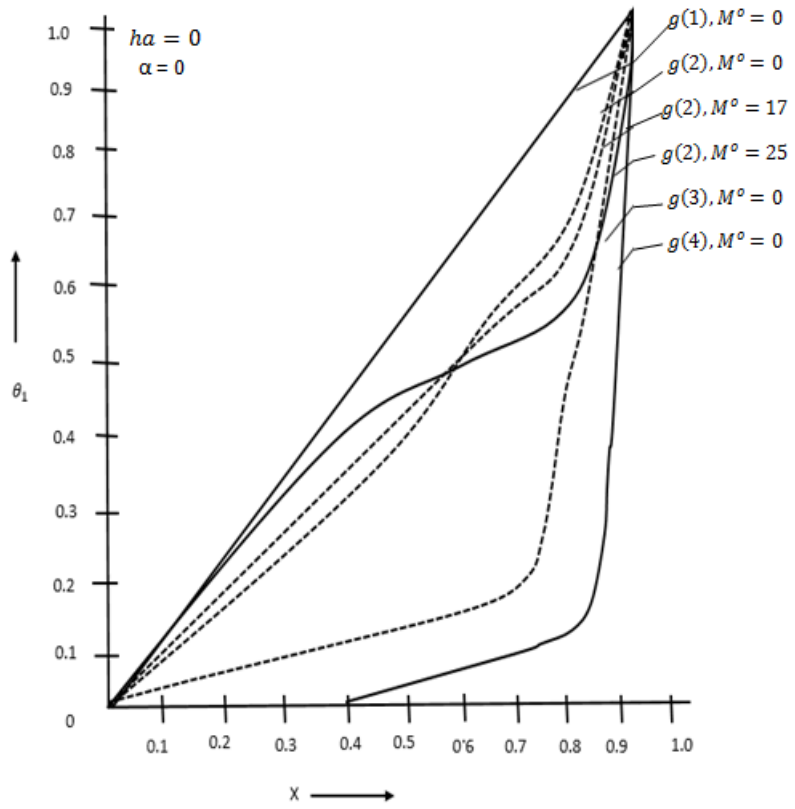

Figure 2.3: Tissue temperature distribution for various perfusion rates and metabolism.

Figure 2.3. portrays the variety of tissue temperature distribution for the different worth of pivotal distance. For negligible blood perfusion rate, the diagram is practically straight. This might happen because the majority of the heat is moved by conduction measure. In this situation the heat perfusion in the capillary is little. The temperature profiles stray linearly as the blood perfusion rates increment. For exceptionally perfused tissue the temperature profile gets parabolic. Thinking about the impact of M^o, it is obvious from the fig that for the fixed perfusion rate [for example poorly perfused tissue of g(2)] the temperature near the core region decreases with an increase in M^o and temperature in the outer region increases with increase in M^o.

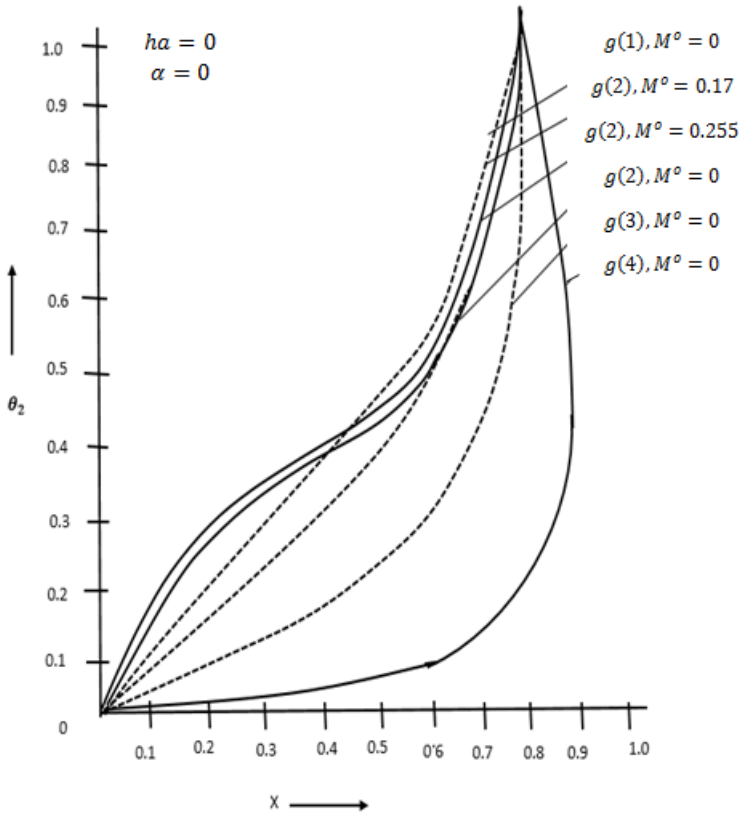

Figure 2.4: Various temperature distribution for various perfusion rates and metabolism.

Figure 2.4. describe the difference in venous temperature dispersion for different values of axial distance. For negligible and low blood perfusion rates the outcomes are like those of tissue temperature with slight modifications in amount. It is obvious from the diagram that the approximate distribution is identical for a wide range of blood perfusion rates. Considering the impact of M^o, it is obvious from the diagram that for poorly perfused tissue the venous temperature increments with expansion in the characteristic boundary.

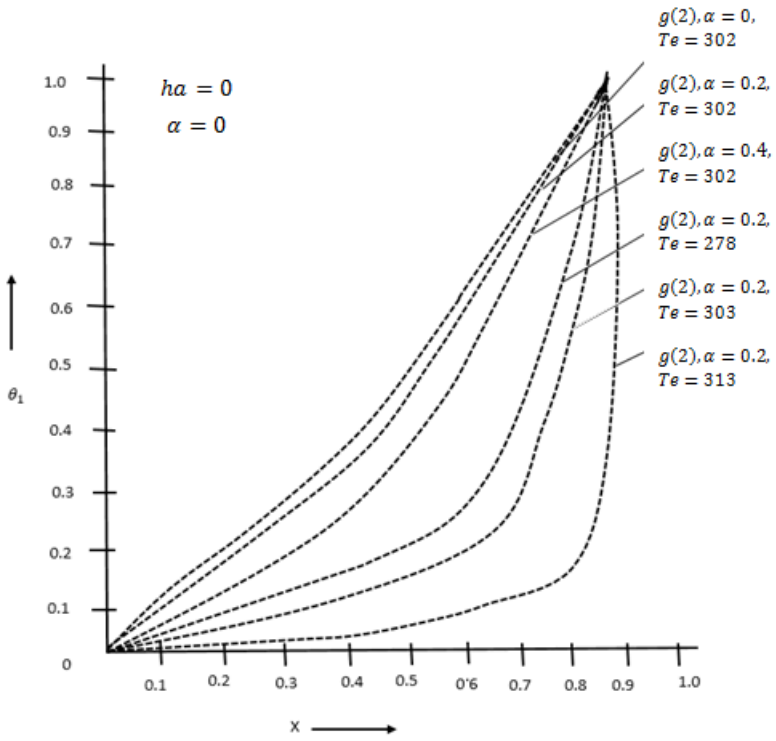

Figure 2.5: Tissue temperature profile for various coefficient metabolism and environmental temperature

Figure 2.5. illustrate the variety of tissue temperature conveyance with axial distance for various climate temperatures and co-proficient metabolism. For poorly perfusion rate the temperature increments with the diminishing value of co-effective of metabolism. On account of very much perfused tissue i.e. g(3), the temperature in the internal region diminishes with the climate temperature when the barometrical temperature is lower than that of the core. In any case, in the external locale, inverted conduct has been noticed. This is because of the way that the heat misfortune from the surface to the climate declines with expansion in the air temperature.

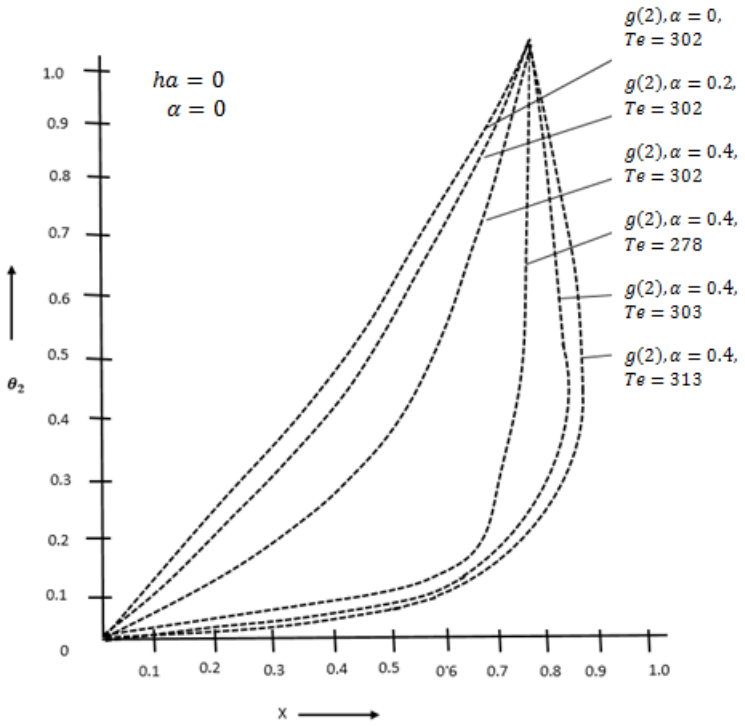

Figure 2.6: Various temperature profiles for various coefficients of metabolism and environment temperature

In Figure 2.6. the impact of the co-efficient of metabolism and air temperature on venous temperature appropriation has been considered. The venous temperature diminishes with expanding the co-productive metabolism. A similar qualitative conduct has been seen with atmospheric temperature as tissue temperature circulation. Subsequently, we can infer that the tissue temperature impacts the venous temperature distribution. Accordingly, we cannot take the temperature distribution of venous beds as consistent. Along these lines, the above investigation shows that the blood perfusion rate impacts the temperature appropriation of tissue and venous beds significantly more in contrast with different boundaries.

2.4 CONCLUSION

This chapter is about the study of heat transfer between skin and core with the help of biomechanics modelling. Skin is the biggest organ and it covers and secures the complete body from mechanical injuries bacterial infections etc. The skin is especially accountable for temperature control and heat reconciliation in the human body. The work of Keller and Seller, who have developed a very simple model for heat transfer between an isothermal core and an ambient atmosphere is considered in this chapter. One dimensional steady state condition taken in the equations (2.1 to 2.3) to solve the problem and also use the non-dimensional scheme to care of the issue of heat moving among skin and core is also discussed. Some values of physical and physiological parameters along with table (2.1) are used for obtaining the temperature with which blood perfusion rates are obtained for various types of tissue. Finally, radiation impacts, convection of blood flow, and tissue metabolism in a body are described. Lastly, outcomes of different flow conditions with some reasonable information are mentioned graphically.

2.5 SIGNIFICANCE OF THIS CHAPTER

The significance of heat transfer between the skin and core of the human body lies in its critical role in maintaining thermal equilibrium and overall well-being. Here are some key aspects of its significance:

1. Regulation of Body Temperature: Heat transfer between the skin and core helps in regulating the body's temperature within a narrow range. This is essential for normal physiological functions and to prevent overheating or hypothermia.

2. Health and Comfort: Understanding heat transfer mechanisms is crucial for ensuring thermal comfort and preventing heat-related illnesses or conditions like heat

stroke or hypothermia.

3. Medical Applications: Knowledge of heat transfer between skin and core is valuable in medical treatments such as managing fever, hypothermia, or hyperthermia, as well as in therapeutic applications like localized heating or cooling for pain relief.

4. Performance Optimization: In sports and physical activities, managing heat transfer between skin and core can improve performance, endurance, and recovery by regulating body temperature effectively.

5. Safety in Extreme Environments: For individuals working in extreme environmental conditions, such as firefighters, soldiers, or industrial workers, understanding heat transfer is crucial for developing protective gear and strategies to prevent heat-related injuries.

6. Personalized Medicine: Advances in understanding individual variations in heat transfer can lead to personalized interventions for thermal regulation, especially for vulnerable populations like the elderly or infants.

Overall, studying heat transfer between the skin and core is essential for maintaining homeostasis, optimizing performance, ensuring safety, and improving overall quality of life.

Chapter 3

MODEL ON TRANSPORT OF O_2 AND CO_2 IN A RED BLOOD CELL

Keywords: Oxygen, Carbon dioxide, Eryhrocyte, Diffusion, Hemoglobin, Radial distance, Concentration, Oxy-hemoglobin.

3.1 INTRODUCTION

The primary functions of the human lungs are obviously to supply oxygen to the blood from the atmosphere and dispose of CO_2. The oxygen is transported to all of the cells of the body for sustaining metabolic processes. The other functions of the lungs are to strain out and digest small blood clots etc. The thickness of the membrane is ranging from 0.2 to 0.5 [Guyton[64]]. The balance between the speeds at which oxygen and carbon dioxide are taken in and exhaled through breathing and the rates at which they are used up and produced by metabolism will determine the

composition of the exhaled air. For a typical male adult, the respiratory membrane has an astounding surface area of $70m^2$, although there is seldom more than roughly 70 to 100 ml of blood in the lung capillaries at any given time. The thickness and surface area of the membrane affect how quickly gases may pass across it. The membrane provides some barrier to the movement of respiration gases. Several authors [Singh. et al.[179, 180, 131] Sharan and Singh[191, 193]] Researchers have developed several mathematical models to explain the transfer of gases from the lungs to the blood. These models consider mechanisms such as molecular diffusion, convection, and facilitated diffusion when hemoglobin acts as a gas carrier. Additionally, the influence of wall permeability on substance transport in the blood has been emphasized by many researchers. [Leonard and Jorgenson[194], Bloch[195], Renkin[196], Gonzalez-Fernandez and Alta[197], Kumar[198]]. Several authors [Kumar[188], Singh, et al.[200]; Sharan et al.[201]] have created several mathematical models to handle the simultaneous movement of oxygen and carbon dioxide in capillaries and surrounding tissue. These studies, however, only take into account permeability, facilitated diffusion, convection, or membrane resistance as they pertain to the pulmonary capillaries. For therapeutic reasons, the study of gaseous diffusion in the red blood cell is the most significant process. By beginning with a flat layer cell model, Nicholson and Roughton[98] were able to successfully simulate the early phases of O_2 absorption by red blood cells. An approximation that a flat disc of uniform thickness has roughly the same uptake rate as a biconcave cell with the same volume as the earlier author is therefore not implausible, according to some additional numerical calculations by [Froster [202]], which have shown that the shape of the red blood cell has only a minor impact on gas uptake. Red blood cells have a diameter that is significantly more than their thickness. As a result, a model like this, which ignores the curvature of the cell surface, turns out to be quite accurate. By avoiding unstable general differential equations and accounting for the back re-

action, [Moll [203] and Kutchai [204]] were able to arrive at the solution for oxygen absorption in red blood cells. Further, these models have not taken into account the role of CO_2 transporting the red blood cell. Rhodes and Varacallo [184] measures of adequate oxygen transportation are hemoglobin concentration and oxygen saturation; the latter is often measured clinically using pulse oximetry. Richardson et al. [185] explain the changes in RBC shape and hemoglobin concentration, which are common manifestations of hematological disorders, can have hitherto unrecognized and clinically significant implications on gas exchange.

A mathematical model is created in this chapter to describe how oxygen and carbon dioxide are transported simultaneously inside red blood cells. The model considers how species are transported as a result of assisted diffusion as well as molecular diffusion.

3.2 FORMULATION OF THE PROBLEM

In the current chapter, we have taken into account the transport of O_2 and $CO2$ due to the red blood cell's enhanced diffusion and response rates as well as its pure diffusional flow. With hemoglobin in its different forms, oxygen, and CO_2 are known to go through a number of reactions. Some of these responses have undergone extensive quantitative research, and the results are well understood [Ulanovier and Frazier[205]]. The following reversible process included the combination of oxygen and carbon dioxide with hemoglobin.

$$\mathrm{Hb} + \mathrm{O_2} \underset{\mathrm{K''}}{\overset{\mathrm{K'}}{\longrightarrow}} \mathrm{HbO_2}$$

$$\mathrm{Hb} + \mathrm{CO_2} \underset{\mathrm{m''}}{\overset{\mathrm{m'}}{\longrightarrow}} \mathrm{HbCO_2}$$

where K',m' are forward rate coefficients and K" and m" are backward rate coefficients.

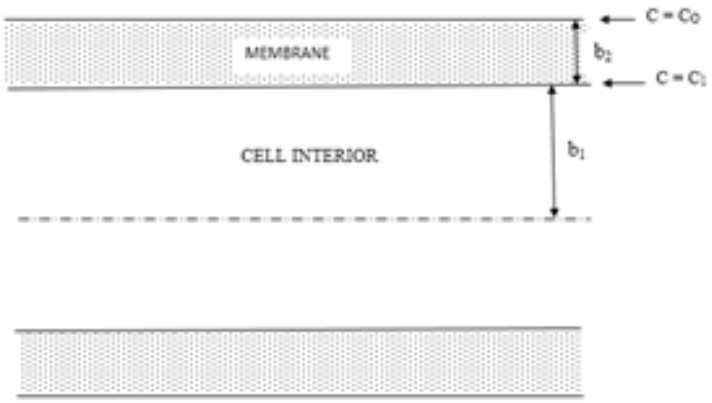

Figure 3.1: Planar model of the red cell for modeling diffusion and reaction

For the dispersion of the O_2 and CO_2, a red blood cell planner model has been provided in Figure 3.1. The membrane equations describe the simultaneous diffusion reaction mechanisms in the interior of the cell and the transport of gases over the membrane.

$$\frac{\partial c^{'}}{\partial t} = D_m \frac{\partial^2 c^{'}}{\partial x^2} \tag{3.1}$$

The model depicts the constant reaction and diffusion of elements as blood moves through capillaries at a rapid pace. The mass balance for the five species, accounting for diffusion, convection, and the chemical interaction of oxygen and carbon dioxide with haemoglobin, yields the parabolic equations shown below.

Cell interior

$$\frac{\partial c^{''}}{\partial t} = D_o \frac{\partial^2 c}{\partial x^2} - K^{'} c^{''} c^{vi} + K^{''} c^{'''} \tag{3.2}$$

$$\frac{\partial c^{'''}}{\partial t} = D_H \frac{\partial^2 c^{'''}}{\partial x^2} - K^{'} c^{''} c^{vi} + K^{''} c^{'''} \tag{3.3}$$

$$\frac{\partial c^{iv}}{\partial t} = D_c \frac{\partial^2 c^{iv}}{\partial x^2} - m^{'} c^{iv} c^{vi} + m^{''} c^{v} \tag{3.4}$$

$$\frac{\partial c^{v}}{\partial t} = D_H \frac{\partial^2 c^{v}}{\partial x^2} - m^{'} c^{iv} c^{vi} + m^{''} c^{v} \tag{3.5}$$

$$\frac{\partial c^{iv}}{\partial t} = D_H \frac{\partial^2 c^{vi}}{\partial x^2} - K^{'} c^{''} c^{vi} + K^{''} c^{'''} - m^{'} c^{iv} c^{vi} + m^{''} c^{v} \tag{3.6}$$

Where $c^{'}$ is the concentration of O_2 in the membrane, $c^{''}$, $c^{'''}$, c^{iV},c^{V} and c^{Vi} are respectively the concentration of O_2, HbO_2, CO_2, $HbCO_2$ and Hb; D_m and DH represents the diffusion coefficient remembrance and hemoglobin present in the cell interior respectively. D_o and D_c are the diffusion coefficient of O_2 and CO_2. HbO_2 at $HbCO_2$ is seen as being the same for all species[Ulanowicz and Frazier [195]].

3.2.1 BOUNDARY CONDITIONS

At x = 0, due to symmetry, the flow of the species will be zero, i.e.

$$\frac{\partial c^{i}}{\partial x} \qquad at \qquad x = 0, i, ...vi.$$

As the membrane is thin, we assume that the gas concentration at the walls (x = a) is the same at all times. In addition, Hb, HbO_2, and $HbCO_2$ cannot permeate the wall, hence there will be no movement of these species across the capillary wall.

$$\begin{cases} c^{'} = c^{''} = c^{iv} = 0 & \text{at} & t = 0 & \\ c^{'''} = c^{v} = c^{vi} = c^{'''} & \text{at} & t = 0 & \text{in the cell interior} \\ c^{'} = c_o & \text{at} & t = 0 & \text{at} \quad X = a + b \\ \frac{\partial c^{''}}{\partial x} = \frac{\partial c^{iv}}{\partial x} = 0 \qquad \text{at} \quad X = 0 \qquad \text{at all time} & & & \end{cases} \tag{3.7}$$

$$\begin{cases} \frac{\partial c^{'''}}{\partial x} = \frac{\partial c^{v}}{\partial x} = \frac{\partial c^{vi}}{\partial x} = 0 \qquad \text{at} \qquad X = 0 \\ c^{'} = \alpha^{'} c^{''} \qquad at \qquad X = a \qquad \text{at all time} \\ c^{'} = \alpha^{''} c^{iv} \qquad \text{at} \qquad X = a \\ D_o = \frac{\partial c^{''}}{\partial x} = \alpha^{'} D_m \frac{\partial c^{'}}{\partial x} \qquad \text{at} \qquad X = a \\ D_c = \frac{\partial c^{iv}}{\partial x} = \alpha^{''} D_m \frac{\partial c^{'}}{\partial x} \qquad \text{at} \qquad X = a \end{cases} \tag{3.8}$$

Now we define the following non-dimensionless variables.

$$\begin{cases} \overline{C_1} = \frac{c^{'}}{c_o}, \qquad \overline{C_2} = \frac{c^{''}}{c_o}, \qquad \overline{C_4} = \frac{c^{iv}}{c_o} \\ \overline{C_3} = \frac{c^{'''}}{c_o^{'''}} \qquad \overline{C_5} = \frac{c^{v}}{c_o^{'''}} \qquad \overline{C_6} = \frac{c^{vi}}{c_o^{'''}} \\ \eta = \frac{x}{a} \qquad D_1 = \frac{D_m}{D_o} \qquad D_2 = \frac{D_H}{D_o} \\ D_3 = \frac{D_c}{D_o} \qquad \tau = \frac{tD_o}{a^2} \\ \omega_1^2 = \frac{K^{'} c_o^{'''} a^2}{D_o} \qquad \omega_2^2 = \frac{K^{''} c_o^{'''} a^2}{c_o D_o} \\ \omega_3^2 = \frac{m^{'} c_o^{'''} a^2}{D_o} \qquad \omega_4^2 = \frac{m^{''} c_o^{'''} a^2}{c_o D_o} \end{cases} \tag{3.9}$$

Here 2a is the effective thickness of the RBC and b is the thickness of the membrane. Using the above nondimensional variables the governing equations (3.3 - 3.9) become membrane.

$$\frac{\partial \overline{C_1}}{\partial \tau} = D_1 \frac{\partial^2 \overline{C_1}}{\partial \eta^2} \tag{3.10}$$

Cell interior

$$\frac{\partial \overline{C_2}}{\partial \tau} = \frac{\partial^2 \overline{C_2}}{\partial \eta^2} - \omega_1^2 \overline{C_2 C_6} + \omega_2^2 \overline{C_3} \tag{3.11}$$

$$\frac{\partial \overline{C_3}}{\partial \tau} = D_2 \frac{\partial^2 \overline{C_3}}{\partial \eta^2} \pm \omega_1^2 \overline{C_2 C_6} \mp \omega_2^2 \overline{C_3} \tag{3.12}$$

$$\frac{\partial \overline{C_4}}{\partial \tau} = D_3 \frac{\partial^2 \overline{C_4}}{\partial \eta^2} - \omega_3^2 \overline{C_4 C_6} + \omega_4^2 \overline{C_5} \tag{3.13}$$

$$\frac{\partial \overline{C_5}}{\partial \tau} = D_2 \frac{\partial^2 \overline{C_5}}{\partial \eta^2} \pm \omega_3^2 \overline{C_4 C_6} \mp \omega_4^2 \overline{C_5} \tag{3.14}$$

$$\frac{\partial \overline{C_6}}{\partial \tau} = D_2 \frac{\partial^2 \overline{C_6}}{\partial \eta^2} - \omega_1^2 \overline{C_2 C_6} + \omega_2^2 \overline{C_3} - \omega_3^2 \overline{C_4 C_6} + \omega_4^2 \overline{C_5} \tag{3.15}$$

And the boundary conditions transform to

$$\begin{cases} \overline{C_1} = \overline{C_2} = \overline{C_4} = 0 \qquad at \qquad \tau = 0 \\ \overline{C_3} = \overline{C_5} = \overline{C_6} = 1 \qquad at \qquad \tau = 0 \end{cases} \tag{3.16}$$

In the cell interior

$$\begin{cases} \overline{C_1} = 1 \qquad at \qquad \tau = 0 \qquad at \qquad X = 1 + \overline{b} \\ \frac{\partial \overline{C_2}}{\partial \eta} = \frac{\partial \overline{C_4}}{\partial \eta} = 0 \qquad \eta = 0 \qquad at \qquad all \qquad time \\ \qquad\qquad\qquad \frac{\partial \overline{C_3}}{\partial \eta} = \frac{\partial \overline{C_5}}{\partial \eta} = \frac{\partial \overline{C_6}}{\partial \eta} = 0 \qquad X = 1 \\ \overline{C_1} = \alpha' \overline{C_2} \qquad X = 1 \qquad at \qquad all \qquad time \\ \overline{C_1} = \alpha'' \overline{C_4} \qquad X = 1 \qquad at \qquad all \qquad time \\ \qquad\qquad\qquad \frac{\partial \overline{C_2}}{\partial \eta} = \alpha' D_1 \frac{\partial \overline{C_1}}{\partial \eta} \qquad at \qquad X = 1 \\ \qquad\qquad\qquad \frac{\partial \overline{C_4}}{\partial \eta} = \alpha'' \frac{D_1}{D_3} \frac{\partial \overline{C_1}}{\partial \eta} \qquad at \qquad X = 1 \end{cases} \tag{3.17}$$

3.3 NUMERICAL SOLUTION AND DISCUSSION OF RESULTS

To solve the governing equations (3.11-3.16) and the boundary conditions (3.17), a numerical approach employing the finite difference method is utilized. The equations are discretized using a semi-implicit scheme. The following physical and physiological parameter values are utilized in conjunction with Table 3.1 and are used for obtaining the concentration of O_2, HbO_2, CO_2, and $HbCO_2$ in the region under study.

Table 3.1: Experimently determined initial rate of gas exchange of human red cell suspension at 37^o C.

Reaction	Experimental rate
$\mathrm{Hb} + \mathrm{Mo} \longrightarrow \mathrm{HbMo}$	2640
$\mathrm{Hb} + \mathrm{O_2} \longrightarrow \mathrm{HbO_2}$	970
$\mathrm{HbO_2} \longrightarrow \mathrm{Hb} + \mathrm{O_2}$	1800
$\mathrm{Hb} + \mathrm{CO} \longrightarrow \mathrm{HbCO}$	790
$\mathrm{HbO_2} + \mathrm{CO} \longrightarrow \mathrm{HbCO} + \mathrm{O_2}$	118
$\mathrm{Hb_4(CO)_4} \longrightarrow \mathrm{CO} + \mathrm{Hb_4(CO)_3}$	6.6

$D_H = 4.5 \times 10^{-8} cm^2/Sec$

$D_o = 7.6 \times 10^{-6} cm^2/Sec$

$D_c = 1.19 \times 10^{-6} cm^2/Sec$

$a = 0.8\mu m, b = 0.06\mu m$

$\alpha^{'} \cong \alpha^{''} \cong 1$

$K^{'} = 2.85 \times 10^9$

$K^{''} = 40$

$m^{'} = 10^7, m^{''} = 5 \times 10^8$

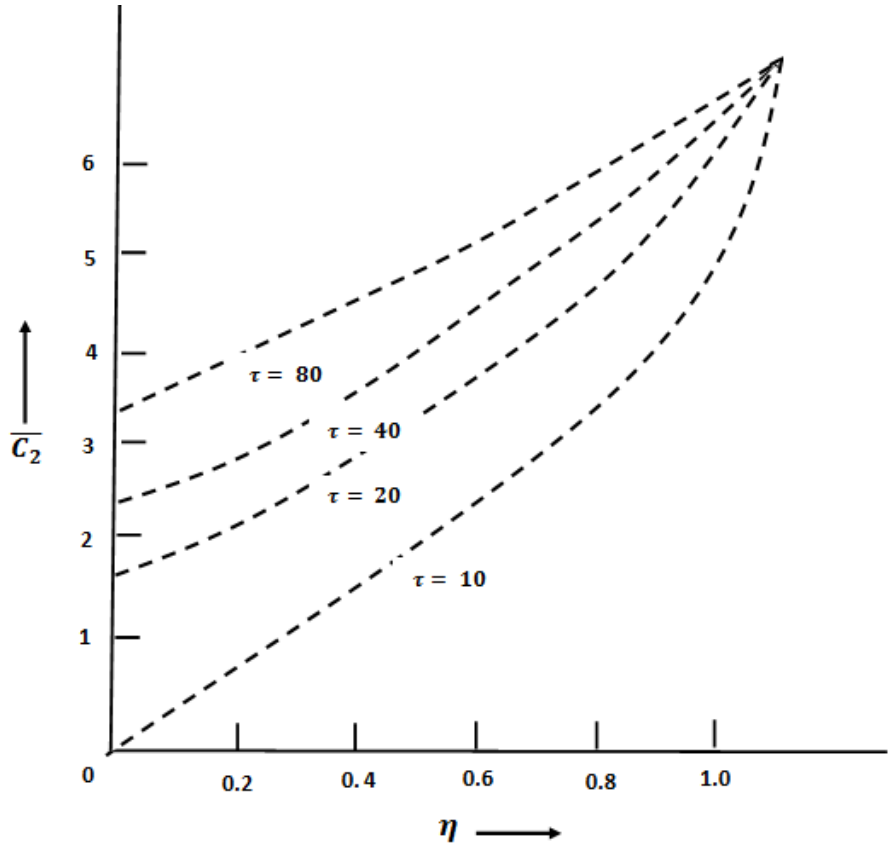

Figure 3.2: Radial variation of O_2 concentration for different value of time

According to radial distance and various values of time, Figure 3.2 shows how oxygen concentration varies. It is clear from the sap that the O_2 concentration increases as the radial distance increases. Also as time increases O_2 concentration increases.

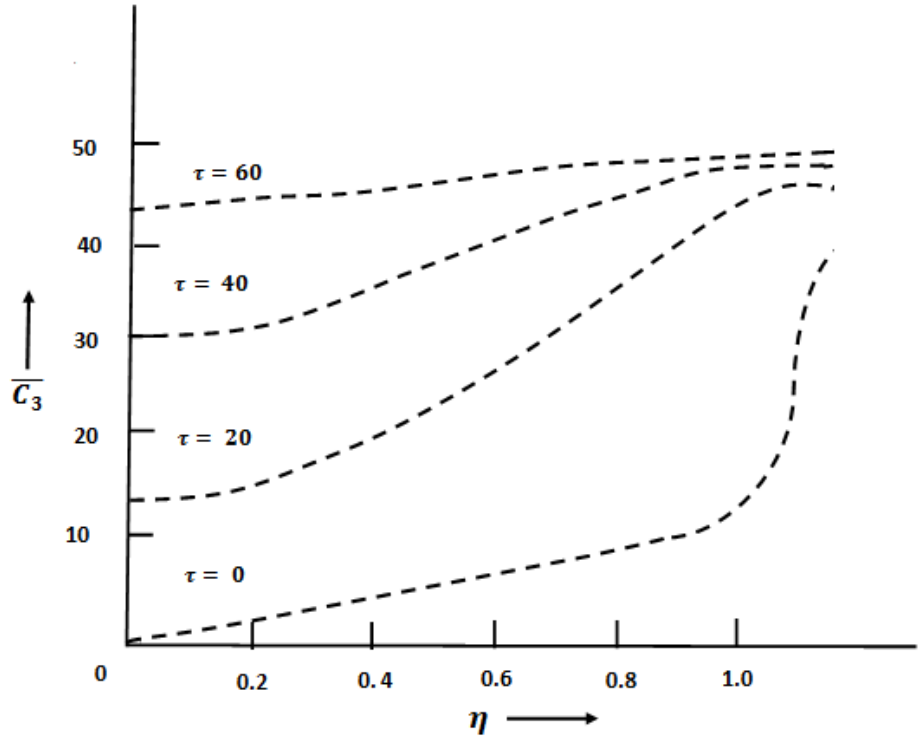

Figure 3.3: Radial variation of oxy-hemoglobin concentration for different values of time

Figure 3.3 describes the variation of oxy-hemoglobin concentration with radial distance for different values of time, we can conclude from the graph that as time increases the concentration of HbO_2 increases it also increases with radial distance. This shows that more O_2 combine with hemoglobin in the span of time.

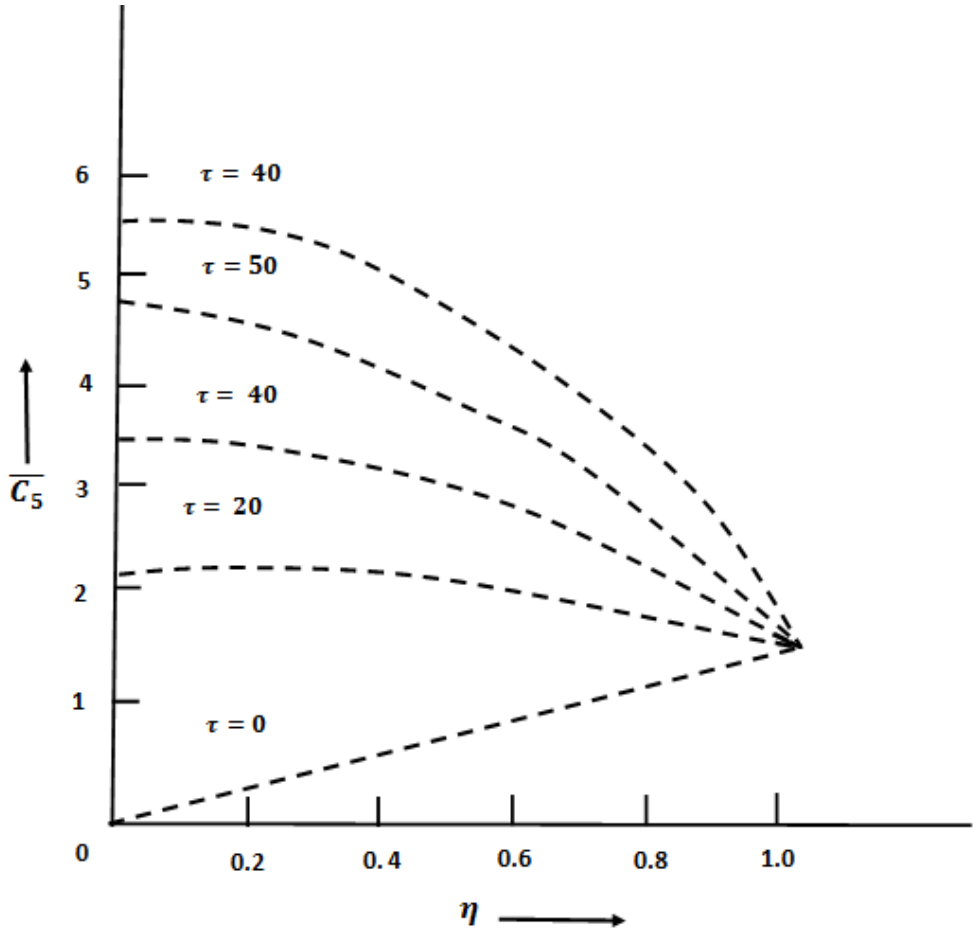

Figure 3.4: Radial variation of CO_2 concentration for different value of time

Figure 3.4 depicts the fluctuation in CO_2 concentration with radial distance for various time values. The graph clearly shows that while CO_2 concentration rises with time, it falls with axial distance.

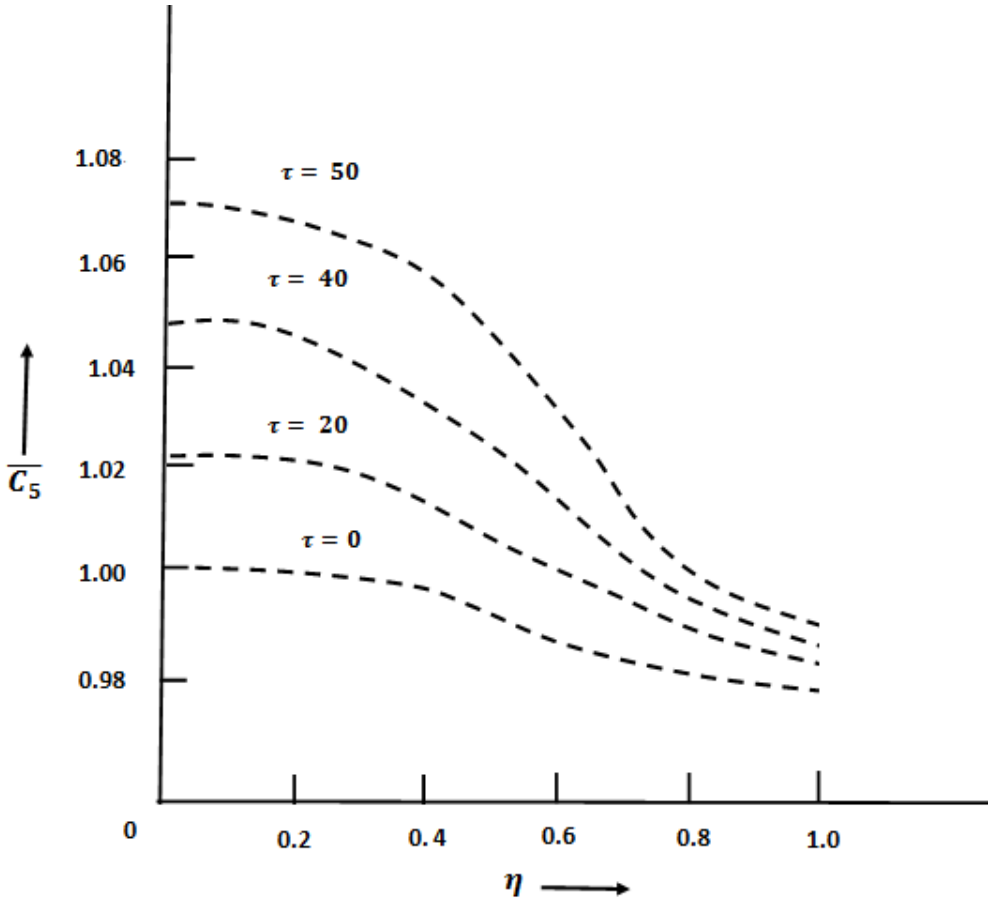

Figure 3.5: Radial variation of $HbCO_2$ concentration for different values of time

Figure 3.5 shows the fluctuation in $HbCO_2$ concentration with radial distance for various values of the time. The graph clearly shows that the concentration of $HbCO_2$ grows with time but decreases with radial distance. This confirms the results obtained from Figure 3.4 because more concentration of CO_2 gives more quantity of $HbCO_2$.

3.4 CONCLUSION

RBCs, are called erythrocytes, are the transcendent cell type in the blood. RBCs perform oxygenation of blood by transporting oxygen from the lungs to every cell of the body. At the same time, it removes carbon dioxide in the reverse direction. This method perfectly depicts the mathematical data and study of oxygen and carbon dioxide in red blood cells taking into consideration the main transport mechanism because of the presence of hemoglobin plus physiologically relevant parameters and various initial data. In the RBC, the transport of O_2 and CO_2 was studied numerically for the present report. According to this study, the finite difference method is adopted to come up with the model signifying the transport of species due to molecular diffusion and facilitated diffusion. Furthermore, it is shown that O_2 takes the longest, and CO_2 is the quickest to attain equilibration. Finally, radiation impacts, convection of blood flow, and concentration of O_2 and CO_2 are described. Lastly, outcomes of different flow conditions with some reasonable information are mentioned graphically.

3.5 FUTURE SCOPE

The future scope of studying the transport of oxygen and carbon dioxide in red blood cells holds great potential for advancements in understanding human physiology and disease. Researchers could explore new technologies for visualizing and analyzing the process at a molecular level, leading to insights on optimizing oxygen delivery in various health conditions. Additionally, advancements in targeted drug delivery systems could be developed based on the understanding of how red blood cells efficiently transport gases. The possibilities are endless and excited to see the innovative discoveries that lie ahead in this field.

Chapter 4

MODEL FOR DIFFUSION THROUGH STENOSIS

Keywords: Stenosis, Diffusion, Peripheral layer, Viscosity, Wall shearing, Disease, Velocity, Symmetric axially, Bessel functions.

4.1 INTRODUCTION

Stenosis is the term for the abnormal growth in the artery's lumen that occurs as a result of intravascular plaque formation, ligament or spur impingement, or both, or as a result of the development of these abnormal growths. As the disease progresses, it affects severely the coronary flow rate and perfusion. The pressure, shear, and other flow parameters, among others, are significant in an arterial system. These are linked to an increase in flow resistance and the presence of a low-pressure area that creates a suction effect, the potential for red and endothelial cell damage as a result of a high shear region, and the potential for the blood artery to transition from laminar to turbulent flow, resulting in high-intensity shear zones that are harmful to

blood flow and the arterial wall. In order to understand and avoid arterial disorders, it is crucial to have a thorough grasp of the flow characteristics in a channel with constriction.

Lee and Fung[36] obtained a numerical solution for flows in tubes with local dumbbell-shaped constriction. Harpreet Kaur[178] solved the problem of heat transfer by one-dimensional steady-state conditions. The solution for flow in a tube with a cosine curve-shaped constriction was discovered by Forrester and Young[35] using approximation techniques. Numerous studies that viewed the blood as a Newtonian or non-Newtonian fluid examined the features of blood flow in an artery with minor stenosis[Caro et al.[31], Shukla et al.[49], Forrester and Young[111], Rodbard[25], Fox and Hugh[112] May et al.[28]]. Recently, Awasthi and Kaur[196] explained finite difference method is adopted to come up with the model signifying the movement of organisms as a result of molecular and facilitated diffusion. Shukla et al.[50, 51] investigated the effect of peripheral larger affecting the blood flow via the artery with modest stenosis. In these investigations, the core region and peripheral layer fluid are represented by two Newtonian fluids of different viscosities, and both fluids are represented by Law fluids of different consistencies m_1 and m_2 completely independent of each other. However, experimental evidence by Bugliarello and Sevilla demonstrates that blood exhibits a blunted velocity profile and while passing through tubes of very small diameter, a cell-free plasma layer close to the tube wall. This layer's fluid is the medium that holds the cells in place rather than a distinct Newtonian or non-Newtonian fluid. Awasthi et al.[189] solved the problem of displacement components and stress components at the interface of two mediums. Recently, Tandon et al.[198, 199] investigated the blood flow through an artery with modest stenosis is affected by microstructural and peripheral layer viscosity. In these papers, Modelling the blood as a micro-polar fluid in the core encompassed

by a peripheral layer with the same viscosity as that of the suspending medium of the whole blood allowed researchers to study the properties of blood flow through an artery with modest stenosis. The effects of percent stenosis, micro-structure, and peripheral layer viscosity have been discussed. It may be observed that the work reported above introduces a constant width of the peripheral layer in almost every paper. The width depends on the size and shape of the stenosis under consideration to create a more accurate model. Numerous researchers have explored the steady flow of blood through a narrowed tube, describing blood as a Newtonian fluid[Deshpande et al.[40], McDonald[41], Shukla, et al.[49], Young[111]].

In microcirculation, where the peripheral layer thickness and viscosity effects predominate the flow characteristics, the consequences of stenosis are significantly more significant. In their investigations, assumptions of rigid wall symmetric constriction seem to be the reason because the changes induced by the stenosis predominate in comparison to the distensibility and the pulsatile character of the blood flow and the taperness of the walls [Young[148]]. As peripheral layer thickness and viscosity effects rule the flow characteristics in micro-circulation, the effect of stenosis is considerably more significant.

[Fung[3], Burns[210], and Bergel[12]] have attempted to identify the diffusion pathways of low-molecular-weight substances that are water-soluble, such as ions, sugars, and amino acids. When combined with the evidence from electron microscopy, it would appear that intercellular spaces are the main diffusion pathways for these molecules, and endothelial cells are relatively impermeable to these substances. Now till date, the emphasis has been laid down on fluid dynamical aspects and the only discussion of mass transfer was undertaken concerning the transfer between red cells and the surrounding plasma, Only peripheral comments have been made regarding the mass transfer from blood to the tissue Fleteher[94]. Buradi metal. [186] investi-

gate the locations where hydrodynamic diffusion of RBCs occurs and the effects of stenosis severity on shear-induced diffusion (SID) of RBCs, concentration distribution and wall shear stress (WSS). Munir et al. [187] focuses on the effect of catheter radius and stenosis height on the blood flow and solute dispersion behavior. The problem is modelled using the Herschel-Bulkley fluid to represent the blood rheology, with catheter and stenosis as the boundary conditions. Ramana et al. [188] studied the hemodynamics of nanofluid flow through the modelled stenosis-aneurysm models in the presence of the catheter.

As blood flows through capillaries, various substances are exchanged between plasma and the surrounding tissue. Some of these substances, such as glucose, package, and albumin, are naturally present in the body under normal physiological conditions, while others are artificially added to the blood or tissue as indicators in an experimental program. The determination of intra-vascular and extra-vascular concentrations of these substances is quite significant in most situations and pathological states [Crone and Lassen[211]]. Although it is believed that a zone of disturbance surrounds each capillary, the disturbances linked to many capillaries do overlap. The issue is caused by the intricate linkage of several micro-circulatory processes, such as fluid exchange in capillary tissue and fluid movement in the interstitial space. Since diabetes individuals' peripheral layer fluid viscosity is two to three times greater than that of healthy ones. These subjects are more prone to such diseases.

As a result, an effort has been made in this chapter to identify the concentration profiles and related physiological diffusion for both healthy and diseased systems connected to stenosis brought on by local lipid accumulation. The results of the analysis may prove to be more useful in the identification and location of such diseases. An iterative scheme based on the Picard-type iteration method has been developed which yields approximate results but this contributes to many complexi-

ties such as the possible effect of micro-structural and peripheral layer viscosity effect on the blood flow, and diffusion through a tube with mild stenosis in pathological states including tapering and inertial effects which are difficult to handle with other techniques. The results for wall shearing stress resistance to flow and concentration profiles have been obtained and discussed.

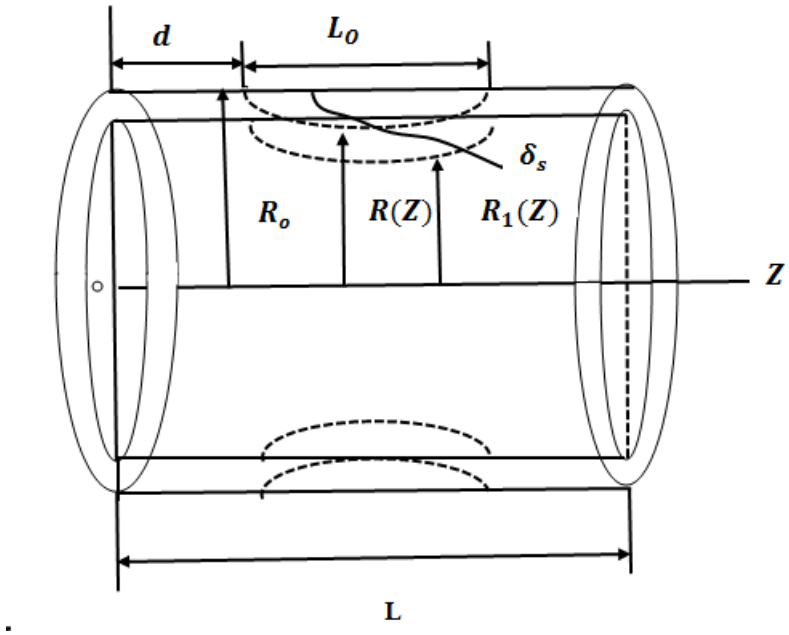

Figure 4.1: The geometry of the artery with stenosis

4.2 FORMULATION OF THE PROBLEM

The geometry of stenosis in a cylindrical polar coordinate system has been developed in Fig. 4.1 the laminar and constant flow of a fluid whose velocity changes along the radial direction [Caro et al.[31]] and it is also considered that stenosis formed in the artery wall in an axially symmetric way and that it is dependent on the axial distance Z and thickness of its growth δ_S. The radius of the wall in the affected

region is given below

$$\frac{R_2}{R_o} = 1 - \frac{\delta_S}{2R_o}\left[1 + cos\frac{2\pi}{L_o}\left(Z - d - \frac{L_o}{2}\right)\right], d \leq Z \leq L_o + d \tag{4.1}$$
$$= 1 \quad \text{elsewhere}$$

The radius of the artery with the stenosis, its length, and its position are shown by the letters R_o, L_o, and d, respectively. The maximal height of the stenosis is indicated by the symbol δ_S.

The governing equation of flow and diffusion for micro-polar fluids (suspension) in the core region $[0 \leq r \leq R_1(Z)]$ and peripheral layer $[R_1(Z) \leq r \leq R_o(Z)]$ may be written in the form.

$$(\mu + K)\frac{1}{r}\frac{\partial}{\partial r}\left(r\frac{\partial V_1}{\partial r}\right) + \frac{K}{r}\frac{\partial}{\partial r}(r\omega) = \frac{dp}{dz}, \qquad 0 \leq r \leq R_1(Z) \tag{4.2}$$

$$(\beta + \gamma)\frac{\partial}{\partial r}\left[\frac{1}{r}\frac{\partial}{\partial r}(r\omega)\right] - K\frac{\partial V_1}{\partial r} - 2K\omega = 0 \tag{4.3}$$

$$\frac{\mu}{r}\frac{\partial}{\partial r}\left(r\frac{\partial V_2}{\partial r}\right) = \frac{dp}{dz}, \qquad R_1(Z) \leq r \leq R_2(Z) \tag{4.4}$$

$$\frac{\partial C_1}{\partial t} + V_1\frac{\partial C_1}{\partial Z} = D_1\left(\frac{\partial^2 C_1}{\partial r^2} + \frac{1}{r}\frac{\partial C_1}{\partial r}\right) + m_1, \qquad 0 \leq r \leq R_1 \tag{4.5}$$

$$\frac{\partial C_2}{\partial t} + V_2\frac{\partial C_2}{\partial Z} = D_2\left(\frac{\partial^2 C_1}{\partial r^2} + \frac{1}{r}\frac{\partial C_2}{\partial r}\right) + m_2, \qquad R_1 \leq r \leq R_2 \tag{4.6}$$

Where the (V_1, ω) are the velocity and suspending particle rotation in the region $[0 \leq r \leq R_1]$ and V_2 is the velocity of the fluid in the region $[R_1 \leq r \leq R_2]$, K is the relative rotational viscosity, (μ, β, γ) are viscosities and the gradients of particle angular velocity, and $\frac{dp}{dZ}$ is constant pressure gradient and r is the radial coordinate and C_1, m_1, D_1, V_1 are the solute concentration, rate of production or

degeneration of cells, diffusion co-efficient of under-solved cells and velocity in the region $[0 \leq r \leq R_1]$ respectively and C_2, m_2, D_2, V_2 is the solute concentration, rate of production or degeneration of cells, diffusion co-efficient of under solved cells and velocity in the region $[R_1 \leq r \leq R_2]$.

4.2.1 BOUNDARY CONDITION

$$\begin{aligned} & & & & w = 0, \quad and \quad V_1 \quad is \quad finite \quad at \quad r \quad = 0 & & \\ V_1 \;=\; V_2, & \qquad \tau_1 = \tau_2, & \frac{\partial V_1}{\partial r} \;=\; - \quad (2+s)w & \qquad at\ r = R_1 & & (4.7) \\ & & & V_2 \;=\; 0, \qquad at \quad r \;=\; R_2 & & \end{aligned}$$

$$\begin{aligned} C_1 \;&=\; C_A, \qquad at \quad Z \;=\; 0 \\ C_2 \;&=\; C_A, \qquad at \quad Z \;=\; 0 \\ \frac{\partial C_1}{\partial r} \;&=\; 0 \quad at \quad r \;=\; 0 \qquad (4.8) \\ -D_1 \left(\frac{\partial C_1}{\partial r}\right) \;&=\; -\, D_2 \left(\frac{\partial C_2}{\partial r}\right) \quad at \quad r \;=\; R_1 \qquad (4.9) \\ C_1 \;&=\; C_2, \qquad at \quad r \;=\; R_1 \\ -D_2 \left(\frac{\partial C_2}{\partial r}\right) \;&=\; N \left(C_2 - C_0\right) \quad at \quad r \;=\; R_2 \end{aligned}$$

Where s is the boundary condition parameter ranging over the interval $0 \leq s \leq \infty$, τ_1 & τ_2 are the shear stress in the two regions described above. N is the retention parameter. C_0 is the same reference concentration of solute.

4.2.2 SOLUTIONS TO THE PROBLEM

The solutions of the equation (4.2) to (4.4) with boundary condition (4.7) are

$$V_1 = \frac{\frac{-dp}{dZ}}{2(2\mu+K)}\left[R_2^2 - r^2 + \frac{K}{2\mu}\left[R_2^2 - R_1^2\right]\right] + \left[\frac{R_1\bar{S}K\left(I_0(r) - I_0(R_1)\right)}{\lambda\left(\mu+K\right)I_1(R_1)}\right] \quad (4.10)$$

$$V_2 = \frac{\frac{-dp}{dZ}}{4\mu}\left[R_2^2 - r^2\right] \quad (4.11)$$

Where

$$\lambda^2 = \frac{K(2\mu+K)}{(\beta+\gamma)(\mu+K)}, \quad \bar{S} = \left[\frac{1+2\mu}{(S\mu+SK)}\right]^{-1} \quad (4.12)$$

Where I_0 and I_1 represent the modified Bessel functions of order V and can approximate the small modified Bessel functions as

$$I_0 \cong 1 + \frac{x^2}{4}$$

$$I_1 \cong \frac{x}{2} + \frac{x^3}{16}$$

The solutions of the equation (4.5) and (4.6) with boundary condition (4.8) are.

$$C_1(r) = C_1(R_1) + \frac{m_1}{4D_1}\left(R^2 - r^2\right) + \frac{\frac{dp}{dZ}}{2(2\mu+K)D_1}\left[\frac{R_2^2}{4}\left(R_1^2 - r^2\right) - \frac{1}{16}\left(R_1^4 - r^4\right) + \frac{K}{8\mu}\left(R_2^2 - R_1^2\right)\left(R_1^2 - r^2\right)\right] + \frac{\partial C_1}{\partial Z}\left[\frac{R_1\bar{S}K}{D_1\left(\mu+K\right)I_1(R_1)}\left[I_0(R_1) - I_0(r)\right]\right] - \frac{1}{D_1}\frac{\left(R_1^2 - r^2\right)}{4(\mu+K)}\frac{\partial C_1}{\partial Z} \quad (4.13)$$

Where

$$C_1(R_1) = C_2(R_2) + \frac{m_2}{D_2}\left[\frac{(R_2^2 - R_1^2)}{2} - R_1^2\left(log\frac{R_2}{R_1}\right) + \frac{dp}{dz}\frac{R_2^2\alpha}{8\mu D_2}\left[\frac{1}{2}\left[log\left(R_2 - \frac{1}{2}\right) - R_1^2\ log\left(R_1 - \frac{1}{2}\right) - \frac{1}{4}\left(R_2^2 - R_1^2\right) - R_1^2\left(log\ R_1 - \frac{1}{2}\right) - \frac{1}{4}\left(R_2^2 - R_1^2\right) - R_1^2\left(logR_1 - \frac{1}{2}\right)log\left(\frac{R_2}{R_1}\right)\right]\right]\right] - \frac{dp}{dz}\frac{\alpha}{16\mu D_2}\left[\frac{1}{4}\left[R_2^4\ log\left(R^2 - \frac{1}{4}\right) - R_1^4\left(log\ R_1 - \frac{1}{4}\right)\right] - \frac{1}{16}\left(R_2^2 - r^4\right) - R_1^4\left(log\left(R_1 - \frac{1}{4}\right)\right)X\ log\frac{R_2}{R_1}\right] + \frac{\left(\frac{dp}{dz}\right)\beta}{4\mu D_2}\left[\frac{R_2^2}{2}\left(\frac{1}{2}\left(R_2^2 - R_1^2\right) - R_1^2\left(log\frac{R_2}{R_1}\right) - \frac{1}{4}\left(R_2^4 - R_1^4\right) - R_1^4\left(log\frac{R_2}{R_1}\right)\right] - G\ log\ \frac{R_2}{R_1} \quad (4.14)$$

$$G = \frac{1}{2}\left(\frac{m_1}{D_1} - \frac{m_2}{D_2}\right)R_1\frac{dR_1}{dZ} + \frac{(m_2 - m_1)}{2D_2}\left[2R_1\frac{dR_1}{dZ}log\frac{R_1}{R_2} + R_1\frac{dR_1}{dZ} - \frac{R_1^2}{R_2}\frac{dR_2}{dZ}\right] + \frac{1}{2N}\left[m_2\frac{dR_2}{dZ} - 2(m_2 - m_1)\frac{R_1}{R_2}\frac{dR_1}{dZ} + (m_2 - m_1)\frac{R_1^2}{R_2^2}\frac{dR_2}{dZ}\right] + \frac{m_2R_2}{2D_2}\frac{dR_2}{dZ} \quad (4.15)$$

$$C_2(R_2) = -\frac{m_2}{2N}\frac{(R_2^2 - R_1^2)}{R_2} - \frac{1}{8\mu}\frac{dp}{dZ}\frac{R_2^2\alpha}{N}\left[R_2^2\left(logR_2 - \frac{1}{2}\right) - \frac{R_1^2}{R_2}\left(logR_1 - \frac{1}{2}\right)\right] + \frac{\frac{dp}{dz}}{16\mu N}\left[R_2^3\left(logR_2 - \frac{1}{4}\right) - \frac{R_1^4}{R_2}\left(logR_1 - \frac{1}{4}\right)\right] - \frac{dp}{dZ}\frac{\beta}{4\mu N}\left[\frac{R_2^2}{2}\frac{(R_2^2 - R_1^2)}{R_2} - \frac{1}{4}\frac{(R_2^2 - R_1^4)}{R_2}\right] + \frac{G}{R_2} + C_0 \quad (4.16)$$

$$\alpha = \frac{(m_2 - m_1)}{2D_2}\left(2R_1\frac{dR_1}{dZ}\right) \quad (4.17)$$

$$\beta = \frac{(m_2 - m_1)}{2D_2}\left[-2R_1\frac{dR_1}{dZ}logR_2 + \frac{R_1^2}{R_2}\frac{dR_2}{dZ}\right] + \frac{1}{2N}\left[m_2\frac{dR_2}{dZ} - 2(m_2 - m_1)\frac{R_1}{R_2}\frac{dR_1}{dZ} + (m_2 - m_1)\frac{R_1^2}{R_2^2}\frac{dR_2}{dZ}\right] + \frac{m_2R_2}{2D_2}\frac{dR_2}{dZ} + \frac{1}{D_2}\left[-\frac{m_1}{2}R_1^2 - \frac{\frac{dp}{dz}\left(\frac{\partial C_1}{\partial Z}\right)}{2(2\mu + K)}\left(\frac{R_2^2R_1^2}{2} - \frac{R_1^4}{4} + \frac{K}{4\mu}(R_2^2 - R_1^2)R_1^2\right) + \frac{1}{D}\frac{\partial C_1}{\partial Z}\frac{R_1^2\bar{S}K}{\mu + K} - \frac{1}{D_1}\frac{\partial C_1}{\partial Z}\frac{R_1^2}{2(\mu + K)}\right] \quad (4.18)$$

After using the above equations (4.14 to 4.18), we get

$$C_2(r) = C_2(R_2) + \frac{m_2}{2D_2}\left[\frac{(R_2^2 - r^2)}{2} - R_1^2\left(logR_2 - log\ r\right)\right] + \frac{dp}{dz}\frac{R_2^2\alpha}{8\mu D_2}\left[\frac{1}{2}\left(R_2^2\left(log\ R_2 - \frac{1}{2}\right) - r^2\left(log\ r - \frac{1}{2}\right)\right) - \frac{1}{4}\left(R_2^2 - r^2\right) - R_1^2\left(log\ R_1 - \frac{1}{2}\right)\{log\ R_2 - log\ r\}\right] - \frac{\frac{dp}{dz}\alpha}{16\mu D_2}\left[\frac{1}{4}\left(R_2^4\left(log\ R_2 - \frac{1}{4}\right) - r^4\left(log\ r - \frac{1}{4}\right)\right) - \frac{1}{16}\left(R_2^2 - r^4\right) - R_1^4\left(log\ R_1 - \frac{1}{4}\right)\{log\ R_2 - log\ r\}\right] + \frac{\left(\frac{dp}{dz}\right)\beta}{4\mu D_2}\left[\frac{R_2^2}{2}\left(\frac{1}{2}\left(R_2^2 - r^2\right) - R_1^2\left(log\ R_2 - log\ r\right)\right) - \frac{1}{4}\left(\frac{1}{4}\left(R_2^4 - r^4\right) - R_1^4\left(log\ R_2 - log\ r\right)\right)\right] - G\left(log\ R_2 - log\ r\right) \quad (4.19)$$

4.3 RESULTS AND DISCUSSION

This chapter examines a two-fluid blood model with a micro-polar fluid core and a Newtonian fluid layer at the periphery in the presence of minor stenosis. In terms of first- and zero-order modified Bessels functions, analytical formulas for resistance to flow, wall shear stress, and diffusion through stenosis have been found for the maximum height of the stenosis. It is discussed that the analysis of this article is a generalization of the [Shukla[50], Tandon et al.[208]], two-fluid model, and [Young[148, 111]], Newtonian fluid model. Since earlier studies have not considered diffusion through stenosis. Therefore, these cases are obtained as certain limiting cases of

the present study. Further, It has been noted that past models either assumed that blood was a Newtonian fluid or that it was a double-layered model of a fluid with differing viscosities in the core and the periphery. However experimental results [Gould[212] and Cokelet[20]] demonstrate the presence of a central non-Newtonian fluid (R.B.C. Suspension) and a central layer of a Newtonian fluid. Therefore, it is obvious that the preceding models are incorrect. Additionally, It has been found that in addition to hematocrit, the velocity profiles in the core also depend on the tube diameter and particle size ratio. Shukla et al.'s [50, 51] two-fluid models with a Casson or power-law fluid core do not account for the effects of particle size. There are certain restrictions on it. The current model has a greater agreement with the experimental findings and contains all of the effects mentioned above with diffusion. Tables 4.1 and 4.2 depict the effects of the boundary conditions parameter $\bar{S}$ on re-

Table 4.1: Variation of resistance to flow (RF) and wall shearing stress(τ_ω) with boundary condition parameter ($\bar{S}$) at 60% stenosis.

$\bar{S}$	0	0.237	0.727
$RF \times 10\ gm/cm^4\ sec$	3.6089	3.6110	3.6161
$\tau_\omega\ gm/cm\ sec^{-2}$	3.0096	3.0099	3.0150

Table 4.2: Variation of wall shearing stress τ_ω with hematocrit at 60% stenosis.

%H	40	20	10
$\tau_\omega\ gm/cm\ sec^{-2}$	6.9378	6.9357	6.9335

sistance to flow and wall shearing stress. Chaturani and Mahagan have determined the values of boundary condition parameter $\bar{S}$ by using the experimental values of the other parameters of the fluid. We have used the same values ($0 \leq \bar{S} \leq 1$). It may be noted that $\bar{S}$ decreases as concentration (i.e. hematocrit) decreases or particle size increases. The wall shearing stress increases with $\bar{S}$ and the resistance

to flow also increases. It has been noted that the boundary condition parameter is directly proportional to apparent viscosity and therefore, we conclude that the wall shearing stress as well as resistance to flow increases with the apparent viscosity of the blood. These results are also consistent with our results reported above and with the literature.

Figure 4.2 describes the variation of resistance to flow with percentage stenosis for different values of peripheral layer viscosity. It may be observed that the resistance to flow increases, slowly up to 40%. Stenosis and thereafter increase very rapidly. It also increases with the viscosity of the peripheral layer. Thus we can conclude that the disease affects more several in patients with higher peripheral layer viscosity.

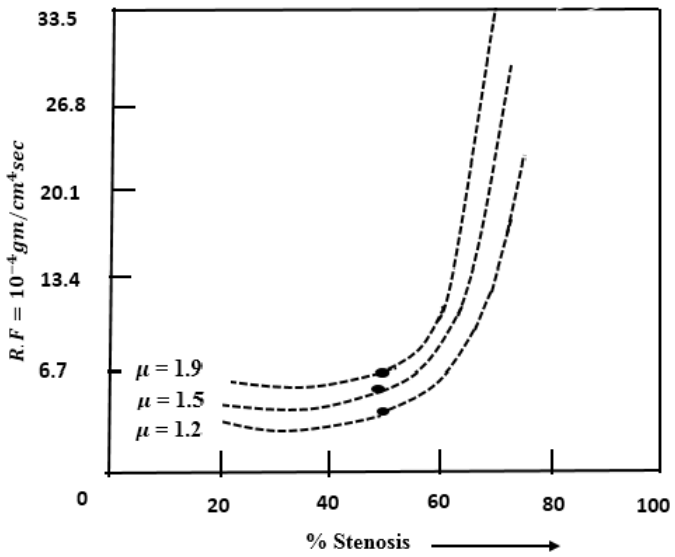

Figure 4.2: Variations of resistance to flow with stenosis percentage for different values of peripheral layer viscosity and fixed values of $s = 0.231, H = 40\%, \frac{L_0}{L} = 0.02$.

Figure 4.3 shows how the flow resistance might vary depending on the hematocrit levels and percentage of stenosis. As the hematocrit value rises, it is seen that the flow resistance also rises. This is the case since the blood's apparent viscosity consistently rises as hematocrit does.

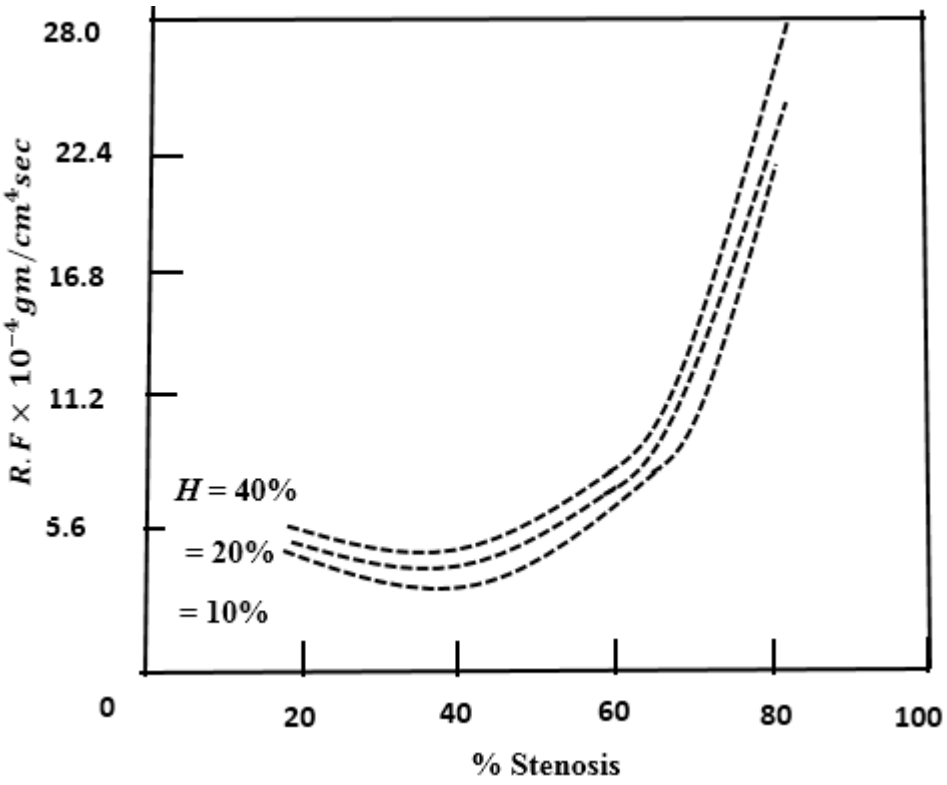

Figure 4.3: Variations of resistance to flow with stenosis percentage for different values of Hematocrit and fixed values of $s = 0.231, \mu = 1.5cP, \frac{L_0}{L} = 0.02$.

Figure 4.4 describes that as the length of the stenosis increases for a particular percentage of stenosis, the resistance to flow increases.

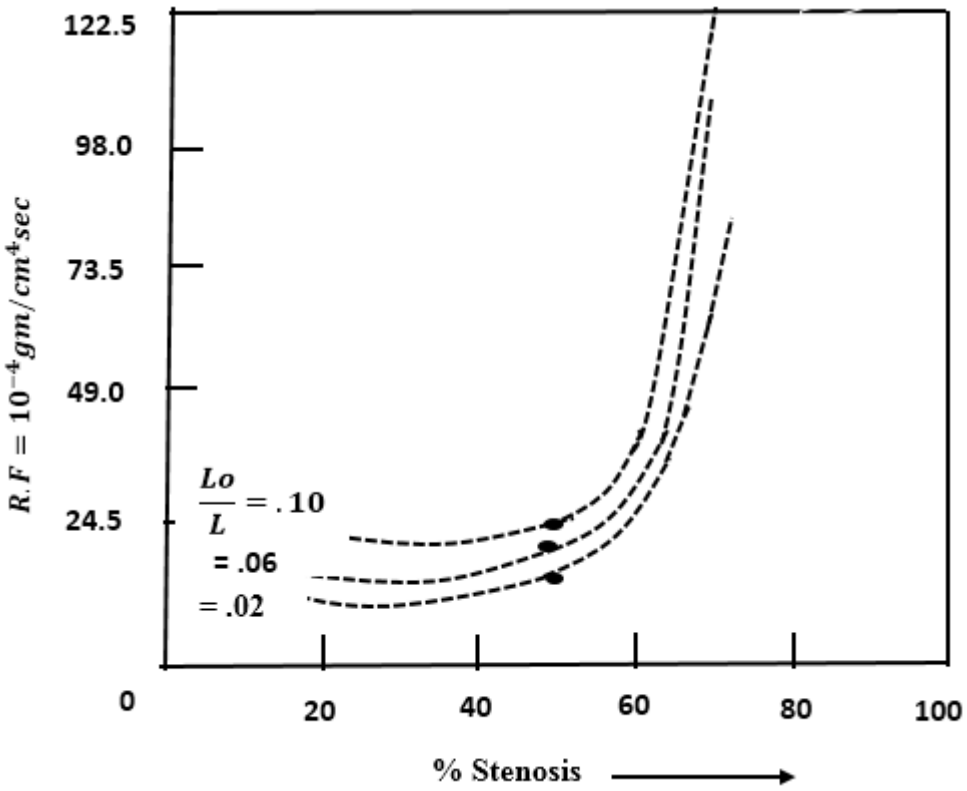

Figure 4.4: Variations of resistance to flow with stenosis percentage for different values of length of the stenosis and fixed values of $s = 0.727, H = 40\%, \mu = 1.5cP$.

Figure 4.5 shows that the length of the stenosis causes a reduction in the wall shearing stress, whereas the percentage of stenosis causes an increase. similar result has earlier been obtained by Chow and Soda[213]. These results further agree in respect of small constrictions when the effect of stenosis is negligible but the effects are more severe as the percentage of stenosis increases. The energy dissipation and the average pressure drop along the tube also increase rapidly as the percentage of stenosis.

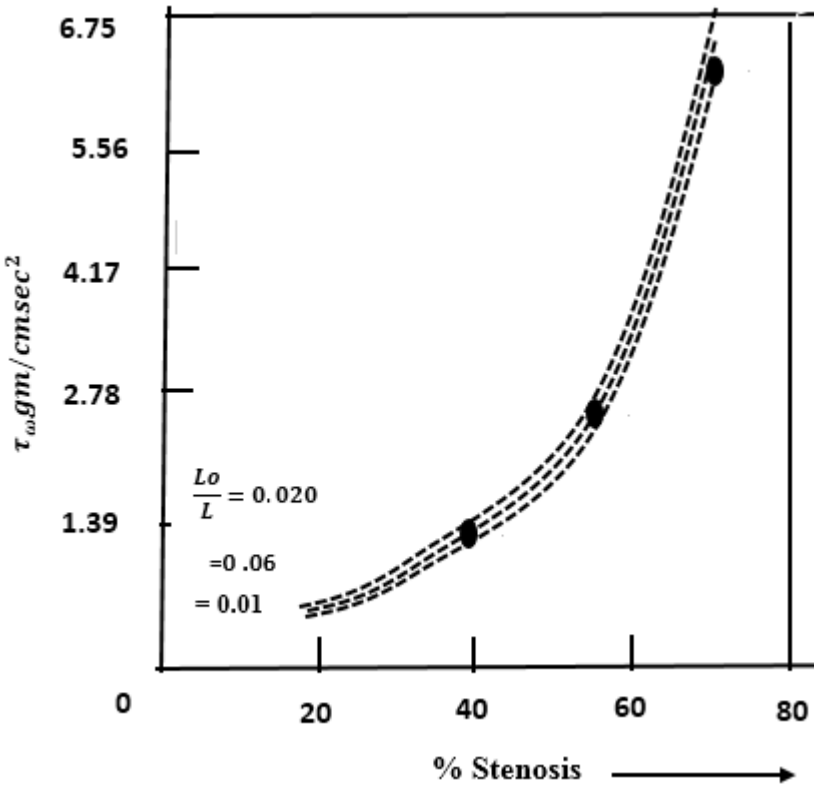

Figure 4.5: Variations of wall shearing stress with stenosis and fixed value of $s = 0.727, H = 40\%, \mu = 1.5cP$.

Figure 4.6 displays the diffusion of dissolved nutrients in the capillary as well as n peripheral layer region. We observe that the concentration in the peripheral layer is much less than that in the capillary region. The concentration in the capillary region is maximum near the central line and decreases towards the peripheral layer and the concentration in the peripheral layer also decreases towards the wall. We have also observed from this figure that as S increases concentration increases due to the axial migration of the cells because of the narrowing of the region of flow.

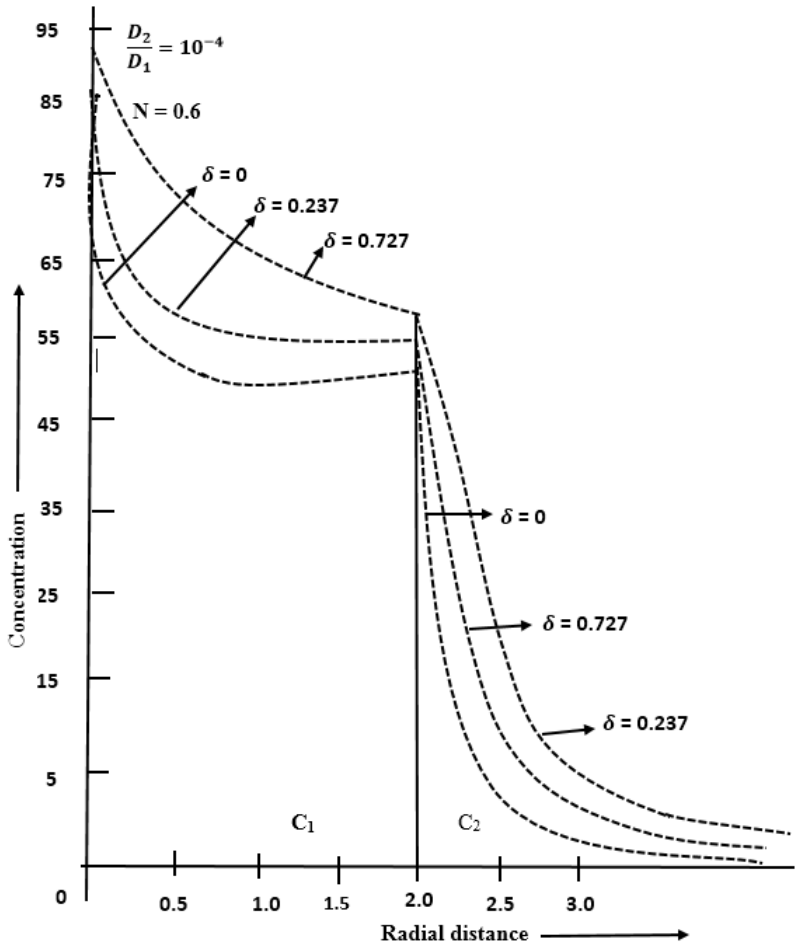

Figure 4.6: Concentration profile in the capillary for different values of the parameters s.

Figure 4.7 describes the diffusion of dissolved nutrients in normal and stenosis capillary the effect of increasing stenosis is to increase the concentration in the peripheral layer as well as in the capillary region. As the stenosis progresses the concentration near the surface increases more rapidly. From this we may conclude once the stenosis is formed, it further increases more rapidly due to the deposition of more cells.

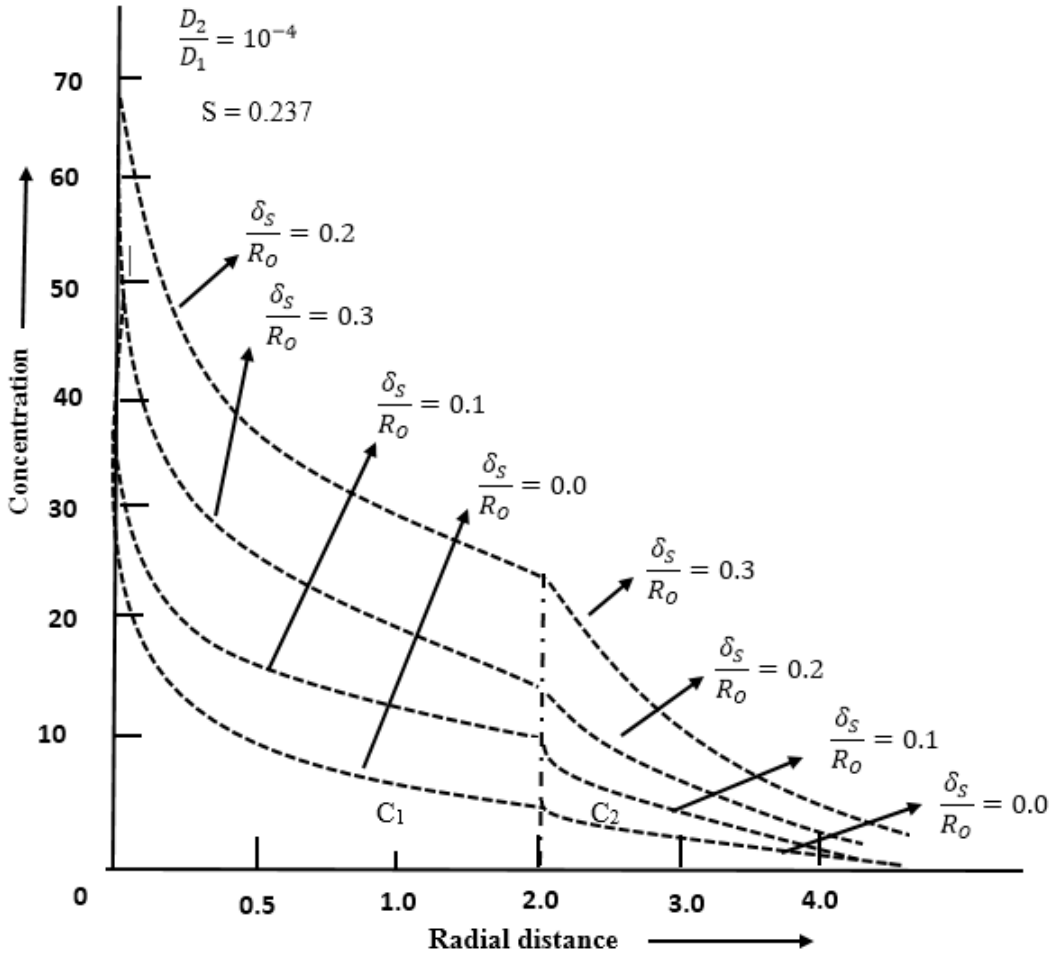

Figure 4.7: Concentration profiles in the capillary for different values of $\frac{\partial_s}{R_0}$.

Figure 4.8 demonstrates the impact of the retention parameter on concentration as well as on the area of the periphery layer. Rising N values signify an increase in the solute's retention in the capillary area. As the retention parameters increase from 1 to 2, more solute diffuses into the tissue region, reducing the concentration in the capillary region as well as in the peripheral layer region. The retention parameter $N = 1$ denotes total retention, meaning no solute diffuses into the tissue region.

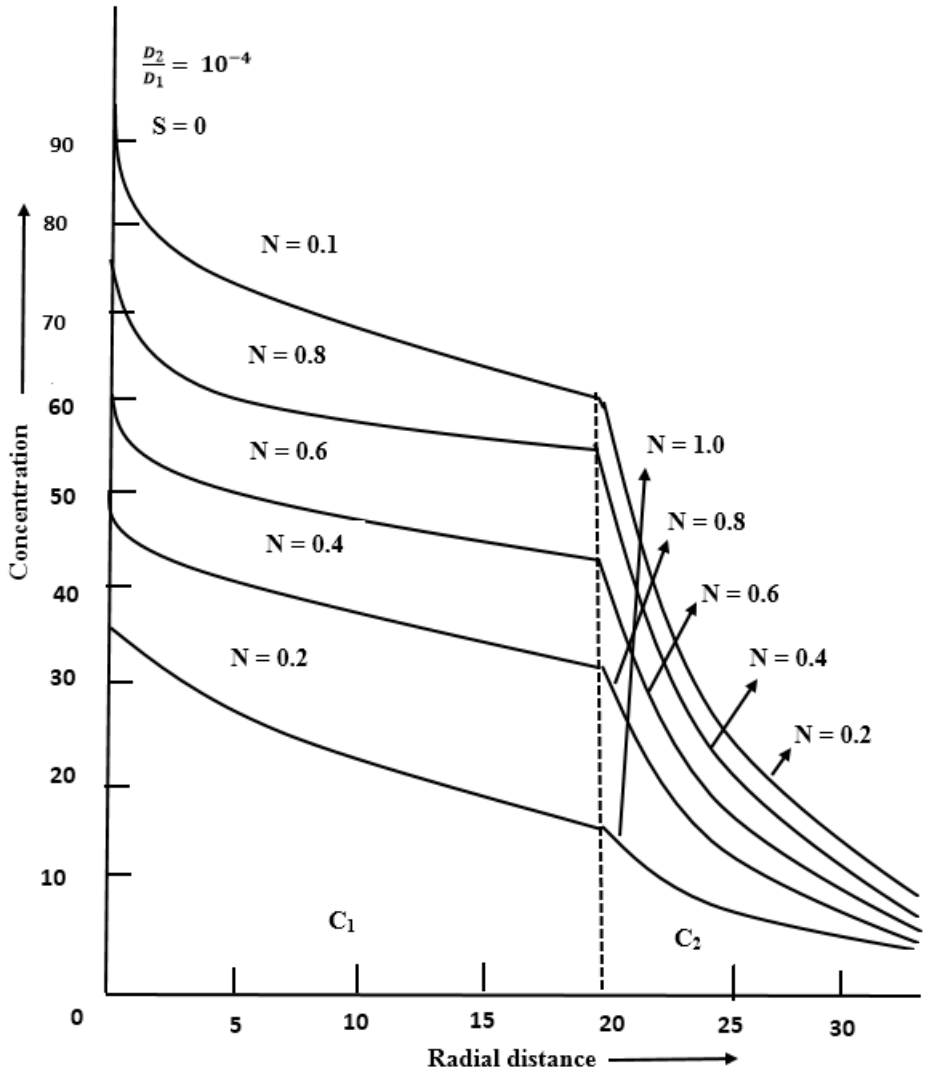

Figure 4.8: Concentration profiles for different values of retention parameter.

Figure 4.9 shows the fluctuation in concentration in the area of the peripheral and capillary layer for various ratios of diffusivities. The concentration in the capillary area rises as the ratio falls.

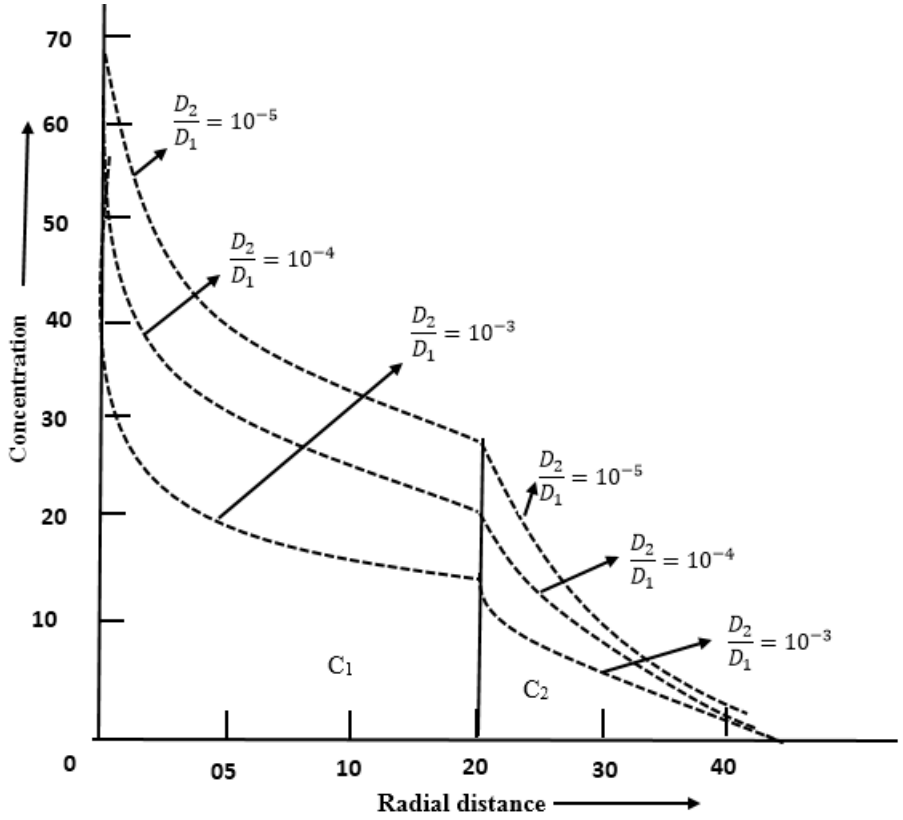

Figure 4.9: Concentration profiles in the capillary for different values of $\frac{D_2}{D_1}$.

4.4 CONCLUSION

In this chapter, concentrates on deriving analytical formulas for flow resistance and wall shear stress at the highest point of the stenosis and also investigates the diffusion process through the stenosis using modified Bessel functions of zero and first order. Additionally, explore the enhanced apparent velocity of blood. These results are consistent with our development reported above and the literature review. As a result, it will undoubtedly assist researchers who are working in this field. The

outcomes acquired prove helpful for doctorly uses such as enhancing effectiveness and sensitivity.

4.5 SIGNIFICANCE OF THIS CHAPTER

The most serious biological reaction is the formation of stenosis, which causes several complications in cardiovascular illnesses. The exciting findings from the studies listed above, as well as the practical applications highlighted, will help medical practitioners predict blood flow behavior in stenotic arteries. Medical practitioners may use the physical information gathered from individuals diagnosed with diabetes and a variety of other conditions to identify the medicine needed to treat them.

Chapter 5

MODEL ON THE TRANSPORT OF NUTRIENTS IN PULSATILE BLOOD THROUGH TIME-BASED STENOTIC TUBE

Keywords: Narrowing, Disease, Resistance, Arteries, Stenosis, Blood flow, Physiological, Velocity, Couple stress, Isotropic, Shear stress.

5.1 INTRODUCTION

To comprehend and model the transport processes in capillaries and the dynamic behavior of the circulatory system within the body, it is essential to have a comprehensive understanding of the physical, chemical, and flow characteristics of blood. It is understood that the narrowing of the tube offers greater resistance to flow and diffusion in the capillary tissue exchange phenomenon. This research may contribute

to the advancement of biomedical engineering, particularly in the development of computational models and experimental techniques to study nutritional transport in complex cardiovascular systems. By providing insights into the intricate interplay between fluid dynamics, nutrient transport, and stenosis, your study can aid in the refinement and validation of existing models and techniques. The study can contribute to a deeper understanding of how nutrition is transported in pulsatile blood flow through stenotic tubes. By investigating the dynamics and mechanisms involved, your research can shed light on how nutritional substances travel and distribute within the cardiovascular system under specific conditions. Cardiovascular disease, i.e. (atherosclerosis) mainly are responsible for nearly half of the deaths every year. It is a disease of the inner layers of the arteries. In its early stages, it is manifested by local deposition of lipids which may begin on the interface between blood and arterial wall or just within the intima. At a later stage, fibrous protein may be incorporated into the lipid deposits may protrude into the bloodstream, and provide a site for the deposition of cellular material from the blood. The deposit is termed as a thrombus and sometimes the stresses are to the extent of breaking it off. If the plugged vessel dominates the blood supply to the region it serves, it may lead to paralysis or sudden death.

An intravascular plexus develops on the inner surface of the artery walls, narrowing the artery and this disease is called stenosis. The coronary flow rate and perfusion are substantially impacted when the stenosis progresses. Due to the fact that myocardial oxygen supply is related to the associated blood flow rate, the schema becomes severely stenotic when there is an increase in oxygen demand. For example, during heavy physical work or exercise, the flow rate reduces and it leads to either a myocardial infarction or angina, extremity discomfort and loss of function are frequently caused by partial or complete obstruction of the arteries supplying the limbs. A cerebral accident might occur if one or more of the major arteries

supplying the brain become stenosed. Various mechanisms like abnormal cellular growth and coupling between the growth of the stenosis and blood flow etc. play very important roles in the continued development of the stenosis. The main cause of atherosclerosis is the arterial blood flow transport material to the arterial wall, which occurs at a specific site within the arterial system, for example at the bifurcation sites or in the neighborhood of bends in the arterial system. These are mainly associated with the development of turbulent eddies such types of eddies generate a large variety of local shearing stress and enhance the deposition of blood particulates. The flow of blood through a small tube 20-300 is of physiological and clinical importance[214]. Because of its complication and atypical way of behaving, it is difficult to analyze it. There are a number of theoretical models to describe the abnormal behavior of blood [215, 216, 217]. In a series of papers Chaturani and his associates have examined micro-polar fluid [217, 218] and couple stress fluid [219, 220] models as true representatives for the blood flows in small diameter tubes.
Recently, The effects of radiation on tissue metabolism, blood flow convection, oxygen and carbon dioxide concentrations, and body temperature have all been discussed [178, 196]. Ramasamy and Murugan [189] discuss a mathematical modeling of electro-hydrodynamic distribution in a pulsatile flow of Carreau fluid in a circular conduit taking chemical reaction and externally applied electric field. Ponalagusamy and Murugan [190] highlights the clinical aspect of the electrohydrodynamic solute dispersion's nature in normal as well as disease-affected blood. The present study might contribute to the design and fabrication of surgical tools and development of laboratory equipment in the fields of medical and bioengineering. Furthermore, the results obtained could play a key role in understanding the transportation of nutrients and dispersion process of drugs in the blood circulation. A substantial number of theoretical analyses of probable blood flow patterns at these places have been conducted [36, 35, 111, 39, 40, 49, 50, 221, 79, 224] have been undertaken

increment past. The main problem is to identify and locate the site right at the developing stage. This can be located by measuring stresses and pressure in the arterial system if there is a sudden change in stress and pressure at any place then it suggests some sort of abnormality in the system under consideration. [222, 209] have made an effort to explain a number of abnormalities related to blood flow via a tube with minor stenosis indicated by the artery's radius.

$$R_3(Z,t) = R_0 - \frac{\delta}{2}\left(1 - e^{\frac{t}{T}}\right)\left[1 + \cos\frac{2\pi}{L_0}\left(Z - d - \frac{L_0}{2}\right)\right], \quad d \le Z \le L_0 + d \tag{5.1}$$

$$= 1, \qquad elsewhere \tag{5.2}$$

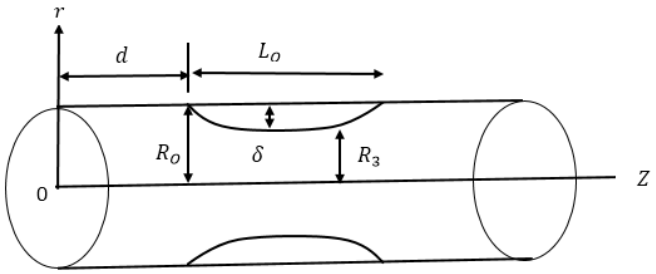

Figure 5.1: Idealized geometry of Stenotic tube

Under the assumption of mild stenosis, the developing stenosis does not introduce any radial component of velocity, it only accelerates the axial velocity component. Further if assumed that pulsatile blood flows are generalized from the steady flows are further generalized to pulsatile flows in time-dependent stenotic tubes [57] have shown to present a formidable barrier to the diffusion of particles as small as the extracellular ions, several attempts to identify the diffusion pathway for (red cell) and further water-soluble substance of low molecular weights such as ions, sugar, amino acid, etc. have been made by light microscopists. A major re-interpretation of the Ultra Structural basis of Capillary permeability was made by [215]. He believed

that the tight regions between the endothelial cells might represent the fusion of adjacent cell membranes but might still be permeable to water and low molecular weight water-soluble molecules. If the Membrane separates two solutions of the same solute which are initially at different concentrations solute moves from the more concentrated to the less concentrated solution and the solvents move in the opposite direction.

Stress components and Displacement components problems are solved with the help of an integral equation [199]. Diffusion through stenosis model is solved by Bessel functions of zero and first order[258]. Several theoretical and experimental studies of blood flow through tubes to date validate the pulsatile nature of the blood. The nature of blood chosen flow to be pulsatile by considering blood as a couple stresses fluid model for the real phenomenon of flow in the Circulatory system. This paper extended the energy integral method to find out the approximate solutions for the velocity profile. The energy integral method is most suitable for these studies since not introduce any initial velocity profile in this analytical method there is nothing like an initial or steady state in blood flow analysis introducing the velocity profile into the diffusion equation, the problem of the Nutritional transport has been undertaken in this paper the governing equation was solved using picards types method and find investigation the effects of different physiological ($\bar{\eta}$, ϵ, $\propto$, T) Parameters on the concentration profile in a stenotic tube.

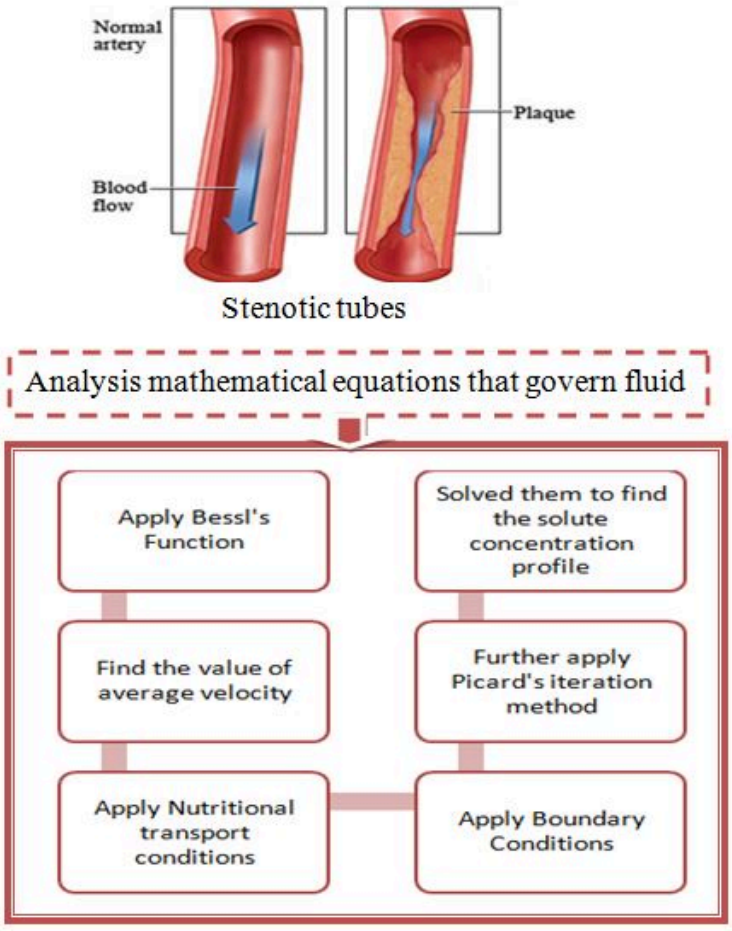

Figure 5.2: Schematic Diagram of the Chapter

5.2 MATHEMATICAL FORMULATION AND ANALYSIS

The equation governing the entirely formed incompressible non-Newtonian fluid in a tube is given by

$$\frac{\partial v}{\partial t} = -\frac{1}{\rho}\frac{\partial p}{\partial z} + \frac{1}{\rho}\frac{1}{r}\frac{d}{dr}(r, \tau_{(r,z)}) \tag{5.3}$$

In the steady case, the velocity profile for an isotropic incompressible couple stresses

fluid with couple stress vanishing near the boundary[226].

$$V = \frac{K}{4\mu}\left[R_3^2 - r^2 - H_1\left(1 - \frac{I_0(\propto_1 r)}{I_0(\propto_1 R_3)}\right)\right] \tag{5.4}$$

$$\propto_1 = \left[\frac{\mu}{\eta}\right]^{\frac{1}{2}} \tag{5.5}$$

$$H_1 = \frac{2(1-\bar{\eta})}{\propto_1^2}\left[\frac{(\propto_1 R_3)I_0(\propto_1 R_3)}{(\propto_1 R_3)I_0(\propto_1 R_3) - (1+\eta)I_1(\propto_1 R_3)}\right] \tag{5.6}$$

$$\bar{\eta} = \frac{\eta_1}{\eta}, \qquad K = -\frac{\partial p}{\partial z} \tag{5.7}$$

And v is the axial velocity, R_3 is the tube radius, μ is the viscosity coefficient, η, and $\bar{\eta}$ are couple stress parameters, r is radial coordinate, $I_0$and I, are zeroth and first-order modified Bessel functions.

The tube radius R_3, which depends on the axial distance, Z, and the passage of time, t, is not constant throughout the flow zone.

The average velocity $\langle \mathrm{V} \rangle$ is defined by

$$\langle V \rangle = \frac{1}{\pi R_3^2}\int_0^{R_3} 2\pi r v dr = \frac{K}{8\mu}X \tag{5.8}$$

$$X = \left[R_3^2 - 2H_1 + \frac{4H_1 I_1(\propto_1 R_3)}{\propto_1 R I_0(\propto_1 R_3)}\right] \tag{5.9}$$

Except when rigidity and incompressibility are idealized, the pressure gradient in a rigid pipe filled with an incompressible liquid can fluctuate over time but not concerning the position [225]. According to Ariman et al. [214], the pressure gradient is stated in the following way.

$$-\frac{\partial p}{\partial z} = P(t) = P_m\left(1 + \epsilon sin\omega_0 t)\right) \tag{5.10}$$

Where P_m is the constant mean pressure gradient and equal to $\frac{P_s}{P_m}$. Thus the average velocity can be written as

$$\langle V \rangle = \frac{P(t)}{8\mu} X \tag{5.11}$$

The velocity profile in terms of average velocity can be written as

$$V = 2\langle V \rangle \left[R_3^2 - r^2 - H_1 \left(1 - \frac{I_0(\propto_1 r)}{I_0(\propto_1 R_3)} \right) \right] \tag{5.12}$$

5.2.1 NUTRITIONAL TRANSPORT

The diffusion equations for the dissolved solute in the region are given by

$$\frac{\partial c}{\partial t} + V \frac{\partial c}{\partial z} = D \frac{1}{r} \frac{1}{\partial r} \left(r \frac{\partial c}{\partial r} \right) + m, \qquad 0 < r < R_3 \tag{5.13}$$

Where C is the solute concentration in the region D is the molecular diffusion coefficient. Take the unsteady axial velocity (v) in the region. m is the rate of production or degeneration of cells.

5.2.2 BOUNDARY CONDITIONS

The following conditions have been used for solving the above diffusion equation (5.13).

$$\frac{\partial c}{\partial r} = 0 \;\; at \;\; r = 0 \tag{5.14}$$

$$^{C}\Big|_{r=R_3} = \alpha_1 \quad {}^{\frac{\partial c}{\partial x}}\Big|_{r=R_3} \tag{5.15}$$

$$-\frac{DC}{\partial r} = \propto_2 c \qquad at \quad r = R_3 \tag{5.16}$$

5.2.3 SOLUTION OF THE PROBLEM

The integral energy equation can be obtained by multiplying equation (5.3) by rv and integrating between 0 to R_3 as

$$\frac{1}{2}\frac{d}{dt}\int_0^{R_3} V^2 r dr = -\frac{1}{\rho}\frac{\partial p}{\partial z}\int_0^{R_3} V r dr - \frac{1}{\rho}\int_0^{R_3} V\frac{d}{dr}(r\tau_{rz})dr \tag{5.17}$$

Substituting the velocities and shear stress gets the following expression for the axial pressure gradient.

$$\frac{-\partial p}{\partial z} = \frac{4\rho}{\langle V\rangle R^3}\frac{d}{dt}\left(\frac{\langle V\rangle^2 N_1}{X^2}\right) + \frac{8\langle V\rangle N_2}{X^2 R_3^2} \tag{5.18}$$

Where

$$N_1 = \Big[\frac{R_3^6}{6} - \frac{R_3^4}{2}(R_3^2 - H_1) + \frac{R_2^3}{2}(R_3^2 - H_1)^2 + \frac{\propto_1^2 H_1^2 R_3^2 I_1(\propto_1 R_3)}{I_0^2(\propto_1 R_3)} - \frac{2H_1 R_3}{\propto_1}\Big(H_1 + \frac{4}{\propto_1^2}\Big)\frac{I_1(\propto_1 R_3)}{I_0(\propto_1 R_3)} + \frac{4R_3^2 H_1}{\propto_1^2}\Big] \tag{5.19}$$

$$N_2 = 4R_3^2(4H_1 - R_3^2) - \frac{\eta(\eta+9)H_1^2 \propto_1^2}{2} - 2\eta H_1 \propto_1^2 R_3^2 + \Big[K_1 H_1 R_3 + H_1^2 R_3 \propto_1 (\propto_1^2 - \mu) + \frac{3H_1^2 \propto_1 \eta}{R_3} + \frac{H_1^2(\overline{\eta} - 3)\eta \propto_1}{2}\Big]\frac{I_1(\propto_1 R_3)}{I_0(\propto_1 R_3)} + \frac{K_2(R_3^2 H_1 - H_1^2)}{I_0(\propto_1 R_3)} + \frac{H_1^2 \propto_1^2 (\eta - \overline{\eta})}{2I_0^2(\propto_1 R_3)} + \left[\frac{H_1^2 \propto_1^4}{2} R_3^2(\mu - \eta \propto_1^2 R_3)\right]\frac{I_1^2(\propto_1 R_3)}{I_0(\propto_1 R_3)} \tag{5.20}$$

Where

$$K_1 = (\propto_1 + 1)(2\eta \propto_1^2 - 8\mu) + 2\eta\overline{\eta} \propto_1^2 (1 + 2 \propto_1) \tag{5.21}$$

$$K_2 = \propto_1 \eta K \left[\propto_1 (2 - \overline{\eta}) + \frac{(3 + \overline{\eta})}{2} \right] \tag{5.22}$$

Again write as

$$\frac{-\partial p}{\partial Z} = \frac{\rho N_1}{\mu R_3^2 X} P^1(t) + \frac{N_2 P(t)}{\mu R_3^2 X} \tag{5.23}$$

Hence velocity profile for unsteady pulsatile blood flow is given by

$$V = \frac{1}{4\mu^2 X} \left[\rho N_1 P^1(t) + N_1 P(t) \right] \times \left[1 - \left(\frac{r}{R_3} \right)^2 - \frac{H_1}{R_3^2} \left\{ \frac{1 - I_0(\propto_1 r)}{I_0(\propto_1 R_3)} \right\} \right] \tag{5.24}$$

The rate at which the volume flows can be described as

$$\propto = \int_0^{R_3} 2\pi r dr = \frac{\pi}{8\mu^2} \left[\rho N_1 P^1(t) + N_2 P(t) \right] \tag{5.25}$$

The wall-shearing stress is given by

$$\tau_\omega = \frac{-R_3}{2} \frac{\partial P}{\partial Z} = \frac{P_m}{2\mu R X} \left[\rho N_1 \omega_0 \propto cos\omega_0 t + N_2 (1 + \propto sin\omega_0 t) \right] \tag{5.26}$$

Using velocity profile for unsteady pulsatile blood flow from equation (5.24). The diffusion equation (5.13) with the boundary condition (5.15) has been solved by Picard's type iteration method to obtain the concentration profile as given below.

$$C(r) = C(R_3) - \frac{G(R_3 - r^2)}{4} - \frac{Q^1}{18}(R_3^3 - r^3) + \frac{Q^1(R_3^5 - r^5)}{100 R_3^2} - \frac{H_1 Q^1}{\propto_1 I_0(\propto_1 R_3)} \left[\frac{1}{\propto_1} \left\{ R_3^3 I_3(\propto_1 R_3) - r^3 I_3(\propto_1 r) \right\} - \frac{1}{\propto_1^2} \left\{ I_2(\propto_1 R_3) - I_2(\propto_1 r) \right\} - \frac{4}{\propto_1^2} \left\{ I_1(\propto_1 R_3) - I_1(\propto_1 r) \right\} \right] - \frac{m}{4}(R_3^2 - r^2) \tag{5.27}$$

Where

$$C(R_3) = \propto_3 (R_3^2 - 2R_3)(G+m) - \propto_3 Q^1(R_3^3 - 3R_3^2) + \frac{\propto_3 Q^1}{1000}(R_3^3 - 5R_3^2) - \frac{H_1 Q^1 \propto_3}{\propto_1 I_0(\propto_1 R)}$$
$$\left[\frac{1}{\propto_1}\left\{R_3^3 I_3(\propto_1 R_3) - \propto_1 I_2(\propto_1 R_3)\right\} - \frac{1}{\propto_1^2}\left\{I_2(\propto_1 R_3) - \propto_1 I_1(\propto_1 R_3) - \right.\right.$$
$$\left.\left.\frac{P}{R_3} I_2(\propto_1 R_3)\right\} - \frac{4}{\propto_1^2}\left\{I_1(\propto_1 R_3) - \propto_1 I_0(\propto_1 R_3) - \frac{P}{R_3} I_1(\propto_1 R_3)\right\}\right] \quad (5.28)$$

$$G = \left[\frac{-m}{8D^2}\frac{t}{T}\delta^2 e^{\frac{-t}{T}}\left(1 + cos\frac{2\pi}{L_0}\left(Z - d - \frac{L_0}{L}\right)\right)\left(e^{\frac{-t}{T}} - 1\right) + \frac{m\delta . t^{e^{\frac{-t}{T}}}}{4D^2 T}\left(1 + cos\frac{2\pi}{L_0}\right.\right.$$
$$\left.\left.\left(Z - d - \frac{L_0}{2}\left(R_0 + \propto\right)\right)\right)\right]\frac{r^2}{2}$$

$$Q^1 = \frac{1}{4D\mu^2}\left[\rho N_1 P'(t) + N_2 P(t)\right] \quad (5.29)$$

5.3 RESULTS AND DISCUSSIONS

In this chapter, examined the rhythmic patterns of blood flow through a tube with a gradually narrowing passage that changes over time.[Figure 5.1] and the effect of various physiological parameters (ϵ, $\propto$, $\omega\tau$, $\overline{\eta}$), on concentration profile in a stenotic tube with radial coordinate under the possible physiological conditions. The results are presented below in Figures 5.3 to 5.14. The parameter $\left(\frac{P_s}{P_m}\right)$ i.e. ϵ is directly proportional to the pulsation of blood. The effects of pulsations are shown in Figures 5.3, 5.7, and 5.9. The other parameter $\frac{\delta}{R_0}$ (i.e. the ratio of the unobstructed tube's radius to the greatest height of the stenosis) is directly proportional to the maximum height of the stenosis, Figure 5.11 to Figure 5.14 depicts the impact of various physiological factors on the concentration profile in a radially-coordinated

stenotic tube.

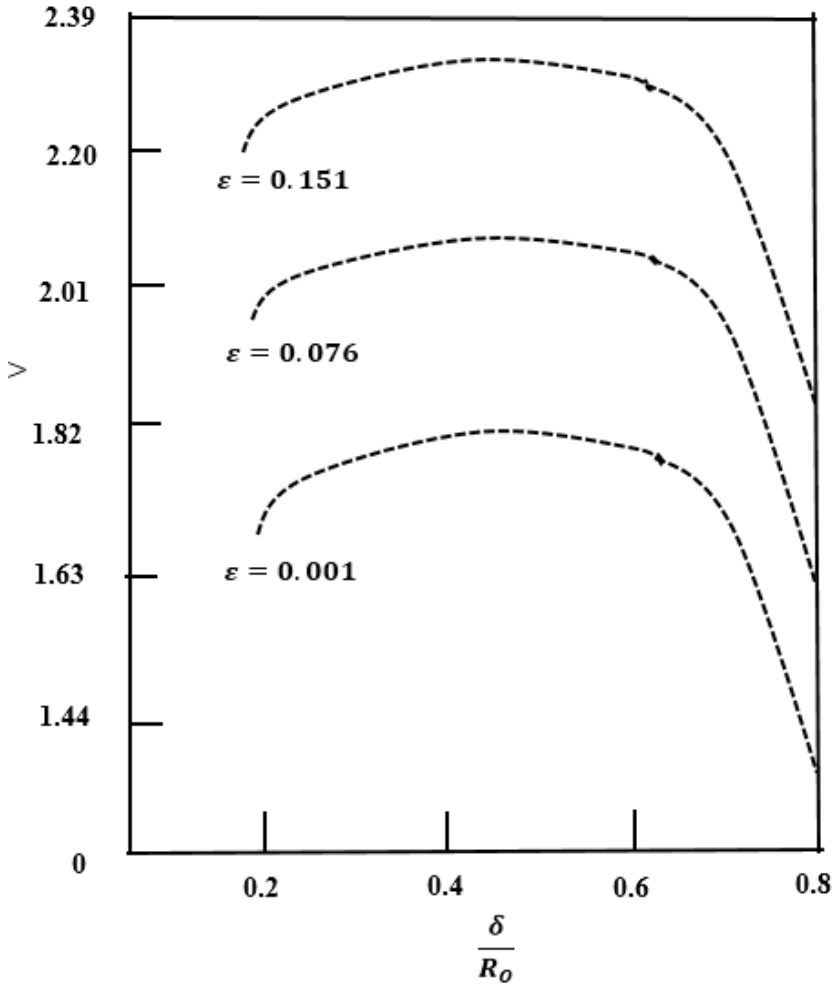

Figure 5.3: Variation of velocity with $\frac{\delta}{R_0}$ for different values of ϵ.

Figure 5.3 depicts the variations of velocity with $\frac{\delta}{R_0}$ different values of ϵ. These figures clearly show that at a fixed value of $\frac{\delta}{R_0}$, blood flow increases as the value increases. The velocity of blood starts decreasing when the stenosis increases beyond $\frac{\delta}{R_0} = 0.4$. An increasing value of ϵ means increases in the pulsation of blood. These pulsations may increase the velocity of blood for the fixed height of stenosis.

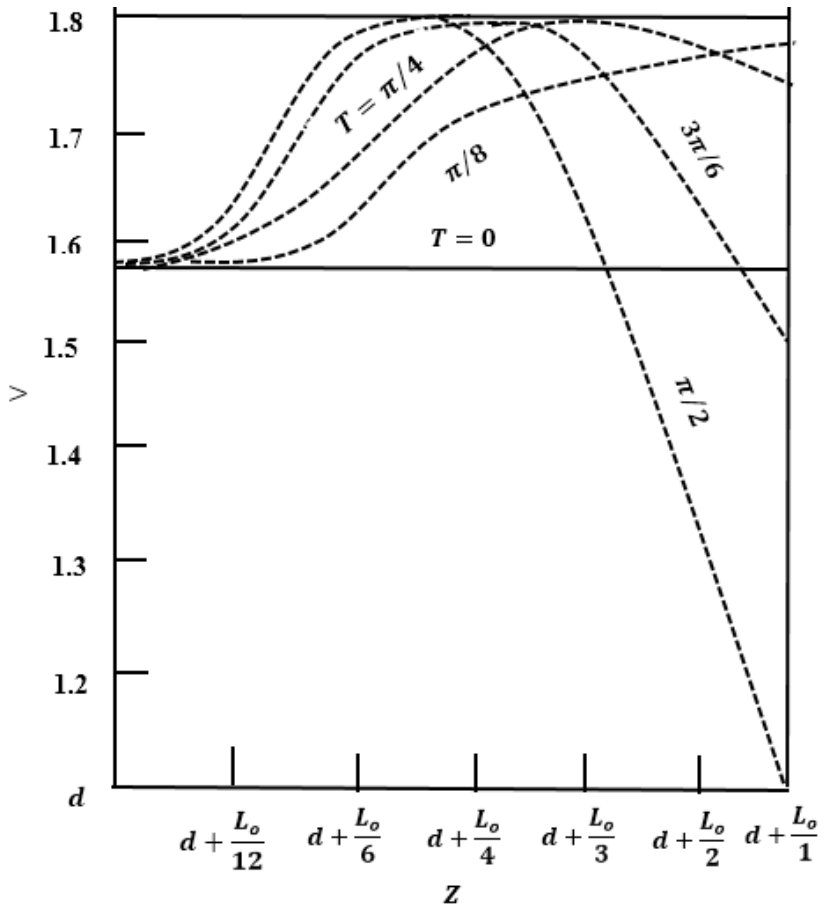

Figure 5.4: Variations of velocity with the axial position of the stenosis for different values of the time.

Figure 5.4 shows the velocity fluctuation for various time values with respect to the axial location of the stenosis. As time increases, the velocity initially increases and then decreases. The initial increase in velocity is due to the increasing growth of the stenosis which increases with time.

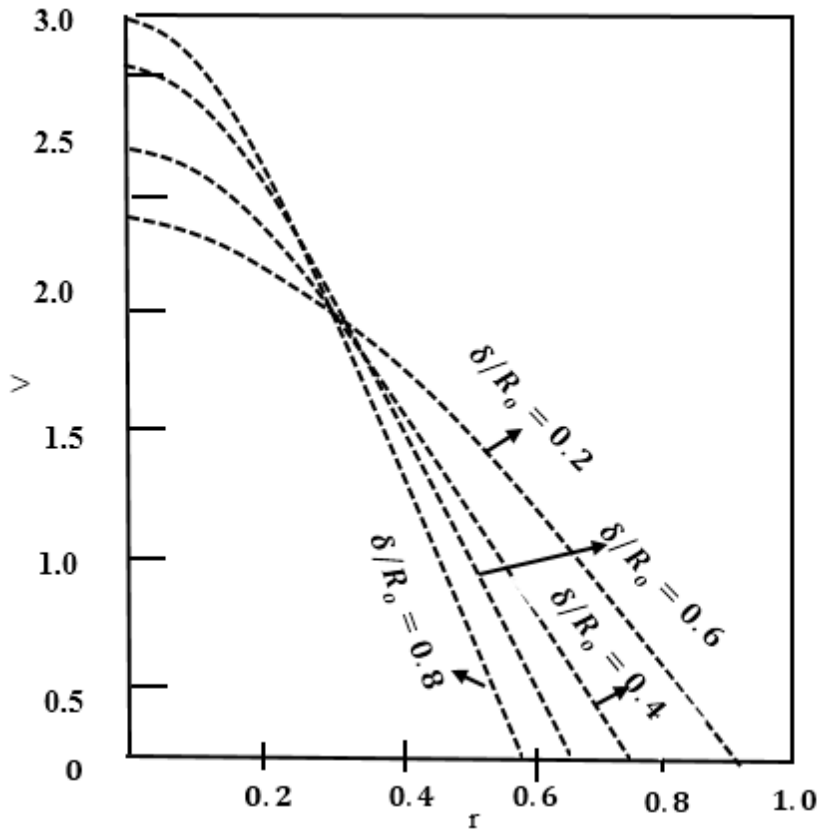

Figure 5.5: Variations of velocity with radial co-ordinate for different values of $\frac{\delta}{R_0}$.

Figure 5.5 shows the variation of velocity with a radial coordinate for different values of $\frac{\delta}{R_0}$. The velocity of blood decreases sharply for greater stenosis as compared to less stenosis.

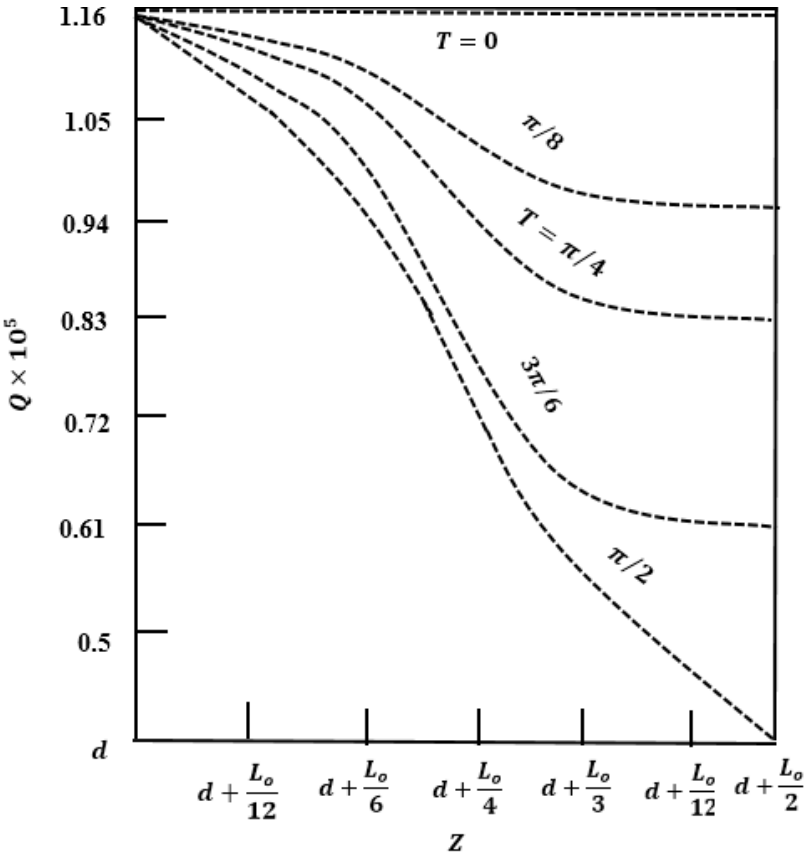

Figure 5.6: Variations of volume flow rate with the axial position of stenosis for different values of the time.

Figure 5.6 shows the axial position of the stenosis increases, and the volume flow rate decreases. This is due to the fact that a higher axial position of the stenosis will increase the resistance to flow, thus reducing the volume flow rate. Furthermore, the volume flow rate decreases with time for a fixed axial position of the stenosis. As time passes, the stenosis gets more severe and the resistance to flow increases, thus reducing the volume flow rate.

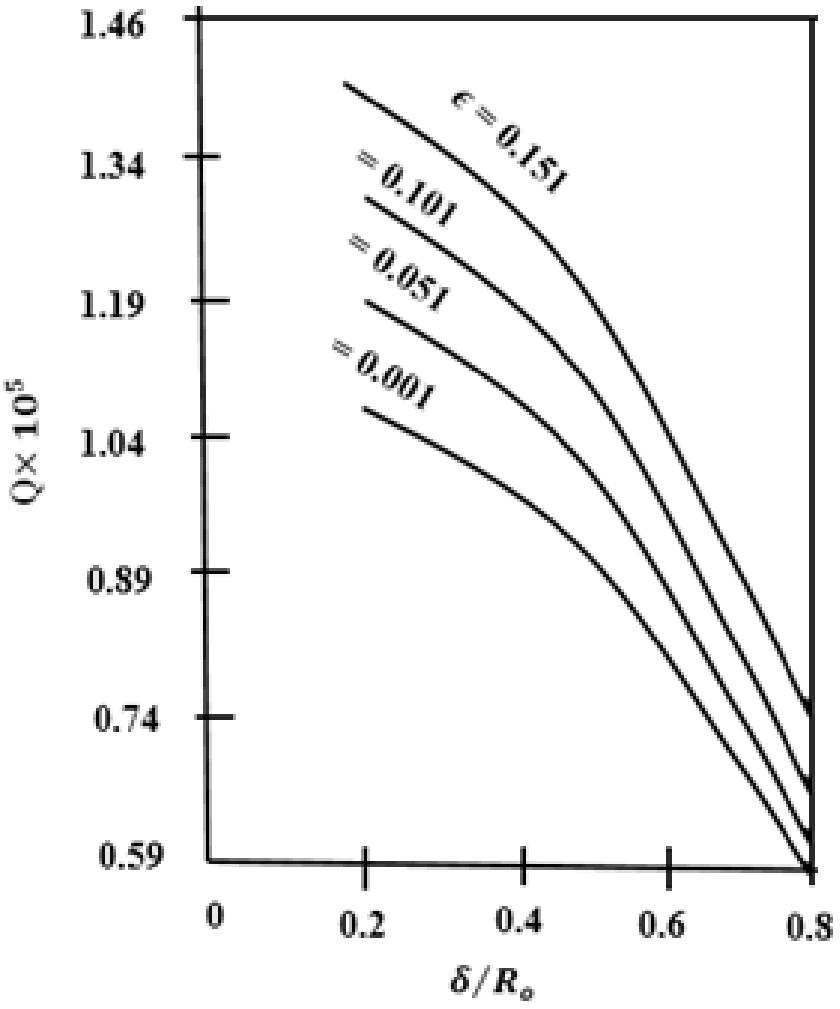

Figure 5.7: Variation of volume flow rate with $\frac{\delta}{R_0}$ for different values of ϵ.

Figure 5.7 illustrates as $\frac{\delta}{R_0}$ increases, the size of the throat area decreases, and the flow velocity increases, resulting in a decrease in the volume flow rate. On the other hand, as ϵ increases, the size of the throat area increases and the flow velocity decreases, resulting in an increase in the volume flow rate.

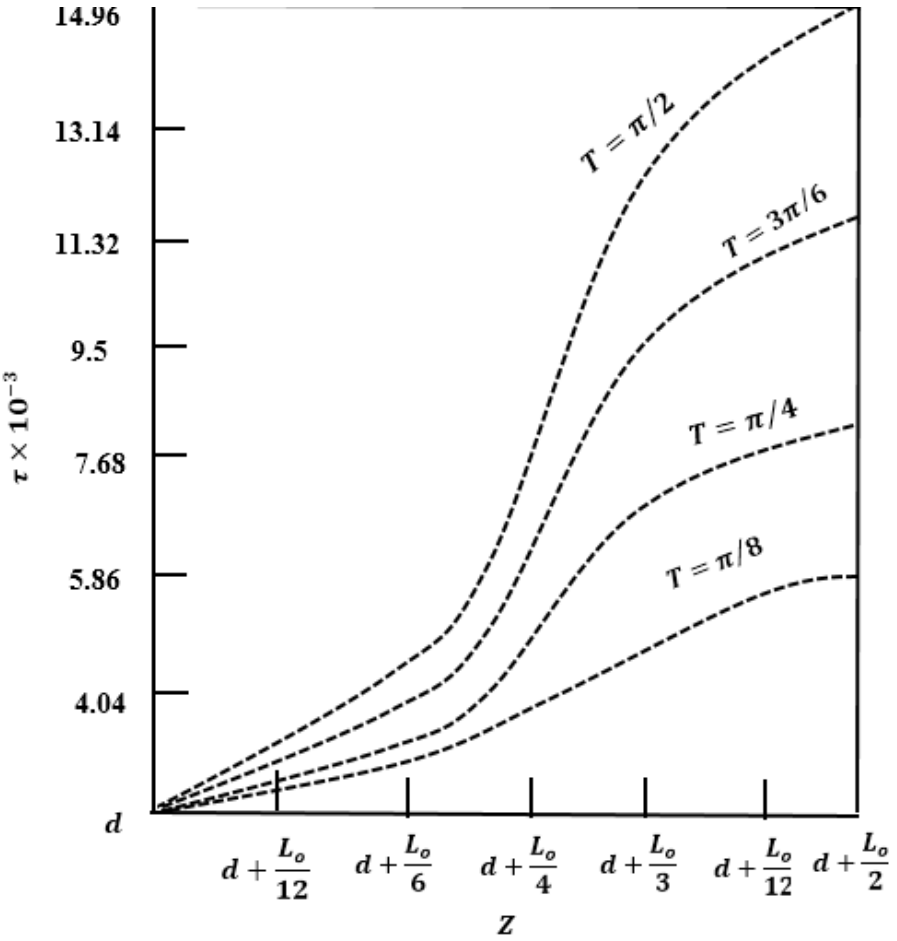

Figure 5.8: Variations of wall shearing stress with the axial position of stenosis for different values of the time.

For various values of time, Figure 5.8 shows the change of wall shearing stress with the axial position of stenosis. Z and time both contribute to an increase in wall shearing stress. Up to the height of the stenosis, the radius of the tube decreases along its axis in an obstruction. This decrease in radius may increase the wall shearing stress. The same behavior can also be observed beyond the maximum height of the stenosis which is not shown in the figure generally growth of the stenosis increases with time. Therefore, wall shearing stress may increase with time.

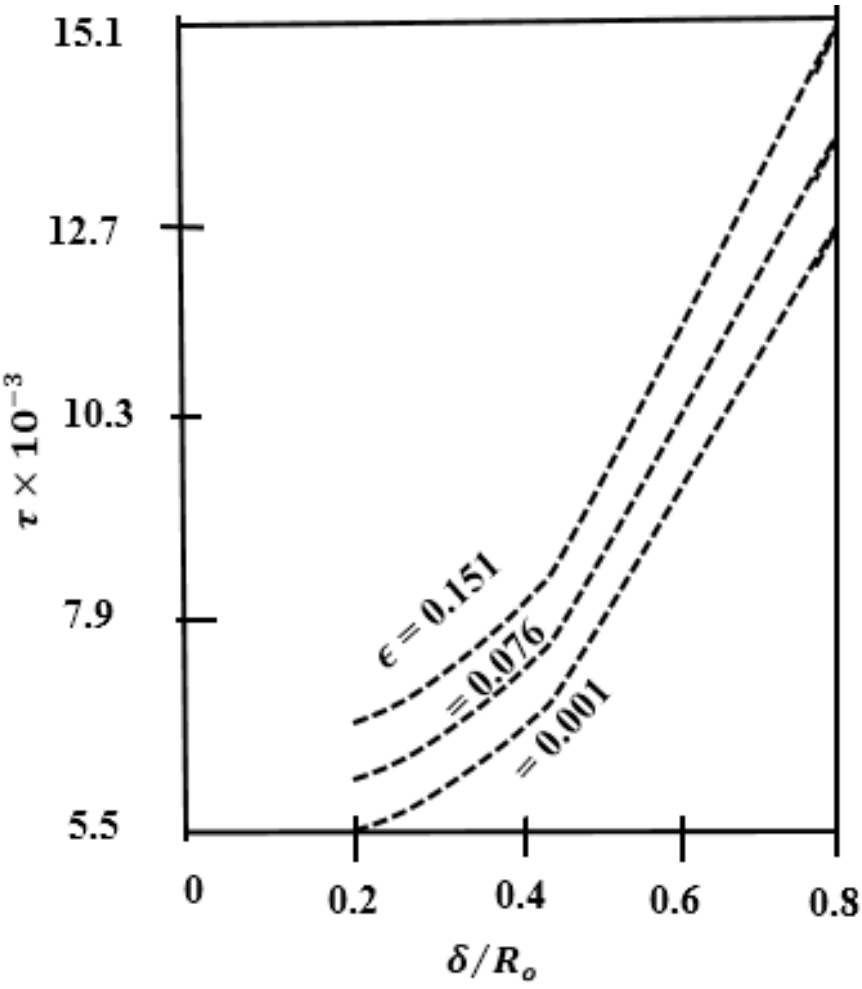

Figure 5.9: Variation of wall shearing stress with $\frac{\delta}{R_0}$ for different values of ϵ

Figure 5.9 describes wall shearing stress changes with $\frac{\delta}{R_0}$ for various values of pulsation parameter. The wall shearing stress increases with and also with $\frac{\delta}{R_0}$. It can be concluded that the wall shear stress is the least for the Newtonian case. Because red blood cells are suspended in blood, it has non-Newtonian behavior. Therefore, the results based on the Newtonian fluid model are quantitatively in error.

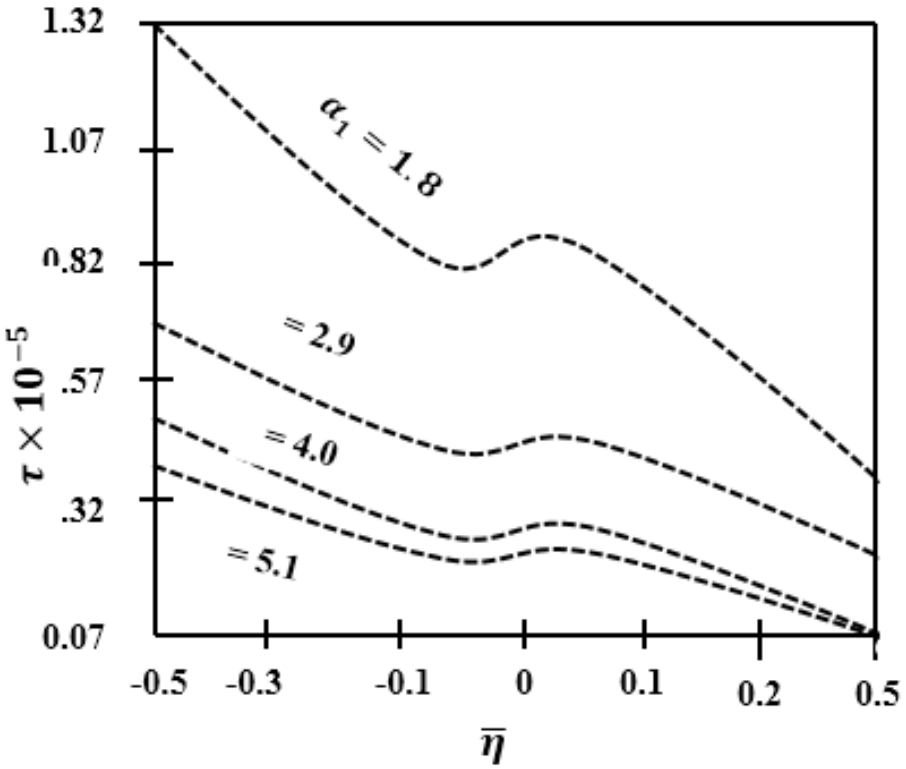

Figure 5.10: Variations of wall shearing stress with couple stress parameter for different values of $\propto_1$

Figure 5.10 demonstrates the various wall shearing stress with a couple of stress parameters for different values of $\propto$. The figure makes it quite evident that as the parameter $\propto$ increases, the wall shearing stress decreases for the fixed value of the couple stress parameter $\overline{\eta}$. Thus, conclude that the parameter $\propto_1$ can play the dominant role in decreasing the wall shearing stress.

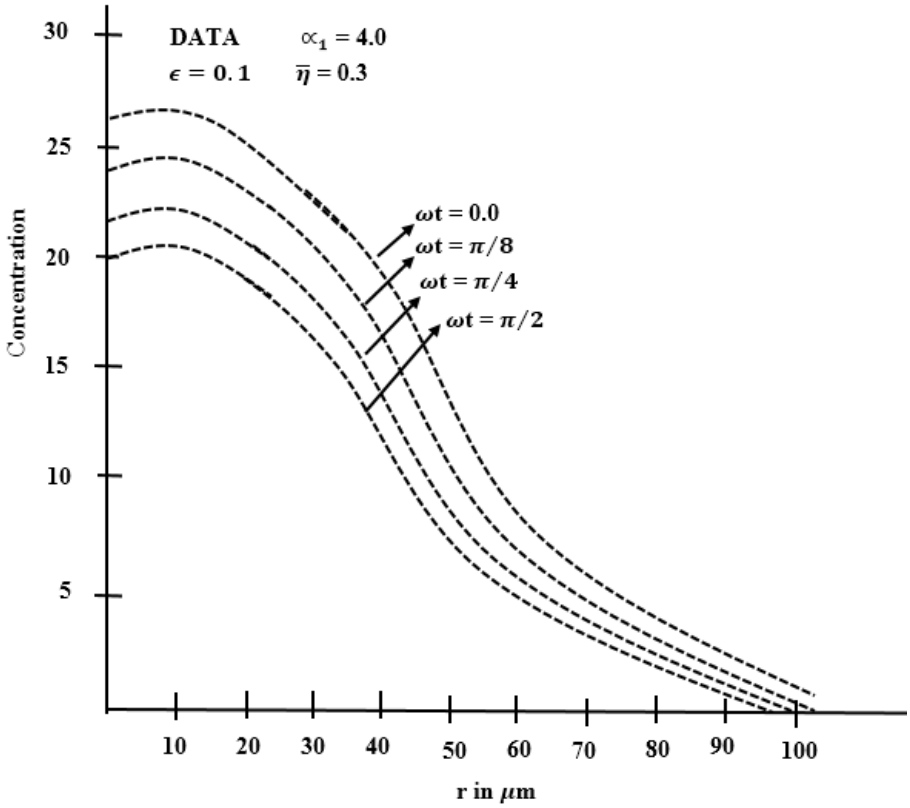

Figure 5.11: Concentration with r for different value of ωt

Figure 5.11 describes the variation of concentration with radial coordinates for different values of wt. As evident from the boundary conditions ($\frac{\partial c}{\partial t} atr = 0$) the concentration decreases as radius increases for a particular value of wt. Because of the pulsatile nature of blood flow the concentration decreases from wt = 0 to wt = π and then further decreases with the negative value from wt = π to wt = 2π. The assessment of the pulsatility of the blood flow has been made in Fig. 11. The concentration decreases as the pulsatility increases. The effect of pulsatile pressure gradient can be observed from this Figure at any radial position for increasing the value of ϵ.

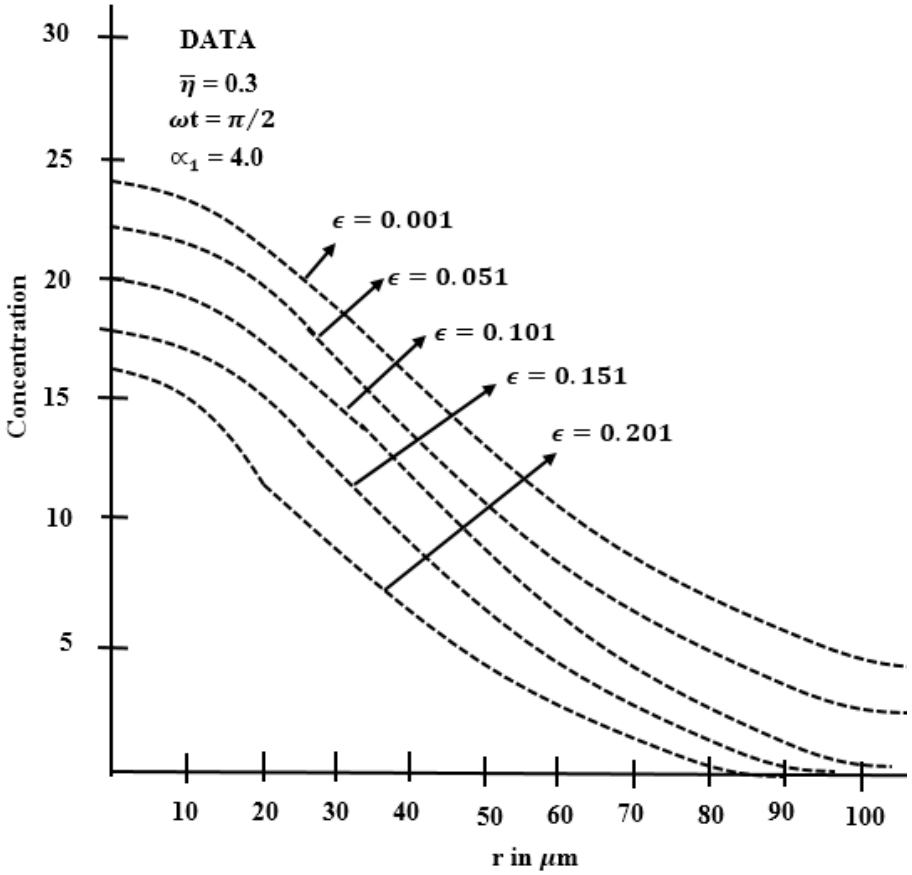

Figure 5.12: Concentration with r for different value of ϵ

Figure 5.12 The concentration decreases as the pulsatility increases. The effect of pulsatile pressure gradient can be observed from this figure at any radial position for increasing the value of ϵ.

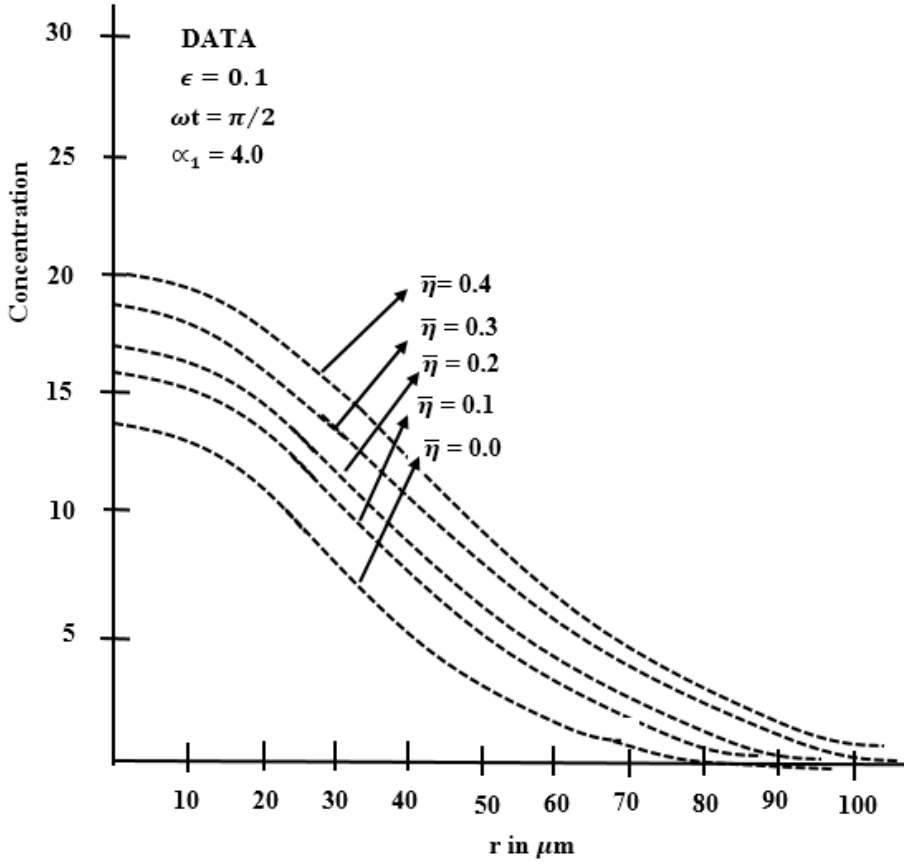

Figure 5.13: Concentration with r for different value $\overline{\eta}$

The effect of couple stress parameter $\overline{\eta}$ has been depicted in Figure 5.13. The concentration increases with increasing values of this parameter. In the model, this parameter represents the effects of the concentration of suspended cells in the blood. The entire blood's viscosity increases as these parameters increase. Therefore, increasing values of this parameter increases the concentration of dissolved nutrients at a point. This will naturally enhance, the nutrition supply to the cells in the tissue when the concentration of the nutrients increases in the capillary.

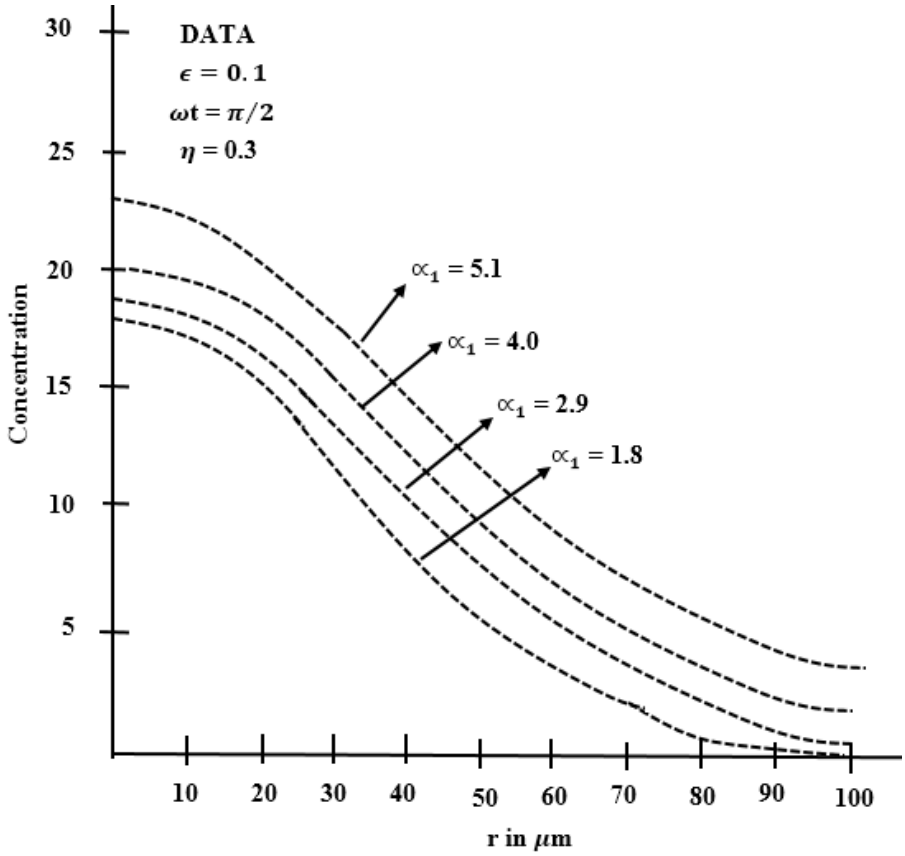

Figure 5.14: Concentration with r for different value of $\propto_1$

Figure 5.14 shows the effect of the parameter on the concentration. The parameter $\propto_1$ in the model representing the blood in the capillaries Illustrates the impact of the size and form of the particles in suspension. The concentration of the nutrients at any position increases as $\propto_1$ increases. The increasing values of $\propto_1$ in the model correspond to the increasing values of the apparent. Viscosity is mentioned in Figure 5.12. Their results are obvious. To the fact that the concentration of dissolved nutrients increases with apparent viscosity.

It is apparent that concentration near the wall increases as δ increases from Zero. This prevents the diffusion from capillary to tissue. This, in turn, presents a barrier to the diffusion of dissolved nutrients into tissue. This, in turn, prevents the supply of nutrition to the cells of the deeper region.

5.4 CONCLUSION

In this research analysis, explored the rhythmic movement of blood flows through a tube that experiences mild narrowing over time, known as stenosis, and also investigated how various physiological factors (ϵ, α, $\omega\tau$, $\overline{\eta}$), influence the concentration profile within the narrowed tube's radial coordinates under different physiological conditions. To begin, derive the equation (5.12) to determine the average velocity. This equation allows us to calculate the average speed of blood flow within the stenotic tube. Additionally, we solved the nutritional transport diffusion using equation (5.13). This step enabled us to understand how nutrients are transported within the narrowed tube. Moreover, proceeded to solve the velocity profile for the unsteady pulsatile blood flow, as described in equation (5.24). To calculate the velocity at different points within the tube during pulsatile flow, we utilized this equation. Next, Picard's type iteration method to solve the diffusion equation with boundary condition (5.15) and obtain the concentration profile, as outlined in equation (5.27). This approach ensures an accurate determination of how the concentration of substances changes within the tube. These results align perfectly with the development we presented earlier in this study, as well as with the findings from existing literature. Consequently, this valuable information will undoubtedly be of great assistance to researchers in this specific field. The outcomes obtained from this research analysis are not only valuable but also have practical applications in the medical field. These findings can be utilized by doctors and healthcare profes-

sionals to enhance effectiveness and sensitivity in their practices. By incorporating these results into their work, doctors can potentially improve the efficiency of their treatments and interventions. Additionally, the newfound sensitivity provided by these outcomes can aid in the accurate diagnosis and monitoring of various medical conditions.

5.5 APPLICATIONS OF THIS CHAPTER

The study of nutritional transport in pulsatile blood through time-dependent stenotic tubes has several potential applications. Here are a few examples:

1. Medical Treatments: Understanding how nutrients are transported through stenotic tubes can help in the development of more effective treatments for conditions such as atherosclerosis or other cardiovascular diseases. This research can provide insights into how to optimize nutrient delivery in patients with compromised blood flow.

2. Medical Device Design: The findings of this study can be utilized in the design and improvement of medical devices such as stents or drug-eluting devices. By considering the pulsatile nature of blood flow and the impact of stenosis, engineers can develop more efficient devices that promote better nutritional transport and overall patient well-being.

3. Clinical Diagnosis: This research can contribute to improved diagnostic techniques for conditions involving stenotic tubes. By understanding the effects of stenosis on nutritional transport, clinicians can better interpret imaging results and make more accurate diagnoses.

4. Patient Education: The outcomes of this study can be used to educate patients

about the importance of maintaining healthy blood flow and managing conditions that can lead to stenosis. By understanding the significance of efficient nutritional transport, patients can make informed lifestyle choices and take proactive steps to improve their health.

Chapter 6

A MODEL ON FIND THE VITAL ROLE OF BIOMECHANICS IN MUSCULOSKELETAL BONES CRACK RESTORATION USING GRIFFITH CRACK

Keywords: Triple integral equations, Fredholm Integral equations, Griffith crack, Isotropic medium, Orthotropic medium, Biomechanics, Bone cracks, stress components, Displacement components, Fourier Transform, Coupled Fredholm Integral Equation, Biomedical, Healthcare Analysis.

6.1 INTRODUCTION

The annals of scientific history show that most physical problems were transformed into mathematical models. The study of physical quantities in the problem of structures is aided by the mathematical theory of elasticity. Mathematically, the structures with cracks are treated as mixed boundary value problems. When a force that causes deformations is removed, a body can be said to be elastic since it will return to its original shape. The structure of bones arises from the properties of the complexity of bones. While describing the structure and properties of bone, terms such as hard tissue, calcified tissue, and mineralized tissue are frequently used for bone as well. Examining any remaining mammalian tissues, which are frequently referred to as delicate tissues, reveals the hard. Independent of its organic capacity, bone is perhaps the most important material known concerning structure-property connections. Bone has a viscoelastic structure that is isotropic, heterogeneous, orthotropic inhomogeneous, non-linear, and thermo-rheologically complex. Kaur [178] and Awasthi and Kaur [206] described radiation impacts, the convention of blood flow, and tissue. Applied Science, Bio-Medical Designing, and Biomechanics are the key areas that the subject of bio-designing covers. Due to these properties, a crack problem occurs in the body. It was Coop4r [252] who investigated the behavior of resistance in the solid structure and gradually Hooke's law came into existence. The mathematical theory of elasticity deals with the calculation of the displacement field under an equilibrium system of forces given the equations of equilibrium by Navier. Awasthi et al.[199] and Kumar et al. [246] solved the problem of stress and displacement components at a general point due to the single crack. Awasthi uses the Fourier transform approach to evaluate the exact expressions of displacement and stress components in the region of crack tips at the common interface of one isotropic and one orthotropic half-plane. A square root singularity may be seen in

these components. Awasthi and Rachna previously gave solutions to the Dual integral equations [253, 229] and also discussed various applications of these equations. Williams [230, 231] used the complex variable method to handle the problem of stress and displacement fields in the vicinity of crack points. Erdogan [232] extended the aforementioned approach to include more Griffith cracks. Rice and Sih [233] solved the problem of cracks in confined dissimilar materials using an R-integral technique. Willis [234] created the cracked design criteria for interfacial cracks as part of his research. Dwivedi et al. [235, 236] tackled the problem of cracks in different mediums.

The structure's hydrostatic pressure is converted to constant pressure at the crack faces. Lowengrub and Sneddon [237] used transform techniques to tackle the problem of a Griffith fracture at the interface of two limited isotropic homogeneous half-planes. Muskhelishvili [251] reduced the Hilbert problem. Logarithmic violent oscillations and the square root singularity are involved in the solutions. In Banach space, Borai and Nadi [238] examined a variety of singular and non-linear singular equations as well as the Fourier transform for Cauchy problems in parabolic and hyperbolic partial differential equations. By using linear and Finite Fourier series, Leontiev [239] describes surface value problems with some boundary problems. The influence that the existence of two cracks has on physical quantities (essential in fracture design criterion) will be investigated in the proposed work. Dwivedi et al. [235, 236] also solved the problems with two cracks and a system of cracks.

The joining of two or more materials, each of which possesses unique mechanical and elastic properties, is a common technique used in the construction of engineered structures. It is necessary for the system made of dissimilar materials to function as a unified whole, and this is accomplished by transferring loads from one material to the next across the interface between the materials. The study of fracture didn't officially begin until 1920 when Griffith published his paper [241]. However,

for the past 26 years, it has been little more than a verbal exercise. The publication of a book by Sneddon [242] served as the impetus for an idea. He utilized the theory of dual integral equations in addition to the methods of Fourier transformation. Sneddon and his co-workers [243] developed an extension of the Griffith theory that accounts for all three dimensions. In the lines that follow, we will talk about the physical features of fractures under mechanical stress, specifically surface forces and body forces. In the theory of the fracture of solids, crack difficulties play an essential role, even though they are not the fundamental cause of many of the problems. When there is an issue with a crack, the distance that separates the two opposing faces of the crack is almost never very great in proportion to the length of the crack. Because of this, the fractures are considered to be discontinuities within the continuous surface. The process of fracture in materials is a time- and space-variant phenomenon that is fundamentally determined by the material's inherent inhomogeneities as well as the stress condition that is applied to the material. It is common knowledge that void nucleation, growth, and coalescence play a role in controlling fracture in ductile materials [135, 244], however, in brittle materials, local cleavage factor, and transgranular cracks are eventually in charge of fracture [117]. The issue of an impact load on a finite crack in an infinite isotropic media, when a magnetic field is present on the fracture surface, is studied by Panja and Mandal [245]. In any event, in order to comprehend the fracture process as well as the toughening mechanism, it is essential to create a system that can analyze the microfractures. The Griffith theory is sufficient on its own to investigate the crack opening mechanism. Surface tension is something that is known to exist in solids, and it is also present in liquids when there is a force from the outside acting on the medium. When a fracture extends, work is done and is subsequently stored as strain energy. This creates an increase in surface area, which in turn causes an increase in surface tension. However, this increase is balanced by the rate at which strain

energy is released.

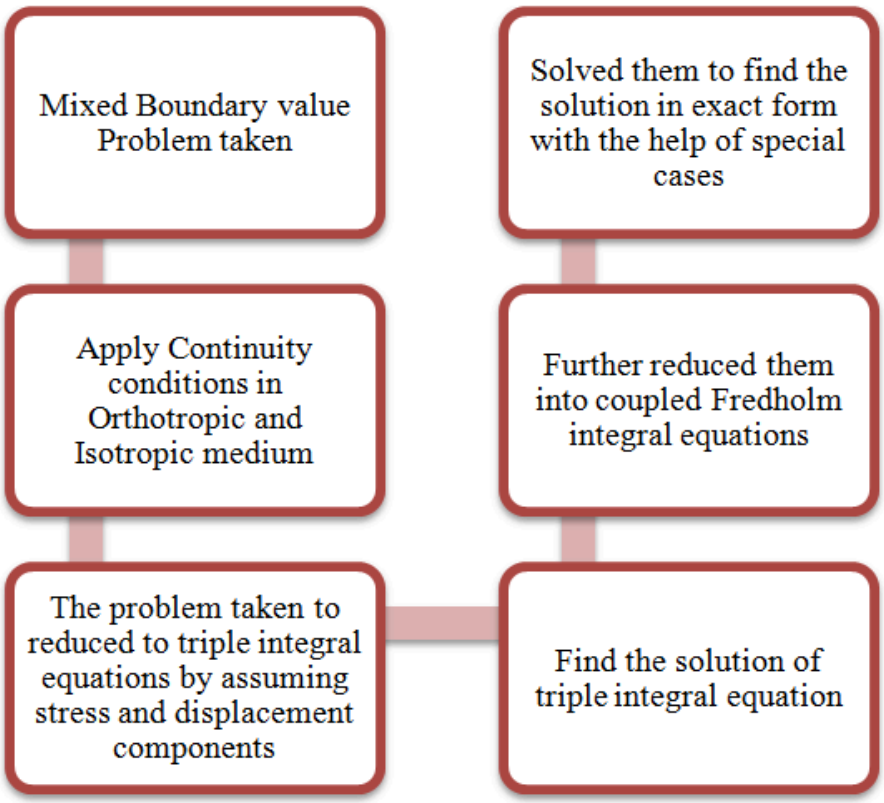

Figure 6.1: Schematic Diagram of the Chapter

6.2 METHOD WITH NECESSITY BACKGROUND FOR SOLVING RAISED ISSUES

The crack will propagate when applied stress Q exceeds the critical value Q_c given as,

$$Q_c = \left(\frac{2ES}{nc(1-\eta^2)} \right)^{\frac{1}{2}}$$

where E, S, η, and c are Young modulus, Surface tension, Poisson ratio, and half crack length respectively. The crack elastic energy of cracking is calculated through

the formula.

$$W = 2\int_0^c p(x)u_y(x,0)dx$$

where p(x) is normally applied stress at crack faces, $u_y(x,0)$ is crack opening displacement while crack occupies the space $y = 0, -c < x < c$ Irwin gave an entirely different approach. He stated that the length of a Griffith crack would be increased from $2c$ to $2(c + \delta c)$ then tensile stress $\sigma_{yy}(x,0)$ would be trying to close the crack which fits the original length. In doing so an account of work $2G_c$ would be done. G_c is called crack extension force. The relation exemplifies the relations between stress intensity factor K, defined as below

$$2\pi(1-\eta^2)K^2 = EG_c$$

$$K = \lim_{x \to c_+} +\sqrt{x-c}d\xi\sigma_{yy}(x,0)$$

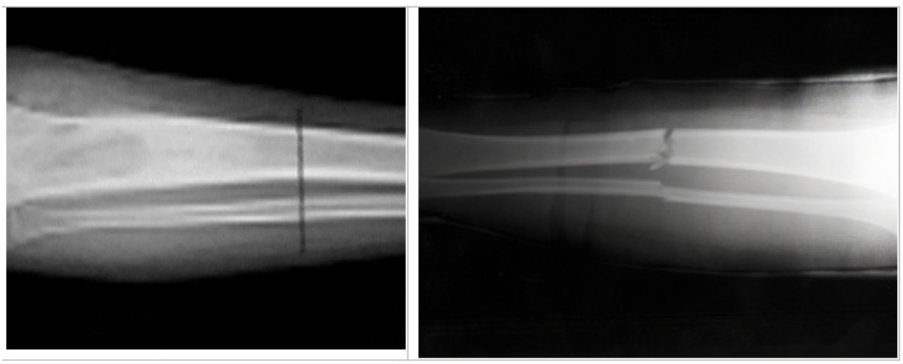

Figure 6.2: Bone Fracture

6.2.1 EXISTING BOUNDARY VALUE PROBLEM

Cracks occupy the region $y = 0$, where $p_1(x)$ and $p_2(x)$ are the crack opening forces, $b < |x| < c$ at the common interface and mathematically the problem is reduced to the following boundary value problem, see Figure 6.4 and Figure 6.5

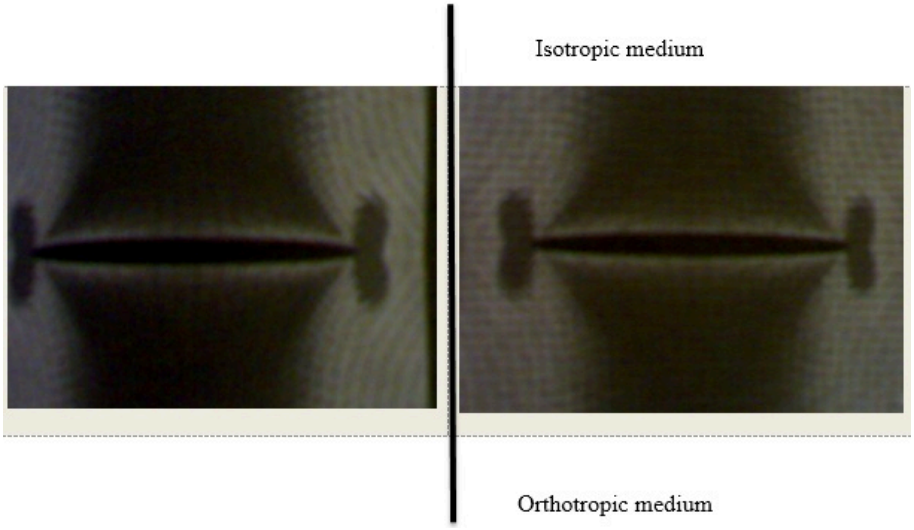

Figure 6.3: Crack Boundary

$$\sigma_{xy}(x,0^+) = \sigma_{xy}(x,0^-) = 0, \qquad b < |x| < c \tag{6.1}$$

$$\sigma_{yy}(x,0^+) = -p_1(x), \qquad b < |x| < c \tag{6.2}$$

$$\sigma_{yy}(x,0^-) = -p_2(x), \qquad b < |x| < c \tag{6.3}$$

with, $b < |x| < c$ and $(\pm)$ sign over 0 refer to the quantities corresponding to $y > 0$ and $y < 0$. There are the following continuity conditions,

$$u_y(x,0^+) = u_y(x,0^-)$$

$$u_x(x,0^+) = u_x(x,0^-)$$

$$\sigma_{xy}(x,0^+) = \sigma_{xy}(x,0^-)$$

$$\sigma_{yy}(x,0^+) = \sigma_{yy}(x,0^-)$$

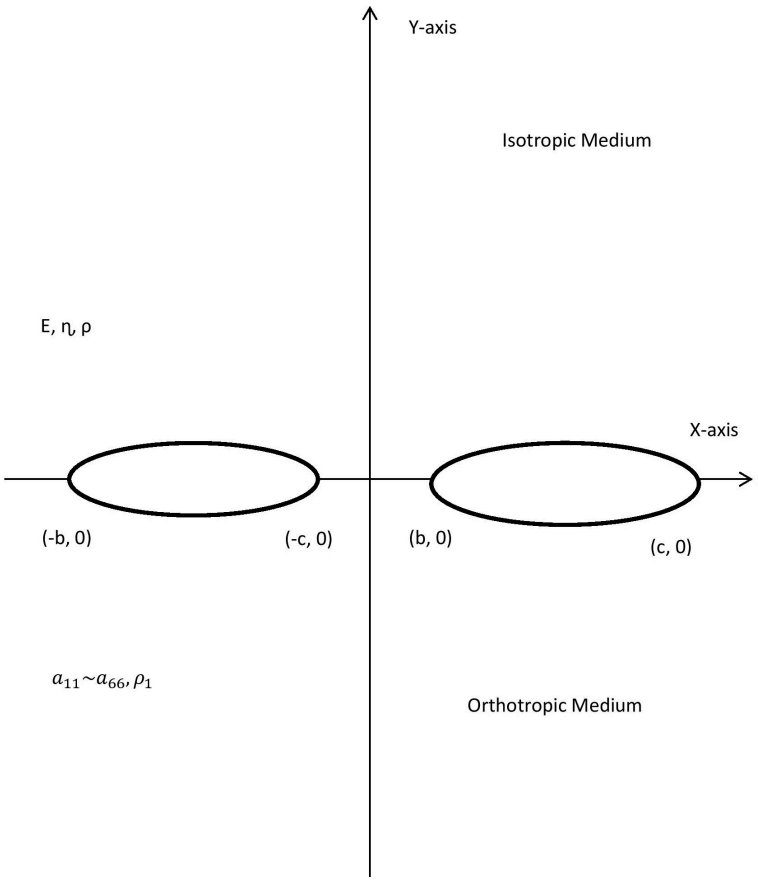

Figure 6.4: Geometry of Problem with two Griffith Cracks

The symmetry in crack geometry gives

$$\sigma_{xy}(x, 0^+) = \sigma_{xy}(x, 0^-), \qquad b < x < c$$

$$\sigma_{yy}(x, 0^+) = \sigma_{yy}(x, 0^-), \qquad b < x < c$$

$$u_y(x, 0^+) = u_y(x, 0^-), \qquad b < x < c$$

$$u_x(x, 0^+) = u_x(x, 0^-), \qquad b < x < c$$

The first and fourth quadrants are the only ones we focus on for analysis. Through

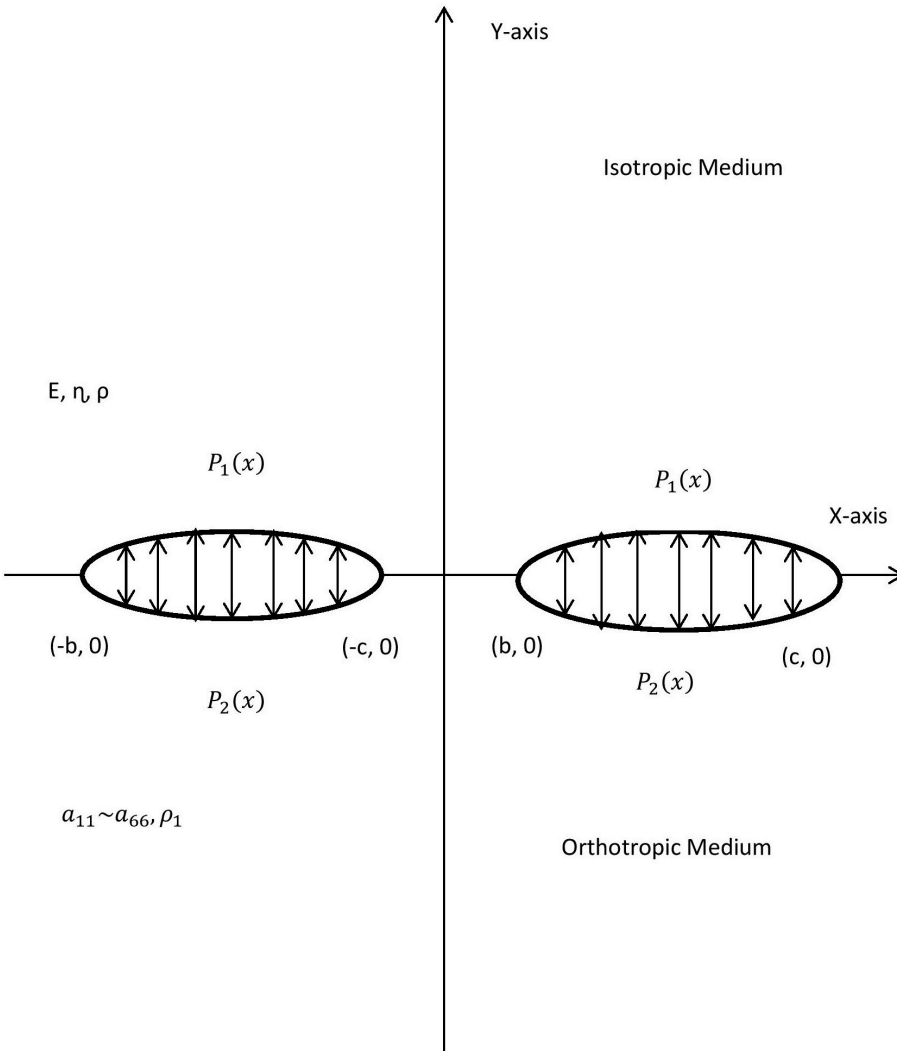

Figure 6.5: Geometry with boundary and continuity conditions

that, we looked

$$u_y(x, 0^+) > 0$$

$$u_y(x, 0^-) > 0$$

which indicates that the cracks enlarge significantly. This paper's structure is as follows: A triple integral equation will be used to solve the boundary value problem in section 6.2.1. This section will provide the triple integral equation's solution. Section 6.2.4 will provide a rough solution for linked Fredholm integral equations of

the second sort. The physical measurements at the crack tip will be taken in the last part. It will be assumed that the surface forces are homogeneous, equal, and constant.

6.2.2 REDUCTION TO TRIPLE INTEGRAL EQUATIONS

The components of stress and displacement will be assumed. The boundary conditions along with the continuity relations and the getting Fourier inversion, we find

$$\xi[r_1 C(\xi) - D(\xi)] + B(\xi) - \xi A(\xi) = 0 \tag{6.4}$$

$$A(\xi) - C(\xi) = \frac{P_1(\xi)}{\xi^2} \tag{6.5}$$

with

$$\bar{P}_1(\xi) = \frac{1}{\pi}\int_b^c (p_1(x) - p_2(x))\cos((\xi x))dx$$

Now, using the relations (6.4) and (6.5), we get the following integral equations

$$\int_b^\infty \xi \sin(\xi x)[K_5 C(\xi) + K_6 D(\xi)]d\xi = P_4(x), \qquad c \le x < \infty, 0 \le x \le b \tag{6.6}$$

$$\int_b^\infty \xi \cos(\xi x)[K_7 C(\xi) + K_8 D(\xi)]d\xi = P_5(x), \qquad c \le x < \infty, 0 \le x \le b \tag{6.7}$$

with K are given by

$K_5 = K_0 - K_1 + 2K_0(1-\eta)(1-r_1)$

$K_6 = K_2 - 2K_0(1-\eta)$

$K_7 = K_0\{1 - 2(1-2\eta)(1-r_1)\} + K_3$

$K_8 = 2K_0(1-2\eta) + K_4$

$K_0 = \frac{2(1+\eta)}{\pi E}, \qquad K_1 = r_1^2 a_{11} - a_{12}$

$K_2 = r_1 a_{11}, \qquad K_3 = r_1(a_{11}r_1^2 - a_{12} - a_{66})$

$K_4 = a_{11}r_2^2 - a_{12} - a_{66}$

where K's is considered an absolutely integrable function and acts as the kernel.

$$P_4 = \int_0^\infty \frac{\bar{P}_1(\xi)\sin(\xi x)}{\xi} d\xi$$

$$P_5 = \int_0^\infty \frac{\bar{P}_1(\xi)\cos(\xi x)}{\xi} d\xi$$

Similarly, now we evaluate

$$\sigma_{xy}(x, 0^+) + \sigma_{xy}(x, 0^-) = 0, \quad b < x < c \tag{6.8}$$

$$\sigma_{yy}(x, 0^+) + \sigma_{yy}(x, 0^-) = -(P_1(x) + P_2(x)), \quad b < x < c \tag{6.9}$$

thus, the above two relations and the corresponding stress-strain relations give

$$\int_0^\infty \xi^2 \sin(\xi x) C(\xi) d\xi = P_6(x), \quad b < x < c \tag{6.10}$$

$$\int_0^\infty \xi^2 \cos(\xi x) C(\xi) d\xi = P_7(x), \quad b < x < c \tag{6.11}$$

with,

$$P_6(x) = \frac{1}{1 + r_1} \int_0^\infty \bar{P}_1(x)\xi \sin(\xi x) dx$$

$$P_7(x) = -\frac{1}{2} \int_0^\infty \bar{P}_1(x)\xi \cos(\xi x) d\xi + \frac{1}{2}(P_1(x) + P_2(x))$$

thus, the boundary value problem is reduced to the solution of triple integral equations.

6.2.3 SOLUTION OF TRIPLE INTEGRAL EQUATION

We assume that,

$$\xi[K_5 C(\xi) + K_6 D(\xi)] = \phi(\xi)$$

$$\xi[K_7 C(\xi) + K_8 D(\xi)] = \psi(\xi)$$

where, ϕ and ψ are two new functions. Then the integral equations become new triple integral equations,

$$\int_0^\infty \phi(\xi) \sin(\xi x) d\xi = P_4(x), \quad x \epsilon I_1 \cup I_3 \tag{6.12}$$

$$\int_0^\infty \psi(\xi) \cos(\xi x) d\xi = P_5(x), \quad x \epsilon I_1 \cup I_3 \tag{6.13}$$

and

$$\int_0^\infty \xi[K_{12}\phi(\xi) + K_{13}\psi(\xi)] \sin(\xi x) d\xi = P_6(x), \qquad x \epsilon I_2 \tag{6.14}$$

$$\int_0^\infty \xi[K_{10}\phi(\xi) - K_{11}\psi(\xi)] \cos(\xi x) d\xi = P_7(x), \qquad x \epsilon I_2 \tag{6.15}$$

where, K_{10} and K_{13} are given, and

$$I_1 = [0, b], I_2 = [b, c], I_3 = [c, \infty]$$

Now, to solve the system of equations we make use of the method of Sneddon and Lowenbrug [123]. We assume that,

$$\pi\xi\phi(\xi) = 2\left[\int_b^c g(t)(1 - \cos\xi t)dt - \left(\int_0^b + \int_c^\infty\right) P_4^1(t)(1 - \cos\xi t)dt\right] \tag{6.16}$$

$$\pi\xi\psi(\xi) = 2\left[\int_b^c h(t) \sin\xi t dt - \left(\int_0^b + \int_c^\infty\right) P_5^1(t) \sin\xi t dt\right] \tag{6.17}$$

then, the equations are satisfied identically. if

$$\int_b^c g(t)dt = P_4(b) - P_4(c) \tag{6.18}$$

$$\int_b^c h(t)dt = P_5(b) - P_5(c) \tag{6.19}$$

Substituting $\phi(\xi)$ and $\psi(\xi)$ evaluating the integrals we get,

$$K_{10}g(x) + \frac{2K_{11}}{\pi}\int_b^c \frac{th(t)dt}{t^2 - x^2} = -P_8(x), \quad x\epsilon I_2 \tag{6.20}$$

$$\frac{2}{\pi}K_{12}x\int_b^c \frac{g(t)dt}{t^2 - x^2} + K_{13}h(x) = P_8(x), \quad x\epsilon I_2 \tag{6.21}$$

where,

$$P_8(x) = P_7(x) - \frac{4K_{11}}{\pi}\left(\int_0^b + \int_c^\infty\right)\frac{P_5(t)}{t^2 - x^2}dt$$

$$P_9(x) = P_6(x) + \frac{4K_{11}x}{\pi}\left(\int_0^b + \int_c^\infty\right)\frac{P_4(t)}{t^2 - x^2}dt$$

Now, rewriting the remaining forms an equation

$$\int_b^c \frac{th(t)dt}{t^2 - x^2} = -\frac{\pi}{2K_{11}}P_{10}(x), \quad x\epsilon I_2 \tag{6.22}$$

$$\int_b^c \frac{xh(t)dt}{t^2 - x^2} = \frac{\pi}{2K_{12}}P_{11}(x), \quad x\epsilon I_2 \tag{6.23}$$

with,

$$P_{10}(x) = P_8(x) + K_{10}g(x)$$

$$P_{11}(x) = P_9(x) - K_{13}h(x)$$

Inverting by using Sneddon and Lowenburg [123] method

$$h(t) = \frac{1}{\pi K_{11}\delta(t)}\left[\int_b^c \frac{x\delta(x)P_{10}(x)}{x^2-t^2}dx + D_1\right] \tag{6.24}$$

$$g(t) = \frac{1}{\pi K_{12}\delta(t)}\left[\int_b^c \frac{x\delta(x)P_{11}(x)}{x^2-t^2}dx + D_2\right] \tag{6.25}$$

$$\delta(t) = [(t^2-b^2)(c^2-t^2)]^2 \tag{6.26}$$

where D_1 and D_2 are two arbitrary constants that will be obtained. Substituting the values of $P_{10}(x)$ and $P_{11}(x)$ and evaluating the integrals.

$$h(t) = P_{12}(t) + \frac{K_{10}}{\pi K_{11}\delta(t)}\int_b^c \frac{x\delta(x)g(x)}{x^2-t^2}dx \tag{6.27}$$

$$g(t) = P_{13}(t) - \frac{K_{13}t}{\pi K_{12}\delta(t)}\int_b^c \frac{\delta(x)h(x)}{x^2-t^2}dx \tag{6.28}$$

$$P_{12}(t) = \left[D_1 + \int_b^c \frac{x\delta(x)P_8(x)}{x^2-t^2}dx\right]\frac{1}{\pi K_{11}\delta(t)} \tag{6.29}$$

$$P_{13}(t) = \left[D_2 + \int_b^c \frac{\delta(x)P_9(x)}{x^2-t^2}dx\right]\frac{1}{\pi K_{12}\delta(t)} \tag{6.30}$$

6.2.4 REDUCTION TO FREDHOLM INTEGRAL EQUATION

We substitute for $g(t)$ and evaluate the certain integrals, we get

$$h(t) = P_{14}(t) - \frac{K_{14}}{\delta(t)}\int_b^c \frac{\delta(\alpha)h(\alpha)}{\alpha^2-t^2}H(t,\alpha)d(\alpha)$$

$$P_{14}(t) = P_{12}(t) + \frac{K_{15}D_2[c-b+H_0(t)]}{2\delta(t)} + \frac{K_{15}}{2\delta(t)}\int_b^c \frac{\delta(\alpha)P_9(\alpha)dx}{\alpha^2-t^2}H^-(t,\alpha)d(\alpha) \tag{6.31}$$

with,

$$H_0(t) = \frac{1}{2} t log \left| \frac{c-t}{c+t} \frac{b+t}{b-t} \right|$$

and

$$H(t, \alpha) = H_0(t) - H_0(\alpha)$$

$$K_{14} = \frac{K_{13} K_{10}}{2\pi^2 K_{11} K_{12}}$$

$$K_{15} = \frac{K_{10}}{2\pi^2 K_{11} K_{12}}$$

Similarly,

$$g(t) = P_{15}(t) + \frac{t K_{16}}{\delta(t)} \int_b^c \frac{\delta(\alpha) h(\alpha)}{\alpha^2 - t^2} \left[\frac{\phi_1(t) H_0^2(\alpha)}{\alpha^2} \right] d\alpha$$

$$P_{15}(t) = \frac{1}{\alpha K_{12} \delta(t)} \left[D_2 + \int_b^c \frac{\delta(x) P_9(x)}{x^2 - t^2} dx - K_{13} \int_b^c \frac{\delta(x) P_{14}(x)}{x^2 - t^2} dx \right] \tag{6.32}$$

$$K_{16} = \frac{K_{13} K_{14}}{\pi K_{12}}$$

$$\phi_1(t) = \int_b^c \frac{H_0(x)}{x^2 - t^2} dx$$

Thus knowing the solution, we will substitute the value to get the solution of $g(t)$.

6.2.5 SOLUTION OF FREDHOLM INTEGRAL EQUATIONS

We assume $h(t)$ as,

$$h(t) = \sum_{n=0}^{\infty} \delta^n h_n(t)$$

where $\delta = K_{14}$ and its properties are discussed by Awasthi et al. [189]. Substituting this value of $h(t)$ and then comparing the coefficients δ^n, we get

$$H_0(t) = P_{14}(t)$$

$$H_1(t) = -K_{15}I_0(t)$$

$$H_2(t) = -K_{15}I_1(t) + r_1K_{15}I_0(t)$$

$$H_3(t) = -K_{15}I_2(t) + r_1K_{15}(1 + K_{15})I_1(t) - r_1K_{15}I_0(t)$$

where,

$$I_n(t) = \int_b^c K_0(\alpha, t)I_{n-1}(\alpha)d\alpha$$

$$I_0(t) = \int_b^c K_0(\alpha, t)P_{14}(\alpha)d\alpha$$

Thus, $h(t)$ can be written as

$$K_0(\alpha, t) = \frac{\delta(\alpha)H^-(t, \alpha)}{\delta(t)(\alpha^2 - t^2)}$$

$$h(t) = P_{14} - \delta K_{15}\phi_2(t)$$

with,

$$\phi_2(t) = K_{20}I_0(t) + K_{21}I_1H + K_{22}I_2(t)$$

and

$$K_{20} = 1 - r_1\delta - r_1\delta^2$$

$$K_{21} = \delta K_{15} - \delta^2 r_1(1 + K_{15})$$

$$K_{22} = \delta^2 K_{15}$$

Substituting this value of $h(t)$ and evaluating the integrals. We get,

$$\phi_3(t) = \phi_1(t)[G_3^{(0)}(t) - \delta K_{15}K_{20}G_0^{(0)}(t) + \delta K_{15}K_{21}G_1^{(0)}(t) + \delta K_{15}K_{22}G_2^{(0)}(t)] - G_3^{(1)}(t) - \delta K_{15}K_{21}G_1^{(1)}(t) + \delta K_{15}K_{20}G_0^{(1)}(t) - \delta K_{15}K_{22}G_2^{(1)}(t) \tag{6.33}$$

and

$$G_m^{(n)}(t) = \int_b^c \frac{\delta(\alpha)}{(\alpha^2 - t^2)} I_m(\alpha) - \left(\frac{H_0(\alpha)}{\alpha}\right)^{2n} d\alpha$$

$$I_3(t) = P_{14}(t)$$

The arbitrary constants D_1 and D_2 are evaluated and given as

$$D_1 = \frac{\pi K_{11}}{J_{31}}[P_5(b) - P_5(c) - J_{33} + J_4] - \frac{2\pi^2 K_{11} K_{15} J_{32}}{J_{32}}[P_4(b) - P_4(c) - K_{16} J_5] \tag{6.34}$$

$$D_2 = 2\pi[P_4(b) - P_4(c) - K_{16} J_5] K_{12}$$

$J_{31} = \frac{1}{b} F\left(\frac{\pi}{2}, p_1\right)$= Complete Elliptic integral of first kind

$$K_1^2 = (c^2 - b^2) b^2$$

$$J_{32} = J_{31} + \int_b^c \frac{H_0(t)}{\delta(t)} dt$$

$$J_{33} = K_{15} \int_b^c \delta(\alpha) P_9(\alpha) \int_b^c \frac{H^-(t,a)}{\delta(t)} dt - \frac{1}{\pi K_{11}(c^2 - b^2)} \int_b^c x\delta(x) P_8(x) \prod \left[\frac{\pi}{2}, K(x)\right] dx \tag{6.35}$$

$\prod$ is the elliptic integral of the third kind.

$$J_4 = \delta K_{15}[J_0 K_{20} + J_1 K_{21} + J_2 K_{22}]$$

$$J_5 = \delta K_{16}\left[M_3^{(0,1)} - \delta K_{15} K_{20} M_0^{(0,1)}\right] + \delta K_{15} \begin{pmatrix} K_{21} M_1^{(0,1)} + K_{22} M_2^{(0,1)} \\ K_{20} M_1^{(1,0)} - K_{21} M_1^{(1,0)} - M_2^{(1,0)} \end{pmatrix} - M_3^{(1,0)} \tag{6.36}$$

$$M_m^{(n,b)} = \int_b^c \frac{t\{\phi_1(t)\}^b}{\delta(t)} G_m^{(n)}(t) dt$$

$$J_m = \int_b^c I_m(t)dt, \quad m = 0, 1, 2, 3$$

6.3 PHYSICAL QUANTITIES

The crack opening displacement and the components of stress around the crack tips are the quantities that are crucial in the fracture design criterion. The following relationship is used to evaluate the components.

Stress Components

Shear Scalar

$$\sigma_{xy}(x, 0^+) - \sigma_{xy}(x, 0^-) = 0, \quad x\epsilon I_1 \cup I_2$$

$$\sigma_{xy}(x, 0^+) - \sigma_{xy}(x, 0^-) = (I + r_1) \int_0^\infty \sin(\xi x) \left[\xi^2 C(\xi) - P_1(\xi)\right] d(\xi)$$

This integral becomes as

$$\sigma_{xy}(x, 0^+) - \sigma_{xy}(x, 0^-) = (I + r_1) \int_0^\infty \xi \left[K_{12}\phi(\xi) + K_{13}\Psi(\xi)\right] \sin(\xi x) d\xi - P_6(x), \quad x\epsilon I_1 \cup I_3$$

Modifying the order of integration, assessing the integrals, and applying relations,

$$\sigma_{xy}(x, 0^+) + \sigma_{xy}(x, 0^-) = K_{12}(1 + r_1) \left[\frac{2x}{\pi} \int_b^c \frac{g(t)dt}{(t^2 - x^2)} - \frac{2x}{\pi} \left(\int_0^b + \int_c^\infty \right) \frac{P_4(t)dt}{(t^2 - x^2)} \right] - (1 + r_1) K_{13} P_5(x) - P_6(x), \quad x\epsilon I_1 \cup I_3 \tag{6.37}$$

Normal Stress

Similarly, the normal components of stresses are given by

$$\sigma_{xy}(x, 0^+) - \sigma_{xy}(x, 0^-) = 0, \qquad x\epsilon I_1 \cup I_3$$

$$\sigma_{yy}(x,0^+)+\sigma_{yy}(x,0^-)=K_{10}P_4(x)-\frac{2x}{\pi}\int_b^c\frac{th(t)dt}{(t^2-x^2)}$$

Now, substituting for $g(t)$ and $h(t)$ and evaluating the integrals, we get

$$\begin{aligned}\sigma_{yy}(x,0^+)+\sigma_{xy}(x,0^-)=K_{12}(1+r_1)\Bigg[2x\bigg(P_{15}(x)+K_{16}\phi_3(x)\bigg)\frac{1}{\delta(x)}\\ -\frac{2x}{\pi}\left(\int_0^b+\int_c^\infty\right)\frac{P_4^1(t)}{(t^2-x^2)}dt\Bigg]-(1+r_1)K_{13}P_5^1(x)-P_6(x),\quad x\epsilon I_1\end{aligned}\tag{6.38}$$

and

$$\begin{aligned}\sigma_{yy}(x,0^+)+\sigma_{xy}(x,0^-)=K_{12}(1+r_1)\Bigg[-2x\bigg(P_{15}(x)+K_{16}\phi_3(x)\frac{1}{|\delta(x)|}\bigg)-\\ \frac{2x}{\pi}\left(\int_0^b+\int_c^\infty\right)\frac{P_4^1(t)}{(t^2-x^2)}dt\Bigg]-(1+r_1)K_{13}P_5^1(x)-P_6(x),\quad x\epsilon I_3\end{aligned}\tag{6.39}$$

and

$$\sigma_{yy}(x,0^+)+\sigma_{xy}(x,0^-)=\begin{cases}\frac{-2K_{11}}{|\delta(x)|}\{P_{14}(x)-\delta K_{15}\phi_3(x)\}-F_0(x), & x\epsilon I_1\\ \frac{2K_{11}}{|\delta(x)|}\{P_{14}(x)-\delta K_{15}\phi_2(x)\}+F_0(x), & x\epsilon I_3\end{cases}\tag{6.40}$$

$$|\delta(x)|=\left[|(b^2-x^2)(c^2-x^2)|\right]^{\frac{1}{2}},\quad x\epsilon I_1$$

$$|\delta(x)|=\left[|(x^2-b^2)(x^2-c^2)|\right]^{\frac{1}{2}},\quad x\epsilon I_3$$

$$\begin{aligned}F_0(x)=K_{10}P_4(x)+\frac{2}{\pi}\left(\int_0^b+\int_c^\infty\right)\frac{P_5^1t}{t^2-x^2}dt+\frac{2}{\pi}K_{11}\left(\int_0^b+\int_c^\infty\right)\\ \frac{P_5^1t}{t^2-x^2}dt-P_7(x),\quad x\epsilon I_1\cup I_3\end{aligned}\tag{6.41}$$

Here we have calculated the stress component by equations (6.39) and (6.40) theoretically. But, this is a very tough and technically challenging attempt due to its intricacy as explained above. The degree to which a structure deforms under a specific load is determined by the type of loading, the geometry of the structure, and the mechanical qualities of the materials used to construct it. A construction that

resembles a long bone will be used to illustrate this concept. The below figure can help us to understand the stress components technically. The stress–strain curve obtained a sample of compact bone in tension. E is the stiffness of the material (Young's modulus for isotropic materials). (Entities in parentheses represent results of whole bone experiments, in which the load–deformation relationship is described).

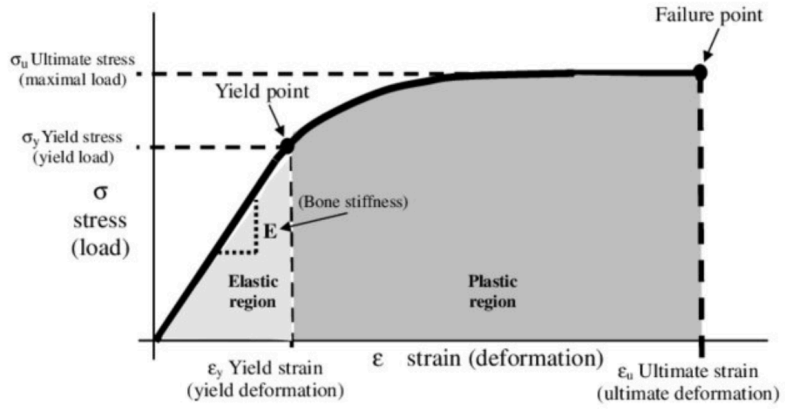

Figure 6.6: Stress component

Displacement Components

The displacement components are evaluated through given relations (6.4), (6.5), (6.12), (6.13), (6.24), (6.25) and the integrals are evaluated, and we obtain

Isotropic Case $(y > 0)$

$$u_y(x,0) = u_y(x,0^+) = \left(\frac{2(1+\eta)}{\pi E}\frac{2(1+\eta)P_5(x)}{\pi E}\right) + \frac{K_{10}^+}{\pi}\left[\left(\int_b^c g(t) - \left(\int_0^b + \int_c^\infty\right)\right.\right.$$
$$\left.\left. P_4^1(t)\log|x^2-t^2|dt + K_{11}^+\left[\int_x^c h(t)dt + P_4(c)\right]\right., \quad x\epsilon I_2 \right. \tag{6.42}$$

with,

$$K_{10}^+ = K_0\left[\frac{r_1K_8 - K_7 - r_1K_6}{K_9}\right]$$

$$K_{11}^{+} = K_0 \left[\frac{(1-2\eta)K_5 - r_1 K_6}{K_9} \right]$$

Further,

Orthotropic Case $(y < 0)$

$$\begin{aligned} u_y(x,0) = u_y(x,0^-) &= \int_0^\infty \cos(\xi x) \left[\xi(K_3 C(\xi) + K_4 D(\xi)) \right] d\xi \\ &= \int_0^\infty \cos(\xi x) \left[K_3 \frac{K_8\phi - K_6\psi}{K_9} - \frac{K_4}{K_9}(K_7\phi - K_5\psi) \right] d\xi \\ = \int_0^\infty \cos(\xi x) &\left[\phi(K_9(K_8K_3 - K_4K_7)) + \frac{K_4K_5 - K_3K_6}{K_9}\psi \right] d\xi \end{aligned} \tag{6.43}$$

Thus,

$$u_y(x,0^-) = \int_0^\infty \cos(\xi x)[\phi K_{13}^{+} + K_{14}^{+}\psi] d\xi$$

$$K_{13}^{+} = \frac{K_3K_8 - K_4K_7}{K_9}$$

$$K_{14}^{+} = \frac{K_4K_5 - K_3K_6}{K_9}$$

$$\begin{aligned} u_y(x,0^-) = P_5(x) + \frac{K_{13}^{+}}{\pi} \left[\int_b^c g(t) \log|x^2 - t^2| dt \right] \left[-\left(\int_0^b + \int_c^\infty \right) P_4(t) \right. \\ \left. \log\left|x^2 - t^2\right| dt + K_{14}^{+} - \left[\int_x^c h(t)dt + P_5(c) \right], x \epsilon I_2 \right. \end{aligned} \tag{6.44}$$

Similarly,

$$\begin{aligned} u_x(x,0^+) = P_4(x)K_0 + K_{16}^{+} \left[\int_x^c g(t)dt + P_4(c) \right] + \frac{K_{17}^{+}}{\pi} \\ \left[\left\{ \int_b^c h(t) - \left(\int_0^b + \int_c^\infty \right) P_4(t) \right\} \log\left| \frac{x-t}{x+t} \right| dt \right], x \epsilon I_2 \end{aligned} \tag{6.45}$$

with,

$$K_{16}^{+} = K_0 \left[\frac{K_{15}^{+}K_8 + 2K_7(1-\eta)}{K_9} \right]$$

$$K_{17}^{+} = K_0 \left[\frac{K_{15}^{+}K_6 + 2K_5(1-\eta)}{K_9} \right]$$

$$K_{15}^{+} = 1 + 2(1-\eta)(1-r_1)$$

$$\begin{aligned} u_x(x,0^-) &= \int_0^\infty \cos(\xi x)\left[c(\xi) - \frac{a_{11}r_2 D}{K_2}\right] d\xi + K_0 P_4(x) \\ &= \int_0^\infty \sin(\xi x)\left[K_1\left(\frac{K_8\phi - K_6\psi}{K_9}\right) + K_2\left(\frac{K_7\phi - K_5\psi}{K_9}\right)\right] \\ &\qquad d\xi \\ &= \int_0^\infty \sin(\xi x)[K_{18}^{+}\phi(\xi) - K_{19}^{+}\psi(\xi)]d\xi + K_0 P_4(x), \quad x\epsilon I_2 \end{aligned} \tag{6.46}$$

$$K_{18}^{+} = \frac{K_1 K_8 - K_2 K_7}{K_9}$$

$$K_{19}^{+} = \frac{K_1 K_6 - K_2 K_5}{K_9}$$

thus,

$$\begin{aligned} u_x(x,0^-) &= P_4(x)K_0 + K_{16}^{+}\left[\int_x^c g(t)dt + P_4(c)\right] \\ &+\frac{K_{19}^{+}}{\pi}\left[\left\{\int_b^c h(t)d(t) - \left(\int_0^b + \int_c^\infty\right) P_5(t)\right\}\log\left|\frac{x-t}{x+t}\right| dt\right], x\epsilon I_2 \end{aligned} \tag{6.47}$$

Here determine the bone crack displacement by equation (6.46) and (6.47). A material's fracture toughness has also been measured using the crack displacement, with the material property being a crucial crack opening displacement. The below figure can help us to understand or visualize the displacement components in a cracK

Special Case

It is assumed that the applied forces at crack faces are constant, uniform, and equal. As a result,

$$p_1(x) = p_2(x) = p_0$$

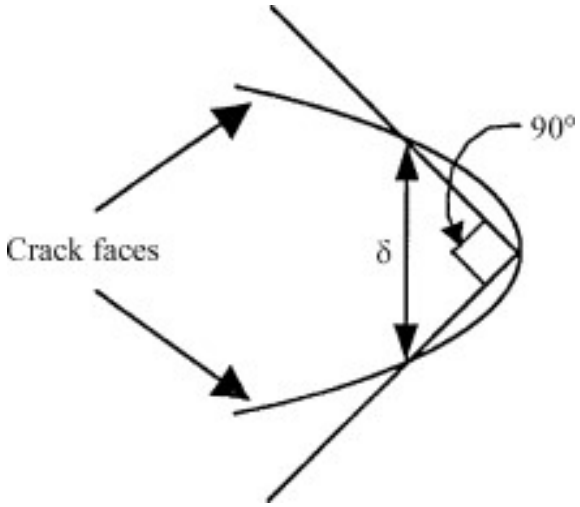

Figure 6.7: Geometry of problem with special force

Then,

$$P_1(\xi) = 0$$

And

$$p_4(x) = p_5(x) = p_6(x) = 0$$

$$P_7(x) = p_0$$

Then, we get

$$\int_b^c g(t)dt = 0$$

$$\int_b^c h(t)dt = 0$$

$$P_8(x) = p_0$$

$$P_9(x) = 0$$

$$P_{10}(x) = K_{10}g(x) + P_0$$

$$P_{11}(x) = -K_{13}h(t)$$

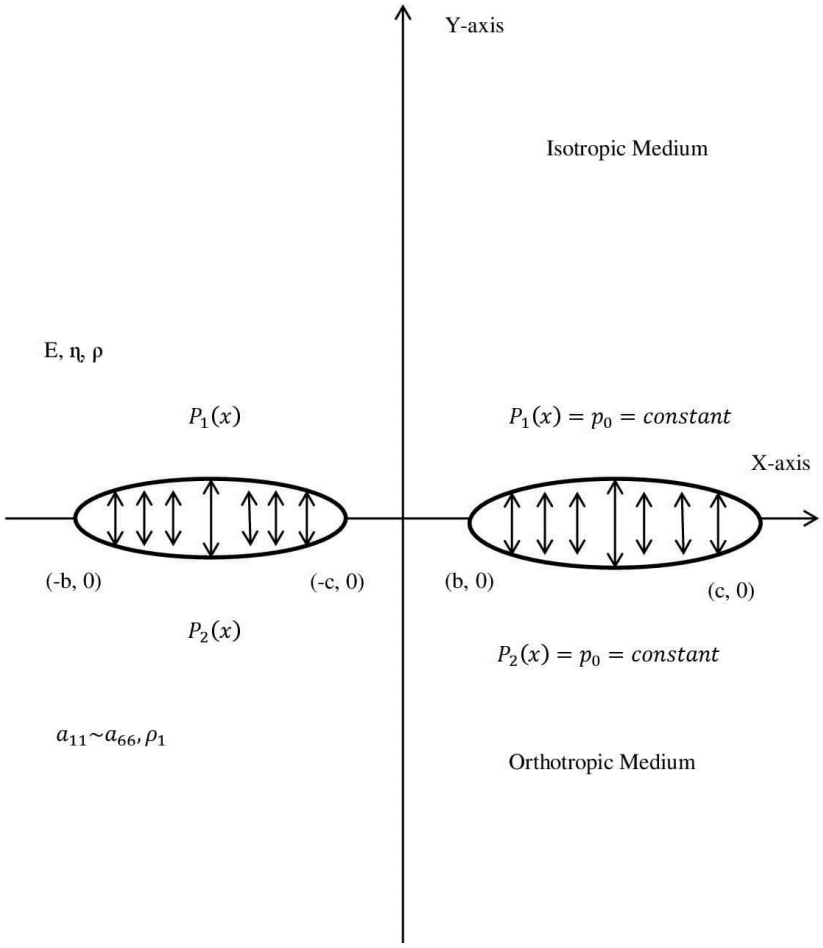

Figure 6.8: Geometry of problem with force

$$P_{12}(t) = \left[D_1 + p_0(2t^2 - c^2 - b^2)\frac{\pi}{2}\right]\frac{1}{\pi K_{11}\delta(t)}$$

$$P_{13}(t) = \frac{tD_2}{\pi K_{11}\delta(t)}$$

$$P_{14}(t) = P_{12}(t) + \frac{K_{15}D_2}{\delta(t)}\big(c - b + H_0(t)\big)$$

$$P_{15}(t) = \frac{1}{\pi K_{12}\delta(t)} + \left[D_2 - \frac{K_{13}}{\pi K_{11}}\left\{\left(D_1 + \frac{\pi p_0}{2}(c^2 - b^2)\right)\frac{H_0(t)}{2t^2}\right.\right.$$

$$\left.\left. + \pi p_0\Big(c - b + H_0(t)\Big)\right\}\right]$$

Now, we get

$$D_1 = \frac{\pi K_{11}}{J_{31}}[J_4 - J_{33}] + \frac{2\pi^2 K_{11} K_{12} K_{16} K_{15} J_{32} J_5}{J_{31}}$$

$$J_{33} = \frac{p_0}{\pi K_{11}}[\pi - 2b^2 J_{31}]$$

These integrals, which must be properly handled for numerical integrations, allow for the numerical evaluation of the constants J_4, J_5, J_{31}, J_{32}.

$$D_2 = -2\pi K_{12} K_{16} J_5$$

The assessment must be done extremely carefully since the constant J_{32} exhibits logarithmic oscillations. The functions $h(t)$ and $g(t)$ are by the equations with P_{14}, P_{15} and constants D_1 and D_2 and remaining constants and functions are evaluated previously.

Therefore, numerical integration can be used to evaluate the physical quantities.

6.4 CONCLUSION

The existing boundary value problem evolved to paper has been reduced to triple integral equations (6.4), (6.5), (6.6), and (6.7) and has been solved in the form of equations (6.27) and (6.28) by assuming stress and displacement components and finding the solution of these triple integral equations by the method of Srivastava and Lowenburg. The triple integral equations are further solved by reducing them into coupled Fredholm integral equations. Finally, the quantities, that are important in the bone fracture design criterion, are the components of stress in the neighborhood of crack tips and the crack opening displacement, which are evaluated by equations (6.40), (6.41), (6.46), and (6.47). Special cases where the forces on bone crack faces

are assumed to be constant, uniform, and equal are also discussed. However, Griffith crack propagation is still widely used for predicting the behavior of brittle materials when stressed or displaced. Even though it has several limitations such as the following:

• It applies exclusively to brittle materials and ignores the effects of plastic deformation or ductility.

• Crack propagation does not have a substantial impact on the effects of temperature or other environmental conditions.

• It presupposes that the fracture is planar and linear, but it's not possible in the real world.

• If the material properties or loading conditions change, the crack is assumed to propagate at a constant velocity, which may not be true in certain circumstances.

6.5 FUTURE SCOPE

In this chapter, the physical problem of bone cracks in biological structure is transformed into the mathematical solution of the triple Integral equation, which is transformed into Fredholm Integral equation, and finally into the decoupled Fredholm Integral equation of the second kind. Finally, the stress and placement components may be simply calculated in their exact form. The research on the topic has certain practical value. The paper only deduces theoretical formulas, and it is believed that presenting stress components and displacements in the form of image texts can be done. Also in future, we can visually demonstrate the effectiveness and correctness of the research content. The technique used for asymmetrical loading of crack faces can be further used in the future for the analysis of crack opening due to heat or thermo elastic problems. Stress components are evaluated for the region x-axis and it is found that it has square root singularity at crack tips. The singularity at crack

tips, it seems, may generate a plastic region around crack tips. This type of problem will be discussed in the future.

Chapter 7

NOMENCLATURE

7.1 LIST OF NOMENCLATURE

1. M = Metabolic heat generation
2. a = Average area for heat transfer
3. C = Capillary perfusion rate
4. ha = Heat transfer coefficient time area
5. T = Temperature
6. Tc and Ts = Core and surface temperature
7. Tv and Ta = Temperature of vein and artery
8. L = Thickness of peripheral layer
9. K = Thermal conductivity of tissue
10. θ_1 and θ_1 = Dimensionless temperature
11. λ = Dimensionless group
12. g = Dimensionless group
13. M^0v and M^0a = Venous and arterial flow rate
14. S = Boundary condition parameters ranging $0 \leq S \leq \infty$

15. ω = Axial velocity
16. τ_1 and τ_2 = Shear stress
17. N = Retention parameters
18. C_0 = Same reference concentration of solute
19. I_0 and I_1 = Bessel functions
20. R_3 = Tube radius
21. μ and $\overline{\mu}$ = Couple stress parameters
22. t = Time
23. $\langle V \rangle$ = Average velocity
24. Pm = Constant mean pressure gradient
25. τ_ω = Wall shearing stress
26. C(r) = Concentration profile
27. α = Volume flow rate
28. Z = Axial distance
29. δ_s = Maximum height of the stenosis
30. R_0 = Radius of artery
31. L_0 = Length of stenosis
32. d = Location of stenosis
33. (V_1, ω) = Rotation suspension speed and velocity in the region $0 \leq r \leq R_1$
34. V_2 = Velocity of fluid in the region $R_1 \leq r \leq R_2$
35. (μ, β, γ) = Viscosities and gradients of particle angular velocities
36. $\frac{dp}{dz}$ = Pressure gradient
37. r = Radial co-ordinate
38. C_1 and C_2 = Solute concentration
39. m_1 and m_2 = Rate of production or degeneration of cells
40. D_1 and D_2 = Diffusion co-efficient of under solved cells
41. $\frac{\partial p}{\partial z}$ = Axial pressure gradient

42. Q_C = Critical value when crack occur
43. E = Young modulus
44. S = Surface tension
45. η = Possion ratio
46. c = Crack length
47. G_c = Crack extension force
48. $(\alpha, \overline{\eta}, \epsilon, T)$ = Various physiological parameters
49. (A, B, C, D) = Arbitary constants
50. a_{11} and a_{66} = Elastic constants of orthotropic medium
51. (ϕ, ψ) = New functions
52. J_{31} = Complete elliptic integral of first kind
53. $(J_4, J_5, ...)$ = Numerically constants
54. ($P_1(x)$, $P_2(x)$) = Crack opening forces
55. ($U_y(x, 0^+)$, $U_y(x, 0^-)$) = Displacement components
56. ($\sigma_{xy}(x, 0^+)$, $\sigma_{xy}(x, 0^-)$) = Stress components
57. $\delta(x)$ = Kernal functions
58. Π = Elliptic integral of third kind

Bibliography

[1] Kapur, J. N. (1985). Mathematical models in biology and medicine. Affiliated East-West Press.

[2] Mitchell, J. W., Myers, G. E. (1968). An analytical model of the counter-current heat exchange phenomena. Biophysical journal, 8(8), 897-911.

[3] Fung, Y. C. (1971). Biomechanics: A survey of the blood flow problem. Advances in Applied Mechanics, 11, 65-130.

[4] Ranvir, L. (1874). Note Sur Les Vasseal Sanguim et al circulation Dansles Muscles Rouges Arch . Physiol. Norm. Path. 1 445.

[5] Spaltcholz, W. (1980). Die vertheiling der bultgefassa in Muske . Apl, Sachs. Ger. Wiss. Phys, 14, 509.

[6] Krogh, A. (1919). The number and distribution of capillaries in muscles with calculations of the oxygen pressure head necessary for supplying the tissue. The Journal of physiology, 52(6), 409.

[7] Krogh, A. (1929). The Anatomy and Physiology of Capillaries. Yale U. Press, New Haven, CT, reprinted 1959. Hafner, NY.

[8] Roughton, F. J. W. (1952). Diffusion and chemical reaction velocity in cylindrical and spherical systems of physiological interest. Proceedings of the Royal Society of London. Series B-Biological Sciences, 140(899), 203-229.

[9] Kety, S. (1970). Determinants of tissue oxygen tension. Fed. Prof. 16, 666.

[10] Taylor, M. G. (1973). Hemodynamics. Annual Review of Physiology, 35(1), 87-116.

[11] Sakalak, R. a·nd Sathis, t. (1966). A po r ous tapered elastic tube of a vascular Bed. symposium on Biomechanics, A.S . ME . , New York, p . 66.

[12] Bergel, D.H. (1972). Cardiovascular Fluid Dyna mics. Acadamic Press, London 2.

[13] Patel, D. J., Vaishnav, R. N., Gow, B. S., Kot, P. A. (1974). Hemodynamics. Annual review of physiology, 36(1), 125-154.

[14] Tammann, G. H. W. Z., Hesse, W. (1926). The dependence of viscosity upon the temperature of supercooled liquids. Z. Anorg. Allg. Chem, 156(1), 245-257.

[15] Harkness, M. L., Harkness, R. D., McDonald, D. A. (1957). The collagen and elastin content of the arterial wall in the dog. Proceedings of the Royal Society of London. Series B-Biological Sciences, 146(925), 541-551.

[16] Švejcar, J. (1962). Biology and psychology in pediatrics. Československá Pediatrie.

[17] Dintenfass, L. (1965). Some observations on the viscosity of pathological human blood plasma. Thrombosis and Haemostasis, 13(02), 492-499.

[18] Chien, S., Usami, S., Dellenback, R. J., Gregersen, M. I. (1970). Shear-dependent interaction of plasma proteins with erythrocytes in blood rheology. American Journal of Physiology-Legacy Content, 219(1), 143-153.

[19] Somer, T. (1966). The viscosity of blood, plasma and serum in dys-and paraproteinemias. Acta medica Scandinavica. Supplementum, 456, 1-97.

[20] Merrill, L.W., Gilliland, E.H. ,Cokelet G. R., Shin, H., Britten, A. and Wells R.E. (1963). Rheology of Hum an Blood, Effect of Temperature and Hematocrit. Biophys. J., 1, p. 199.

[21] Barbee, J. H. (1973). The effect of temperature on the relative viscosity of human blood. Biorheology, 10(1), 1-5.

[22] Mitvalský, V. (1965). Heat transfer in the laminar flow of human blood through tube and annulus. Nature, 206, 307-307.

[23] Charm, S.E. and Kurland, G. S. (1974). Blood Flow and Micro-circulation. John Wiley and sons , New York.

[24] Roach, M.R. (1963). An Experimental study production and time poststenotic Dilatation of course in of the Femoral and carotid Arteries of Adult Dogs. Gire. Res., 13 p. 537.

[25] Rodbard, S. (1966). Dynamics of blood flow in stenotic vascular lesions. American heart journal, 72(5), 698-704.

[26] Nerm R.M. and Guyton J.R. (1980). Hemodynamics and arterial wall. Proc . from a specialists meeting Univ. of Honston Taxas , Nov . 5-7.

[27] Ross, R. (1986). The pathogenesis of atherosclerosis—an update. New England journal of medicine, 314(8), 488-500.

[28] May, A.G., Deweese J.A. and Rob, C.G. (1962). Hemodynamics Effect of Arterial and stenosis. Surgery, 53 p. 513.

[29] Eklöf, B., Schwartz, S. I. (1970). Critical stenosis of the carotid artery in the dog. Scandinavian Journal of Clinical and Laboratory Investigation, 25(4), 349-353.

[30] Fry, P., Harkness, M. L., Harkness, R. D., Nightingale, M. (1962). Mechanical properties of tissues of lathyritic animals. The Journal of Physiology, 164(1), 77

[31] Caro, C. G., Fitz-Gerald, J. M., Schroter, R. C. (1971). Atheroma and arterial wall shear-observation, correlation and proposal of a shear dependent mass transfer mechanism for atherogenesis. Proceedings of the Royal Society of London. Series B. Biological Sciences, 177(1046), 109-133.

[32] Rodkiewicz, C. M. (1974). Atherosclerotic formations in the light of fluid mechanics.

[33] Bergel, D. H., Nerem, R. M., Schwartz, C. J. (1976). Fluid dynamic aspects of arterial disease. Atherosclerosis, 23(2), 253-261.

[34] Young, D. F. (1979). Fluid mechanics of arterial stenoses.

[35] Forrester, J. H., Young, D. F. (1970). Flow through a converging-diverging tube and its implications in occlusive vascular disease—I: Theoretical development. Journal of Biomechanics, 3(3), 297-305.

[36] Lee, J. S., Fung, Y. C. (1970). Flow in locally constricted tubes at low Reynolds numbers.

[37] Hung, T. K., Macagno, E. O. (1966). Laminar eddies in a two-dimensional conduit expansion. La Houille Blanche, (4), 391-401.

[38] Cheng, L. C., Robertson, J. M., Clark, M. E. (1973). Numerical calculations of plane oscillatory non-uniform flow—II. Parametric study of pressure gradient and frequency with square wall obstacles. Journal of Biomechanics, 6(5), 521-538.

[39] Morgan, B. E., Young, D. F. (1974). An intergral method for the analysis of flow in arterial stenoses. Bulletin of Mathematical Biology, 36, 39-53.

[40] Despande, M. D., Gidden, D. P., Mahon, R. F. (1976). Steady laminar flow through modelled vascular stenosis. J Biomech, 9, 165-174.

[41] McDonald, D. A. (1979). On steady flow through modeled vascular stenosis. J. Biomech, 12, 13-20.

[42] Daly, B. J. (1976). A numerical study of pulsatile flow through stenosed canine femoral arteries. Journal of Biomechanics, 9(7), 465-475.

[43] Haynes, R. H., Burton, A. C. (1959). Role of the non-Newtonian behavior of blood in hemodynamics. American Journal of Physiology-Legacy Content, 197(5), 943-950.

[44] Haynes, R. H. (1960). Physical basis of the dependence of blood viscosity on tube radius. American Journal of Physiology-Legacy Content, 198(6), 1193-1200.

[45] Whitmore, R. L. (1968). Rheology of the Circulation. Pergamon.

[46] Lih, M. M. (1969). A mathematical model for the axial migration of suspended particles in tube flow. The bulletin of mathematical biophysics, 31, 143-157.

[47] Lih, M. M. S. (1975). Transport phenomena in medicine and biology. Wiley.

[48] Middleman, S. (1972). Transport phenomena in the cardiovascular system. In Transport phenomena in the cardiovascular system (pp. 299-299).

[49] Shukla, J. B., RS, P. (1980). Biorheological aspects of blood flow through artery with mild stenosis: effects of peripheral layer.

[50] Shukla, J. B., Parihar, R. S., Gupta, S. P. (1980). Effects of peripheral layer viscosity on blood flow through the artery with mild stenosis. Bulletin of Mathematical Biology, 42, 797-805.

[51] Shukla, J. B., Parihar, R. S., Rao, B. R. P. (1980). Effects of stenosis on non-Newtonian flow of the blood in an artery. Bulletin of Mathematical Biology, 42, 283-294.

[52] US Department of Health and Human Services. (1983). The health consequences of smoking: cardiovascular disease. A report of the Surgeon General.

[53] Microrheology, B. (1971). Butterworths.

[54] Dintenfass, L. (1976). Rheology of Blood in Diagnostic and Preventive Medicine: An Introduction to Clinical Haemorheology. Butterworths.

[55] Juhan, I., Buonocore, M., Jouve, R., Vague, P. H., Moulin, J. P., Vialettes, B. (1982). Abnormalities of erythrocyte deformability and platelet aggregation in insulin-dependent diabetics corrected by insulin in vivo and in vitro. The Lancet, 319(8271), 535-537.

[56] Barnes, A. J., Locke, P., Scudder, P. R., Dormandy, T. L., Dormandy, J. A., Slack, J. (1977). Is hyperviscosity a treatable component of diabetic microcirculatory disease?. The Lancet, 310(8042), 789-791.

[57] Tandon, P. N., Agarwal, R. (1989). Pipe a simple model for human bronchial tube. Ganita, 37, 74.

[58] Reid, H. L., Dormandy, J. A., Barnes, A. J., Lock, P. J., Dormandy, T. L. (1976). Impaired red cell deformability in peripheral vascular disease. The Lancet, 307(7961), 666-668.

[59] Dormandy, J., Boyd, M., Ernst, E. (1981). Red cell filterability after myocardial infarction. Scandinavian Journal of Clinical and Laboratory Investigation, 41(sup156), 195-198.

[60] Gordon, R. G., Roemer, R. B., Horvath, S. M. (1976). A mathematical model of the human temperature regulatory system-transient cold exposure response. IEEE Transactions on Biomedical Engineering, (6), 434-444.

[61] Hodson, D. A., Eason, G., Barbenel, J. C. (1986). Modeling transient heat transfer through the skin and superficial tissues—1: Surface insulation.

[62] Hwang, C. L., Konz, S. A. (1977). Engineering models of the human thermoregulatory system-a review. IEEE Transactions on biomedical engineering, (4), 309-325.

[63] Wulff, W. (1974). The energy conservation equation for living tissue. IEEE transactions on biomedical engineering, (6), 494-495.

[64] Guyton A.C. (1976). Textbook of Medical Physiology, W.B. Saunders 904-984.

[65] Clegg, S. T., Roemer, R. B. (1985). A study of the effect of sensor placement and perfusion pattern variations on thermal tomography solutions in hyperthermia. IEEE transactions on biomedical engineering, (9), 677-682.

[66] Antich, P. P., Tokita, N., Kim, J. H., Hahn, E. W. (1978). Selective heating of cutaneous human tumors at 27.12 MHz. IEEE Transactions on Microwave Theory and Techniques, 26(8), 569-572.

[67] Taylor, L. S. (1980). Implantable radiators for cancer therapy by microwave hyperthermia. Proceedings of the IEEE, 68(1), 142-149.

[68] Stauffer, P. R., Cetas, T. C., Jones, R. C. (1984). Magnetic induction heating of ferromagnetic implants for inducing localized hyperthermia in deep-seated tumors. IEEE Transactions on Biomedical Engineering, (2), 235-251.

[69] Elkowitz, A. B., Shitzer, A., Eberhart, R. C. (1982). Transient temperature profiles in tissues with nonuniform blood flow distributions.

[70] Gordon, R. G., Roemer, R. B., Horvath, S. M. (1976). A mathematical model of the human thermal system. Bull. Mathematical Biophys. (26) 147-166.

[71] Stolwijk, J. A. (1971). A mathematical model of physiological temperature regulation in man (No. NASA-CR-1855). NASA.

[72] Fan,L.T., Hsu, F.T. and Hwag C.L. (1971). A Review on Medical Models of Human Thermal System,' IEEE Trans.of BME, 218-234.

[73] Eberhart, R. C., Shitzer, A. (Eds.). (1985). Heat Transfer in Medicine and Biology: Plenum Press, New York. Volume 1.

[74] Gray, H. (1973). Text Book of Gray's Anatomy.

[75] Sinclair, D. C., Ryan, T. J. (1973). The Physiology and Pathophysiology of the Skin. Academic Press.

[76] Montagna, W. (1956). The Structure and Function of Skin Academic Press, I nc New York. N. Y.

[77] Thews,G. (1960). Oxygen diffusion in brain , a contribution to the question of oxygen supply of the organs. Pflugers Archio, 271, 197.

[78] Krogh, A. (1922). The anatomy and physiology of capillaries. Yale University Press.

[79] Fahraeus, R., Lindqvist, T. (1931). The viscosity of the blood in narrow capillary tubes. American Journal of Physiology-Legacy Content, 96(3), 562-568.

[80] Florey, H. W. (1964). The transport of materials across the capillary wall. Quarterly Journal of Experimental Physiology and Cognate Medical Sciences: Translation and Integration, 49(2), 117-128.

[81] Blum, J. J. (1960). Concentration profiles in and around capillaries. American Journal of Physiology-Legacy Content, 198(5), 991-998.

[82] Salathé, E. P., Wang, T. C. (1980). Substrate concentrations in tissue surrounding single capillaries. Mathematical Biosciences, 49(3-4), 235-247.

[83] Ranke O.I. (1934). Die Daemfung derpulswelle and die innire Reelung der Anterten ward' Lalscher Biol. 95 179 (1934)

[84] Gow, B. S., Taylor, M. G. (1968). Measurement of viscoelastic properties of arteries in the living dog. Circulation research, 23(1), 111-122.

[85] Craine, R. E., Green, A. E., Naghdi, P. M. (1969). A mixture of viscous elastic materials with different constituent temperatures. CALIFORNIA UNIV BERKELEY DIV OF APPLIED MECHANICS.

[86] Chien, S., Usami, S., Dellenback, R. J., Gregersen, M. I. (1970). Shear-dependent interaction of plasma proteins with erythrocytes in blood rheology. American Journal of Physiology-Legacy Content, 219(1), 143-153.

[87] Reneau Jr, D. D., Bruley, D. F., Knisely, M. H. (1967). A mathematical simulation of oxygen release, diffusion, and consumption in the capillaries and tissue of the human brain. In Chemical Engineering in Medicine and Biology: Proceedings of the Thirty-Third Annual Chemical Engineering Symposium of the Division of Industrial and Engineering Chemistry of the American Chemical Society, Held at the University of Cincinnati, on October 20–21, 1966 (pp. 135-241). Boston, MA: Springer US.

[88] Reneau Jr, D. D., Bruley, D. F., Knisely, M. H. (1969). A digital simulation of transient oxygen transport in capillary-tissue systems (cerebral grey matter). Development of a numerical method for solution of transport equations describing coupled convection-diffusion systems. AIChE Journal, 15(6), 916-925.

[89] Reneau, D. D., Knisely, M. H. (1971). A mathematical simulation of oxygen transport in the human brain under conditions of countercurrent capillary blood flow(Oxygen distribution in human brain under countercurrent capillary blood flow conditions, presenting mathematical simulation for transport in Krogh system). In Chemical Engineering Progress, Symposium Series (No. 114, pp. 18-27).

[90] Reneau, D. D. (1970). A computer simulation of prediction of oxygen limitations in cerebral gray matter. J. Assoc. Adv. Med. Inst., 4, 211-223.

[91] Thews, G. (1968). The theory of oxygen transport and its application to gaseous exchange in the lung. In Oxygen transport in blood and tissue (pp. 1-20). Thieme Stuttgart.

[92] Gonzalez-Fernandez, J. M., Atta, S. E. (1968). Transport and consumption of oxygen in capillary-tissue structures. Mathematical Biosciences, 2(3-4), 225-262.

[93] Fletcher, J. E. (1973). A mathematical model of the unsteady transport of oxygen to tissues in the microcirculation. Oxygen Transport to Tissue: Pharmacology, mathematical studies, and neonatology, 819-825.

[94] Fletcher, J. E. (1975). A model describing the unsteady transport of substrate to tissue from the microcirculation. SIAM Journal on Applied Mathematics, 29(3), 449-480.

[95] Popel, A. S. (1978). Analysis of capillary-tissue diffusion in multicapillary systems. Mathematical biosciences, 39(3-4), 187-211.

[96] Salathé, E. P. (1982). Mathematical modeling of oxygen transport in skeletal muscle. Mathematical Biosciences, 58(2), 171-184.

[97] Apelblat, A., Katzir-Katchalsky, A., Silberberg, A. (1974). A mathematical analysis of capillary-tissue fluid exchange. Biorheology, 11(1), 1-49.

[98] Nicolson, P., Roughton, F. J. W. (1951). A theoretical study of the influence of diffusion and chemical reaction velocity on the rate of exchange of carbon monoxide and oxygen between the red blood corpuscle and the surrounding fluid. Proceedings of the Royal Society of London. Series B-Biological Sciences, 138(891), 241-264.

[99] Hartridge, H., Roughton, F. J. W. (1923). A method of measuring the velocity of very rapid chemical reactions. Proceedings of the Royal Society of London. Series A, Containing Papers of a Mathematical and Physical Character, 104(726), 376-394.

[100] Roughton, F. J. W. (1964). Transport of oxygen and carbon dioxide. Handbook of physiology, 1, 767-825.

[101] Griffith, A. A. (1920). The phenomenon of rupture and flow in solids. Phil, Trans, Roy. Soc. A221.

[102] Griffith, A. (1924). The theory of rupture. In First Int. Cong. Appl. Mech (pp. 55-63).

[103] Lankford, J. (1980). On the small crack fracture mechanics problem. International Journal of Fracture, 16, R7-R9.

[104] Morozov, E. M. (1980). Some problems in experimental fracture mechanics. Engineering Fracture Mechanics, 13(3), 541-561.

[105] Jarrett, A. (Ed.). (1973). The Physiology and Pathophysiology of the Skin: The sweat glands, skin permeation, lymphatics, the nails (Vol. 5). Academic Press.

[106] Nilsson, F., Brickstad, B. (1985). Dynamic fracture mechanics—rapid crack growth in linear and non-linear materials. In Elastic-Plastic Fracture Mechanics: Proceedings of the 4th Advanced Seminar on Fracture Mechanics, Joint Research Centre, Ispra, Italy, 24–28 October 1983 in collaboration with the European Group on Fracture (pp. 427-478). Springer Netherlands.

[107] Russo, R. (1985). Some classical theorems in fracture theory. Theoretical and applied fracture mechanics, 3(3), 179-184.

[108] Yokobori, T., Kamei, A., Kounosu, S. (1984). A concept of combined micro and macro fracture mechanics to brittle fracture. International Journal of Fracture, 26, 352-354.

[109] Ståhle, P. (1983). On the small crack fracture mechanics. International Journal of Fracture, 22, 203-216.

[110] Lemaitre, J. (1986). Local approach of fracture. Engineering Fracture Mechanics, 25(5-6), 523-537.

[111] Forrester, J. H., Young, D. F. (1970). Flow through a converging-diverging tube and its implications in occlusive vascular disease—II: Theoretical and experimental results and their implications. Journal of biomechanics, 3(3), 307-316.

[112] Fox, J. A., Hugh, A. E. (1966). Localization of atheroma: a theory based on boundary layer separation. British Heart Journal, 28(3), 388.

[113] Ritchie, R. O., Knott, J. F., Rice, J. R. (1973). On the relationship between critical tensile stress and fracture toughness in mild steel. Journal of the Mechanics and Physics of Solids, 21(6), 395-410.

[114] Lal, M. (1982). Some axially symmetric thermal stress distributions in an elastic solid containing an annular crack. International Journal of Engineering Science, 20(11), 1261-1273.

[115] Lal, M. and Pandey, D. (1975). The axisymmetric thermoelastic stress distrubution in an infinite solid containing a penny-shaped crack. Proc. Nat. Acad. Sci., India, 45(A), pp. 175-180.

[116] Tweed, J., Melrose, G. (1988). The thermal stresses due to a uniform heat flow past two collinear cracks. International journal of engineering science, 26(10), 1053-1057.

[117] Kushwaha, P. S., Chandra, U. (1979). The stress intensity factor for a Griffith crack opened by thermal stresses in an infinite solid. Proc. 24th Congress of IST AM pp. I 09- 210.

[118] Kushwaha, P. S., Chandra, U. (1980). The stress intensity factors for Griffith-crack(s) opened by thermal stresses in an infinite solid", Proc. 25th Congress of lSTAM pp. 130-138.

[119] Kushwaha, P. S., Chandra, U. (1982). The stress intensity factors for Griffith-crack opened by thermal stresses in an infinite strip. ActaCincia India, VIII M, No. 3 p. 152.

[120] Dwivedi, A.P., Awasthi, R.D. and Singh, Roli. (1993). Stress intensity factors for two Griffith cracks opened by symmetrical system of body forces in a stress free strip. J.M.A.C.T., pp. 55-68.

[121] Dwivedi A.P ., Kushwaha, P.S. and Awasthi, R.D. (1978). A Griffith crack opened by symmetrical system of body forces in stress free-strip. 1ST AM Proc pp. 15-20.

[122] Dwivedi, A.P. and Awasthi, R.D. (1982). Exterior cracks in a stress free strip opened by body forces. Indian J. Math., 24 pp. 1-12.

[123] Sneddon, I. N., Tweed, J. (1967). The stress intensity factor for a Griffith crack in an elastic body in which body forces are acting. International Journal of Fracture Mechanics, 3, 317-330.

[124] Sneddon, I. N., Tweed, J. (1967). The stress intensity factor for a penny-shaped crack in an elastic body under the action of symmetric body forces. International Journal of Fracture Mechanics, 3, 291-299.

[125] Sneddon, I. N. and Tweed J.(1970). The stress intensity factors for a Griffith-crack an elastic body m which there 1s an asymmetrical distribution of body forces. Proc. Roy. Soc. Edinb., A(68), pp. 309-321.

[126] Kushwaha, P. S. (1978). Stress intensity factor in orthotropic medium in the presence of symmetrical body forces. International Journal of Fracture, 14, 443-451.

[127] Byskov, E. (1984). The calculation of S.I.F. usmg finite element method with cracked elements Int. J. Fracture, 26, pp. 329-337.

[128] Forsythe, G. E., Wasow, W. R. (1960). Finite Difference Method for partial Differential Equations, New York; John WileySons.

[129] Steif, P. S. (1985). A superposition procedure for computing stress intensity factors in cracked elastic composites. International journal of fracture, 29, 223-233.

[130] Bowie, O. L. (1964). Rectangular tensile sheet with symmetric edge cracks.

[131] Ioakimidis, N. I. (1980). A new class of approximate formulas for the evaluation of stress intensity factors. International Journal of Fracture, 16, R143-R146.

[132] Ioakimidis, N. I. (1983). Simple bounds for the stress intensity factors by the method of singular integral equations. Engineering fracture mechanics, 18(6), 1191-1198.

[133] Wei, Lixiao and Wen. (1983). Section method for calculation of stress intensity factors. Engng. Fract. Mech. Vol. ll., pp. 161-169.

[134] Carpenter, W. C. (1983). Extrapolation techniques for determining stress intensity factors. Engineering Fracture Mechanics, 18(2), 325-332.

[135] Hahn, G. T., Rosenfield, A. R. (1975). Metallurgical factors affecting fracture toughness of aluminum alloys. Metallurgical Transactions A, 6, 653-668.

[136] Green, G. (1889). An essay on the application of mathematical analysis to the theories of electricity and magnetism (Vol. 3). author.

[137] Sneddon, I. N., Berry, D. S. (1958). The classical theory of elasticity. Elasticity and Plasticity/Elastizität und Plastizität, 1-126.

[138] Muskhelishvili, N. I. (1953). Some basic problems of the mathematical theory of elasticity (Vol. 15). Groningen: Noordhoff.

[139] Westergaard, H. M. (1997). Bearing pressures and cracks.

[140] Raftopoulos, D. D., Farahmand, B. (1982). An investigation of stress intensity factors for plates with equal and unequal parallel edge cracks. International Journal of Fracture, 20, 223-239.

[141] Navier, S. L. M. H. (1821). Mém. Acad. Sci. Inst. France.

[142] Dwivedi, A.P., Pandey, Sarita and Tiwari, D.N. (1991). Thermal stress in a bonded dissimilar elastic half plane containing a Griffith crack at the interface. J.M.A.C.T., 24, pp. 79 -89.

[143] Florence, A. L., Goodier, J. N. (1963). The linear thermoelastic problem of uniform heat flow disturbed by a penny-shaped insulated crack. International Journal of Engineering Science, 1(4), 533-540.

[144] Georgiadis, H. G., Papadopoulos, G. A. (1987). Determination of SIF in a cracked plane orthotropic strip by the Wiener-Hopf technique. International Journal of Fracture, 34, 57-64.

[145] Kushwaha, P.S.Kushwaha, P.S.ushwaha, P.S.(1974). The stress field m the neighbourhood of Griffith crack in an infinite medium - A new approach. 40th Annual Conference of I.M.S. held at I.LT., Bombay pp. 26-29.

[146] Oleziak, A. and Sneddon, I.N. (1960). The distribution of thermal stresses m an infinite elastic solid containing a penny-shaped crack. Arch. Rat. Mech. And Analysis, 1, p. 238.

[147] Paul, H. S., Sridharan, K. (1980). The penny-shaped crack problem in micropolar thermoelasticity. International Journal of Engineering Science, 18(12), 1431-1448.

[148] Young, D. (1968). Effect of a time-dependent stenosis on flow through a tube.

[149] Shail, R. (1964). Some thermoelastic stress distributions in an infinite solid and a thick plate containing penny-shaped cracks. Mathematika, 11(2), 102-118.

[150] Umesh Chandra (1987). A Ph.D. thesis entitled as Two dimensional mixed boundary value problems in a strip. Agra University.

[151] Transter, C. J. (1952). Fourier Transforms. By IN Sneddon. p. xii, 542. 85s. 1951.(McGraw-Hill). The Mathematical Gazette, 36(318), 290-291.

[152] Sneddon I.N. and Lowengrub, M. (1969). The crack problems in mathematical theory of elasticity. John Wiloy Sons.

[153] Mensheh Ju Ju (1969). The relation between the temperature of the skin and that of Muscles during working and rest. (In Zb the physiological basis of working Regimes) pp 111-18.

[154] Saltin, B., Jagge, A. P. and Stolwijk, I. A. (1968). Muscle temperature during submaximal exercise in man. Journal of Applied physiol, 25, pp 679-688.

[155] Stow, R. W. and Shieve, I.F. (1970). Measurement of blood flow in minute volume of specific tissue in man. Journal of Applied physiology, 14, pp 215.

[156] Zavyalov, V. I. (1969). Temperature change characteristics in skin over the muscles of man at different regime of work. The Physiological basis for working Regimes, pp 75-80.

[157] Hill, A. V. (1910). The possible effects of the aggregation of the molecules of hemoglobin on its dissociation curves. j. physiol., 40, iv-vii.

[158] Shitzer, A. (1975). Studies of bio-heat transfer in mammals. Topics in transport phenomena: Bioprocesses, mathematical treatment, mechanisms.(A 76-23569 09-34) Washington, D. C., Hemisphere Publishing Corp., 211-343.

[159] Stolwizk J. A., (1971). Mathematical Model thermoregulation. In Physiological and Behavioura.

[160] Chato, J. C. (1969). Heat transfer in bioengineering. Advanced Heat Transfer, 111, 395-412.

[161] Shitzer, A., Chato, J. C. (1971). Analytical solutions to the problem of transient heat transfer in living tissue (No. ASME PAPER 71-WA/HT-36).

[162] Zhitomirskii, I. S., Kagna, A. A. (1978). A theoretical study of the temperature distribution in skeletal muscle undergoing rhythmic contractions. Bulletin of Mathematical Biology, 40, 535-540.

[163] Keller, K. H., Seiler Jr, L. (1971). An analysis of peripheral heat transfer in man. Journal of Applied Physiology, 30(5), 779-786.

[164] Torell, L. M., Nilsson, S. K. (1980). Calculation of skin temperature increase caused by subcutaneous veins perpendicular to the skin surface. Physics in Medicine Biology, 25(1), 85.

[165] Steketee, J., Van Der Hoek, M. J. (1979). Thermal recovery of the skin after cooling. Physics in Medicine Biology, 24(3), 583.

[166] Collins, J. C., Pilkington, T. C., Schmidt-Nielsen, K. (1971). A model of respiratory heat transfer in a small mammal. Biophysical journal, 11(11), 886-914.

[167] Burton, A. C. (1934). The application of the theory of heat flow to the study of energy metabolism: Five figures. The Journal of Nutrition, 7(5), 497-533.

[168] Scholander, P. F., Krog, J. (1957). Countercurrent heat exchange and vascular bundles in sloths. Journal of Applied Physiology, 10(3), 405-411.

[169] Pye, G., Bowker, P. (1976). Skin temperature as an indicator of stress in soft tissue. Engineering in medicine, 5(3), 58-60.

[170] Burton, A. C. and Edholm, O. G. (1955). Man in Cold Environment. Williamand Winkins, Baltiomore, Md, chap 5.

[171] Hardy, J. D., Soderstrom, G. F. (1938). Heat Loss from the Nude Body and Peripheral Blood Flow at Temperatures of 22° C. to 35° C. Two Figures. The journal of Nutrition, 16(5), 493-510.

[172] Lefever, J. (1911). Chaleur Animal et' Bioenergetique. Paris Masson, pp 393.

[173] Cooper, K. E., Edholm, O. G., Mottram, R. F. (1955). The blood flow in skin and muscle of the human forearm. The Journal of Physiology, 128(2), 258.

[174] Pennes, H. H. (1948). Analysis of Tissue and Arterial Blood Temperatures in the resting Human Forearm. Journal of Physiol, 1, pp 93-122.

[175] Wissler, E. H. (1966). A mathematical Model of Human thermal System. Chem. Engg Prog sympser, pp 62-65.

[176] Gupta, N. K., Tandon, P. N., Kachhara, N. L. (1986). Temperature Distribution in two layered undergoing Phythmic Contration. Journal of Institution of Engineers, pp 66.

[177] Fu, M., Yu, T., Zhang, H., Arens, E., Weng, W., Yuan, H. (2014). A model of heat and moisture transfer through clothing integrated with the UC Berkeley comfort model. Building and environment, 80, 96-104.

[178] Kaur, H. (2022, May). Heat transfer between skin and core with the help of mathematical modelling. In Journal of Physics: Conference Series (Vol. 2267, No. 1, p. 012067). IOP Publishing.

[179] Singh, M. P., Khetarpal, K., Sharan, M. (1980). A theoretical model for studying the rate of oxygenation of blood in pulmonary capillaries. Journal of Mathematical Biology, 9, 305-330.

[180] Singh, M. P., Sharan, M., Verma, S. B. (1982). Transport of gases in Pulmonary capillaries—a computation of equilibrium constants arising in the oxygen dissociation curve. Journal of Biomedical Engineering, 4(4), 279-284.

[181] Karis, Xu, X., Buller, A. J. Santee, W. R. (2013). Relationship between core temperature, skin temperature, and heat flux during exercise in heat. European journal of applied physiology, 113, 2381-2389.

[182] Salimpour, M. R., Shirani, E. (2017). Heat transfer analysis of skin during thermal therapy using thermal wave equation. Journal of thermal biology, 64, 7-18.

[183] Ichikawa, Y., Ogino, T. (2024). Quantitative Assessment of the Heat Transfer Capacity of Ice Bags and their Cooling Effects on the Skin Surface and Core Temperature. Acta Medica Okayama, 78(1), 53-61.

[184] Rhodes, C. E., Denault, D., Varacallo, M. (2019). Physiology, oxygen transport.

[185] Richardson, S. L., Hulikova, A., Proven, M., Hipkiss, R., Akanni, M., Roy, N. B., Swietach, P. (2020). Single-cell O2 exchange imaging shows that cytoplasmic diffusion is a dominant barrier to efficient gas transport in red blood cells. Proceedings of the National Academy of Sciences, 117(18), 10067-10078.

[186] Buradi, A., Morab, S., Mahalingam, A. (2019). Effect of stenosis severity on shear-induced diffusion of red blood cells in coronary arteries. Journal of Mechanics in Medicine and Biology, 19(05), 1950034.

[187] Munir, I. D., Jaafar, N. A., Shafie, S. (2022). Effect of Catheter and Stenosis on Solute Diffusion in Non-Newtonian Blood Flow through a Catheterized Stenosed Artery. CFD Letters, 14(12), 11-26.

[188] Ramana Reddy, J. V., Ha, H., Sundar, S. (2023). Modelling and simulation of fluid flow through stenosis and aneurysm blood vessel: A computational

hemodynamic analysis. Computer Methods in Biomechanics and Biomedical Engineering, 26(10), 1160-1182.

[189] Ramasamy, P., Murugan, D. (2022). Transport of a reactive solute in electro-osmotic pulsatile flow of non-newtonian fluid through a circular conduit. Authorea Preprints.

[190] Ponalagusamy, R., Murugan, D. (2023). Transport of a reactive solute in electroosmotic pulsatile flow of non-Newtonian fluid through a circular conduit. Chinese Journal of Physics, 81, 243-269

[191] Singh, M. P., Sharan, M., Aminataei, A. (1989). Development of mathematical formulae for O_2 and CO_2 dissociation curves in the blood. Mathematical Medicine and Biology: A Journal of the IMA, 6(1), 25-46.

[192] Sharan, M., Singh, M. P. (1984). Equivalence between one step kinetics and Hill's equation. Journal of biomedical engineering, 6(4), 297-301.

[193] Sharan, M., Singh, M. P. (1985). Numerical simulation of pulmonary O_2 and CO_2 exchange. International journal of bio-medical computing, 16(1), 59-80.

[194] Leonard, E. F., Jørgensen, S. B. (1974). The analysis of convection and diffusion in capillary beds. Annual review of biophysics and bioengineering, 3(1), 293-339.

[195] Bloch, I. (1943). Some theoretical considerations concerning the interchange of metabolites between capillaries and tissue. The bulletin of mathematical biophysics, 5, 1-14.

[196] Renkin, E. M. (1959). Transport of potassium-42 from blood to tissue in isolated mammalian skeletal muscles. American Journal of Physiology-Legacy Content, 197(6), 1205-1210.

[197] Gonzalez-Fernandez, J. M., Atta, S. E. (1973). Maximal substrate transport in capillary networks. Microvascular Research, 5(2), 180-198.

[198] Kumar, P. (1982). Finite element analysis of mass transfer in creeping fluid flow through tubes: applications to blood flow. PhD diss., Indian Institute of Technology.

[199] Awasthi, A. K., Rachna, H. K. (2022). A Griffith Crack at the Interface of an Isotropic and Orthotropic Half Space Bonded Together.

[200] Singh, M. P., Sharan, R. K., Saxena, R. K., Malhotra, I. (1982). A theoretical model for the exchange of gases in the systemic capillaries and the surrounding tissues under compression—an application in underwater phys-

iology. In Finite Element Flow Analysis (pp. 867-875). University of Tokyo Press—North-Holland, Amsterdam.

[201] Sharan, M., Singh, M. P., Saxena, R. K., Sud, I. (1985). A Theoretical Study for the Oxygen and Carbon Dioxide Transport in the Systemic Circulation under Compression. In Physiological Fluid Dynamics I: Proceeding of the First International Conference on Physiological Fluid Mechanics, Madras, India, September 5-7, 1983 (p. 127). Committe on Science and Technology in Developing Countries (ICSU) and Scientific Committee on Physiological Fluid Dynamics, Indian Institute of Technology.

[202] Forster, R. E. (1964). Rate of gas uptake by red cells. Handbook of physiology, 1, 827-837.

[203] Moll, W. (1968). The influence of hemoglobin diffusion on oxygen uptake and release by red cells. Respiration physiology, 6(1), 1-15.

[204] Kutchai, H. (1970). Numerical study of oxygen uptake by layers of hemoglobin solution. Respiration Physiology, 10(3), 273-284.

[205] Ulanowicz, R. E., Frazier Jr, G. C. (1970). The transport of oxygen and carbon dioxide in hemoglobin systems. Mathematical Biosciences, 7(1-2), 111-129.

[206] Awasthi, A. K. Kaur. (2022). A numerical study of transport of O_2 and CO_2 in a red blood cell. AIP Conference series.

[207] Siddiqu, S. U. (1984). Microstructural and Peripheral Layer Viscosity Effects on Blood Flow through a Tube with Small Construction. Journal of the Institution of Engineers (India).: Interdisciplinary general engineering, 65, 60.

[208] P. N. Tandon, Agarwal, Rekha. (1987). A new model of get formation on articular surface in normal and pathological states. Pro. Of 15th National conference on F. M. and F.P. held at Srinagar 22-24 july, 345.

[209] Tandon, P. N., Misra, J. K. (1983). Microstructural and peripheral layer viscosity effects on the flow of blood through an artery with mild stenosis. Annals of the New York Academy of Sciences, 404(1), 59-62.

[210] Burns, J. C., Parkes, T. (1967). Peristaltic motion. Journal of Fluid Mechanics, 29(4), 731-743.

[211] Crone, C., Lassen, N. A. (Eds.). (1970). Capillary permeability (pp. 446-455). Copenhagen: Munksgaard.

[212] Gould, K. L., Lipscomb, K. (1974). Effects of coronary stenoses on coronary flow reserve and resistance. The American journal of cardiology, 34(1), 48-55.

[213] Chow, J. C., Soda, K. (1972). Laminar flow in tubes with constriction. The Physics of Fluids, 15(10), 1700-1706.

[214] Ariman, T., Turk, M. A., Sylvester, N. D. (1974). On steady and pulsatile flow of blood.

[215] Einav, S., Berman, H. J., Fuhro, R. L., DiGiovanni, P. R., Fine, S., Fridman, J. D. (1975). Measurement of velocity profiles of red blood cells 194 in the microcirculation by laser Doppler anemometry (LDA). Biorheology, 12(3-4), 207-210.

[216] Gupta, B. B., Seshadri, V. (1977). Flow of red blood cell suspensions through narrow tubes. Biorheology, 14(2-3), 133-143.

[217] Chaturani, P., Upadhya, V. S. (1979). A two-fluid model for blood flow through small diameter tubes. Biorheology, 16(1-2), 109-118.

[218] Chaturani, P., Mahajan, S. P. (1982). Poiseuille flow of micropolar fluid with non-zero couple stress at boundary with applications to blood flow. Biorheology, 19(4), 507-518.

[219] Chaturani, P. (1979). Flow of couple stress fluid through narrow tubes by sigma phenomenon and marginal zone theory with applications to blood flow. Biorheology, 16(6), 377-386.

[220] Stokes, V. K., Stokes, V. K. (1984). Couple stresses in fluids. Theories of Fluids with Microstructure: An Introduction, 34-80.

[221] Bitoun, J. P., Bellet, D. (1986). Blood flow through a stenosis in microcirculation. Biorheology, 23(1), 51-61.

[222] Radhakrishnamacharya, G., Chandra, P., Kaimal, M. R. (1981). A hydrodynamical study of the flow in renal tubules. Bulletin of mathematical biology, 43(2), 151-163.

[223] Cauchy, A. L. (1825). Memorie sur les integrales definies, prises entre des limites imaginaires. De Bure frères.

[224] Chakravarty, P., Mishra, R. R. (1986). The influence of VA mycorrhizae on the wilting of Albizia procera and Dalbergia sissoo. European journal of forest pathology, 16(2), 91-97.

[225] Perkkiö, J., Keskinen, R. (1983). Hematocrit reduction in bifurcations due to plasma skimming. Bulletin of Mathematical Biology, 45(1), 41-50.

[226] LUFT, J. H. (1965). The ultrastructural basis of capillary permeability. In The inflammatory process (pp. 121-159). Academic press.

[227] Valanis, K. C., Sun, C. T. (1969). Poiseuille flow of a fluid with couple stress with applications to blood flow. Biorheology, 6(2), 85-97.

[228] Awasthi, A. K. (2022, May). Fourier Series And Fourier Integral Equations And Their Applications In Elasticity. In Journal of Physics: Conference Series (Vol. 2267, No. 1, p. 012158). IOP Publishing.

[229] Awasthi, A. K., Rachna, and Rohit. (2023). A Formal Solution of Quadruple Series Equations, Mathematics and Statistics, Vol.11, No.1, 144-148. DOI: 10.13189/ms.2023.110116.

[230] Williams, M. L. (1957). On the stress distribution at the base of a stationary crack.

[231] Williams, M. (1959). The stresses around a fault or crack in dissimilar media. Bulletin of the seismological society of America, 49(2), 199-204.

[232] Erdogan, F. (1965). Stress distribution in bonded dissimilar materials with cracks.

[233] Rice, J. R., Sih, G. C. (1965). Plane problems of cracks in dissimilar media.

[234] Willis, J. R. (1971). Fracture mechanics of interfacial cracks. Journal of the Mechanics and Physics of Solids, 19(6), 353-368.

[235] Dwivedi, A. P., Sharma, J. P. (1980). Pair of coplanar Barenblatt cracks at the interface of two bounded dissimilar elastic half palnes. Ganita, 31.

[236] Dwivedi, P., and Kushwaha, S. P. (1981). The stress field due to a system of Griffith cracks at the interface of two bonded dissimilar wedge. J.M.A.C.T., Vol.14, 35-51.

[237] Lowengrub, M., Sneddon, I. N. (1973). The stress field near a Griffith crack at the interface of two bonded dissimilar elastic half-planes. International Journal of Engineering Science, 11(9), 1025-1034.

[238] El-Borai, M. M., EL-NADI, K. E. S. (2020). The Parabolic Transform and Some singular integral evolution equations. Journal of Mathematics and Statistics, 8(4), 410-415.

[239] Leontiev, V. L. (2020). Orthogonal splines in approximation of functions. Mathematics and Statistics, 8(2), 167-172.

[240] Tweed, J. (1969). The distribution of stress in the vicinity of a Griffith crack in an elastic solid in which body forces are acting. International Journal of Engineering Science, 7(8), 815-842.

[241] Griffith, A. A. (1921). VI. The phenomena of rupture and flow in solids. Philosophical transactions of the royal society of london. Series A, containing papers of a mathematical or physical character, 221(582-593), 163-198.

[242] Sneddon, I. N. (1995). Fourier transforms. Courier Corporation.

[243] Pompe, W. (1971). IN Sneddon/M. Lowengrub, Crack Problems in the Classical Theory of Elasticity.(The SIAM Series in Applied Mathematics). VIII+ 221 S. m. 57 Fig. New York/London/Sydney/Toronto 1969. John Wiley Sons, Inc. Preis geb. 140 s. net.

[244] Rawal, S. P., Gurland, J. (1977). Observations on the effect of cementite particles on the fracture toughness of spheroidized carbon steels. Metallurgical Transactions A, 8, 691-698.

[245] Panja, S. K., Mandal, S. C. (2021). Impact response of a finite crack in the presence of magnetic field. Engineering Fracture Mechanics, 253, 107851.

[246] Kumar, P., Mahanty, M., Singh, A. K., Chattopadhyay, A. (2021). Analytical study on stress intensity factor due to the propagation of Griffith crack in a crystalline monoclinic layer subjected to punch pressure. Fatigue Fracture of Engineering Materials Structures, 44(2), 475-487.

[247] Love, T. J . , Haber-man, J.D. and and Francis, J.E. (1971). A comparision of predicted skin temperature with the thermographic measurement temperature, its measurements and control in science and Industry.

[248] Duhamel, J. M. (1837). Second memoire sur les phenomenes thermomecaniques. Journal de l'École polytechnique, 15(25), 1-57.

[249] Nowacki, W., Thermoelasticity, P. P. (1962). Polish Science Publishers.

[250] Su, C. (1982). Actions of nicotine and smoking on circulation. Pharmacology Therapeutics, 17(1), 129-141.

[251] Muskhelishvili, N. I. (1955). Some basic problems of the mathematical theory of elasticity. 445-447.

[252] Cooper, M. L. (1978). Early contributions to the problems of elasticity. Physics Education, 13(6), 384.

[253] Awasthi, A. K. (2022, May). Fourier Series And Fourier Integral Equations And Their Applications In Elasticity. In Journal of Physics: Conference Series (Vol. 2267, No. 1, p. 012158). IOP Publishing.

[254] Spain, D.M. (1966). Atherosclerosis, Scientific American, 215 p.49.

[255] Divrik, A. M., Romer, R. B. and Catas, T. C. (1984). Inter Face of complete tissue temperature measured unconstrained fields from a few temperature:An Optimization Method. IEEE 150-160.

[256] Osilla, E. V., Marsidi, J. L., Sharma, S. (2018). Physiology, temperature regulation.

[257] Secomb, T. W. (2017). Blood flow in the microcirculation. Annual Review of Fluid Mechanics, 49, 443-461.

[258] Awasthi, A. K., Kaur, H., Tripathi, R. K., Khademi, M., Emadifar, H. (2023). A theoretical model for diffusion through stenosis. Heliyon, 9(11).

List of Publications				
S.no.	Title of paper	Name of Journal	Issn No and Pub. Date	Indexing
1	Bone crack inspired pair of Griffith crack opened by forces at crack faces	Mechanics of Advanced Materials and Structures	1537-6494 and 01/10/2023	SCI and SCOPUS (Q1)
2	A Theoretical Model for Diffusion through Stenosis	Helyion	2405-8440 and 07/11/2023	SCI and SCOPUS (Q1)
3	A Study of Nutritional Transport in Pulsatile Blood Through Time-Dependent Stenotic Tube	PLOS ONE	1932-6203 and Communicated	SCI and SCOPUS (Q1)
4	SIF And DF Of A Griffith Crack Problem Bounded Together Isotropic and Orthotropic Medium	Materials Today: Proceedings	2214-7853 and 2023	SCI and SCOPUS (Q2)
5	A Griffith Crack at the Interface of an Isotropic and Orthotropic Half Space Bonded Together	Mathematics and Statistics	2332-2144 and 27/12/2021	SCOPUS (Q3)

6	Heat transfer between skin and core with the help of mathematical modelling	Journal of Physics, Conference Series	1742-6596 and 9/12/2022	SCOPUS (Q4)
7	A Numerical Study of Transport of O_2 and CO_2 in the Red Blood Cell	AIP Conference Series	1551-7616 and 23/06/2023	SCOPUS (Q4)

List of Conferences			
S. NO.	Name of Conferences	Organization	Date
1	International Conference (RAFAS 2021)	School of Chemical Engineering and Physical Sciences, Lovely Professional University, Phagwara	June 25-26, 2021
2	International Conference on "Computational Applied Sciences and its Application" (AIP Conference Series)	University of Engineering and Management, Jaipur, Rajasthan	April 28-29, 2022

List of Workshops			
S. NO.	Name of Workshop/FDP	Organiser	Date
1	Workshop on Scientific Writing Using Typesetting Software Latex	Lovely Professional University	March 13-14, 2020
2	One Week Online Short Term Course on Mathematics Without Boundaries	NIT Srinagar	November 23-27, 2020
3	FDP on Big Data Analysis	Siddhartha Institute of Engineering and Technology	January 25-29, 2021

Published Paper 1

Heliyon 9 (2023) e20807

Contents lists available at ScienceDirect

Heliyon

journal homepage: www.cell.com/heliyon

Research article

A theoretical model for diffusion through stenosis

A.K. Awasthi [a], Harpreet Kaur [a], Rajendra Kumar Tripathi [b], Masoumeh Khademi [c], Homan Emadifar [c,d,*]

[a] Department of Mathematics, School of Chemical Engineering & Physical Sciences, Lovely Professional University, Phagwara, India
[b] Department of Applied Science & Humanities (Mathematics), Khwaja Moinuddin Chishti Language University, Lucknow, U.P., India
[c] Department of Mathematics, Hamedan Branch, Islamic Azad University, Hamedan, Iran
[d] MEU Research Unit, Middle East University, Amman, Jordan

ARTICLE INFO

Keywords:
Stenosis
Diffusion
Peripheral layer
Viscosity
Wall shearing
Disease
Velocity
Symmetric axially
Bessel functions

ABSTRACT

Stenosis is caused by an abnormal growth in the artery's lumen. This undesirable growth can change the hemodynamic characteristics of the blood flow which could be injurious to normal health. Theoretical results obtained for specific geometrics are given for the velocity distribution, pressure, wall shearing stress, and other different phenomena. Flow resistance has been shown that the wall shear decreases with decreasing peripheral layer viscosity, but these properties increase with increasing stenosis size. A two-fluid blood model with a core of micro-polar fluid and a periphery of Newtonian blood has been researched in the presence of moderate stenosis. In terms of modified Bessels functions of zero and first order, analytical equations for flow resistance, wall shear stress, and diffusion via stenosis have been found. Therefore, understanding and preventing arterial illnesses need a thorough grasp of the specific flow characteristics of a channel with restriction. The results for wall shearing stress resistance to flow and concentration profiles have been obtained and discussed with the help of graphically.

1. Introduction

Stenosis is caused by an abnormal growth in the artery's lumen which is developed due to the formation of intravascular plaques or the impingement of ligaments or spurs on the vessel wall. As the disease progresses, it affects severely the coronary flow rate and perfusion. The pressure, shear, and other flow parameters, among others, are significant in an arterial system. These are linked to an increase in flow resistance and the presence of a low-pressure area that creates a suction effect, the potential for red and endothelial cell damage as a result of a high shear region, and the potential for a change from laminar to turbulent flow inside the blood vessel that results in high-intensity shear zones that are unfavourable to blood flow and the arterial wall.

Lee and Fung [1] described a numerical result for flows in tubes with local dumbbell-shaped constriction. Kaur [2] solved the problem of heat transfer by one dimensional steady state conditions. Forrester and Young [3] employed approximation techniques to find the flow solution in a tube having a constriction in the shape of a cosine curve. Several works have studied the Viewing the blood as a Newtonian or non-Newtonian fluid, one may determine the blood's flow characteristics in an artery with minor stenosis [Caro et al. [4], Shukla et al. [6], Forrester and Young [5], Rodbard [7], Fox and Hugh [8], May et al. [9]]. Recently, Awasthi and Kaur [10]

* Corresponding author at: Department of Mathematics, Hamedan Branch, Islamic Azad University, Hamedan, Iran.
E-mail addresses: dramitawasthi@gmail.com, amit.25155@lpu.co.in (A.K. Awasthi), harpreettalwar47@gmail.com (H. Kaur), drrktripathi_fgiet@rediffmail.com (R.K. Tripathi), dr.amonaft@gmail.com (M. Khademi), homan_emadi@yahoo.com (H. Emadifar).

https://doi.org/10.1016/j.heliyon.2023.e20807
Received 4 April 2023; Received in revised form 12 September 2023; Accepted 6 October 2023

Available online 7 November 2023

Published Paper 2

Mechanics of Advanced Materials and Structures

ISSN: (Print) (Online) Journal homepage: https://www.tandfonline.com/loi/umcm20

Bone crack inspired pair of Griffith crack opened by forces at crack faces

A. K. Awasthi, Harpreet Kaur, Rachna, Shavej Ali Siddiqui & Homan Emadifar

To cite this article: A. K. Awasthi, Harpreet Kaur, Rachna, Shavej Ali Siddiqui & Homan Emadifar (2023): Bone crack inspired pair of Griffith crack opened by forces at crack faces, Mechanics of Advanced Materials and Structures, DOI: 10.1080/15376494.2023.2253019

To link to this article: https://doi.org/10.1080/15376494.2023.2253019

Published online: 12 Sep 2023.

Published Paper 3

Contents lists available at ScienceDirect

Materials Today: Proceedings

journal homepage: www.elsevier.com/locate/matpr

SIF and DF of a Griffith crack problem bounded together isotropic and orthotropic medium

A.K. Awasthi *, Rachna, Harpreet Kaur

Department of Mathematics, School of Chemical Engineering and Physical Sciences, Lovely Professional University, Phagwara 144411, India

ARTICLE INFO

Article history:
Available online xxxx

Keywords:
Displacement component
Stress components
Coupled Fourier Transform
Crack tips
Second Kind Fredholm Integral equation

ABSTRACT

The motive why most materials break suddenly is that they have tiny internal and surface fissures that spread when tension is applied. The development and presentation of reinforced composite materials' properties has received a lot of effort. Composite materials have a very promising future. We will continue to see broader use of composite materials for advanced constructions. In order to properly analyse the cracking mechanisms of these structures, which are being used in engineering buildings using composite materials at an ever-increasing rate. The Griffith crack is the most intricate and peeling is the simplest of the numerous forms in which cracks can spread. After the First World War, Alan Griffith created it as an engineer at the Royal Aircraft Establishment in Farnborough. This paper explores the terms "stress intensity factor," and "displacement factor" of this particular type of fracture at the intersection of two medium half-space bound together, there is a Griffith Crack.

Selection and peer-review under responsibility of the scientific committee of the International Conference on Futuristic Materials.

1. Introduction

Griffith's paper launched the field of fracture research in 1920 [1]. It remained a purely rhetorical exercise, nevertheless, for 26 years. Sneddon's [2] book was the catalyst for it. In addition to the theory of Dual integral equations, he applied Fourier transform techniques. The physical characteristics of cracks that are subject to mechanical forces, particularly surface and body forces, are covered in the following paper. Crack issues are not the majority of them in the theory of solid fracture, but they do play a significant part. In crack-problem scenarios, the gap between the crack's two opposing faces is almost never proportional to the crack's length. The precise expressions of displacement and stress components at crack-tips at the common interface of one isotropic and one orthotropic half plane are assessed using the Fourier transform method. In these elements, we see a square root singularity.

Williams [3,4] used the complex variable method to find a solution to the issue of the stress and displacement fields near crack tips. The problem is stated in the proposed work along the lines of [6]. Don't reduce it to a Hilbert problem, though. The issue is reduced to dual integral equations, then Srivastava and Lowengrub's, Awasthi approaches [5,11] are used to reduce the solutions to coupled Fredholm integral equations. Willis [7] described the cracked design criteria for interfacial fractures were produced in his research study. Dwivedi et al. [3,8,9] resolved the issues with disparate media having fractures. Awasthi et al. [10] also worked on stress and displacements components of a Griffith crack.

There is need to reduces problems into second kind of Fredholm integral equation. So, Now proposed problem of the mixed boundary will be of type with Griffith Crack which occupies the region,

$$\lambda = 0, 0 \le |\gamma| \le b \tag{1}$$

Where λ is on Y-axis and γ on X-axis, shown in Fig. 1.
Boundary conditions,

$$\sigma_{\gamma\lambda}(\gamma, 0^+) = \sigma_{\gamma\lambda}(\gamma, 0^-) = 0,\ 0 \le |\gamma| \le b \tag{2}$$

Suppose, $\sigma_{\gamma\lambda}(\gamma, 0^+) = -p_1(\gamma)$ and $\sigma_{\gamma\lambda}(\gamma, 0^-) = -p_2(\gamma)$
Continuity conditions,

$$\left.\begin{aligned} \sigma_{\gamma\lambda}(\gamma, 0^+) &= \sigma_{\lambda\lambda}(\gamma, 0^-), \quad b \le |\gamma| < \infty \\ \sigma_{\lambda\lambda}(\gamma, 0^+) &= \sigma_{\lambda\lambda}(\gamma, 0^-), \quad b \le |\gamma| < \infty \end{aligned}\right\} \tag{3}$$

* Corresponding author at: epartment of Mathematics, School of Chemical Engineering and Physical Sciences, Lovely Professional University, Phagwara 144411, India
E-mail address: dramitawasthi@gmail.com (A.K. Awasthi).

https://doi.org/10.1016/j.matpr.2023.04.633
2214-7853/
Selection and peer-review under responsibility of the scientific committee of the International Conference on Futuristic Materials.

Published Paper 4

Mathematics and Statistics 10(1): 166-175, 2022
DOI: 10.13189/ms.2022.100115

http://www.hrpub.org

A Griffith Crack at the Interface of an Isotropic and Orthotropic Half Space Bonded Together

A. K. Awasthi*, Rachna, Harpreet Kaur

Department of Mathematics, Lovely Professional University, India

Received April 25, 2021; Revised December 9, 2021; Accepted December 27, 2021

Cite This Paper in the following Citation Styles

(a): *[1] A. K. Awasthi, Rachna, Harpreet Kaur , "A Griffith Crack at the Interface of an Isotropic and Orthotropic Half Space Bonded Together," Mathematics and Statistics, Vol. 10, No. 1, pp. 166 - 175, 2022. DOI: 10.13189/ms.2022.100115.*

(b): *A. K. Awasthi, Rachna, Harpreet Kaur (2022). A Griffith Crack at the Interface of an Isotropic and Orthotropic Half Space Bonded Together. Mathematics and Statistics, 10(1), 166 - 175. DOI: 10.13189/ms.2022.100115.*

Abstract In the past 53 years, many efforts have been contributed to develop and demonstrate the properties of reinforced composite materials. The ever-increasing use of composite materials through engineering structures needs the proper analysis of the mechanical response of these structures. In the proposed work, we have an exact form of Stress components and Displacement components to a Griffith crack at the interface of an Isotropic and Orthotropic half-space bounded together. The expression was evaluated in the vicinity of crack tips by using Fourier transform method but here these components have been evaluated with the help of Fredholm integral equations and then reduce to the coupled Fredholm integral equations. In this paper, we use the problem of Lowengrub and Sneddon and reduce it to dual integral equations. Solution of these equations through the use of the method of Srivastava and Lowengrub is reduced to coupled Fredholm integral equation. Further reduces the problem to decoupled Fredholm integral equation of 2nd kind. We get the solution of dual integral equations and the problem is reduced to coupled Fredholm integral equation. We find the solution of the Fredholm integral equation and reduce it to decoupled Fredholm integral equation of 2nd kind. The Physical interest in fracture design criterion is due to Stress and crack opening Displacement components. In the end, we can easily calculate the Stress components and Displacement components in the exact form.

Keywords Stress Components, Displacement Components, Fourier Transform, Fredholm Integral Equation, Coupled Fredholm Integral Equation

1. Introduction

The exact expressions of the displacement and the stress components in the vicinity of crack-tips at the common interface of the one isotropic and other one orthotropic half-plane are evaluated by using Fourier transform method. A square root singularity is observed in these components.

Williams [1,3] solved the problem of the stress and displacement fields in the neighbourhood of crack tips by using the complex variable method. Erdogan [4] extended the application of the above method to more Griffith-cracks. Rice and Sih [5] used R-integral approach to solve the problem of cracks in the bounded dissimilar materials. Willis [18] in his research endeavor develop the fractured design parameters for interfacial cracks. Dwivedi et al. [13,1,16] solved the problems of dissimilar media containing cracks.

Hydro-static pressure over the structure is transformed to constant pressure at crack faces. Lowengrub and Sneddon [11] solved the problem of a Griffith crack at the interface of two bounded isotropic homogeneous half-planes by using transform techniques. The Hilbert problem is reduced by Muskhelishvili [6]. The solutions involve logarithmic violent oscillations and the square root singularity. Borai and Nadi [21] discussed some singular and non-linear singular equations in Banach space and Fourier transform used for Cauchy problems for parabolic and hyperbolic partial differential equations. Leontiev [22] described surface value problem with some boundary problems by linear and finite Fourier series.

In the proposed work the problem is formulated on the

Published Paper 5

Journal of Physics: Conference Series

Heat transfer between skin and core with the help of mathematical modelling

To cite this article: Harpreet Kaur 2022 *J. Phys.: Conf. Ser.* **2267** 012067

Published Paper 6

A numerical study of transport of O_2 and CO_2 in a red blood cell

A. K. Awasthi ✉; Harpreet Kaur

AIP Conference Proceedings 2768, 020004 (2023)
https://doi.org/10.1063/5.0148441

Copyright/Patent

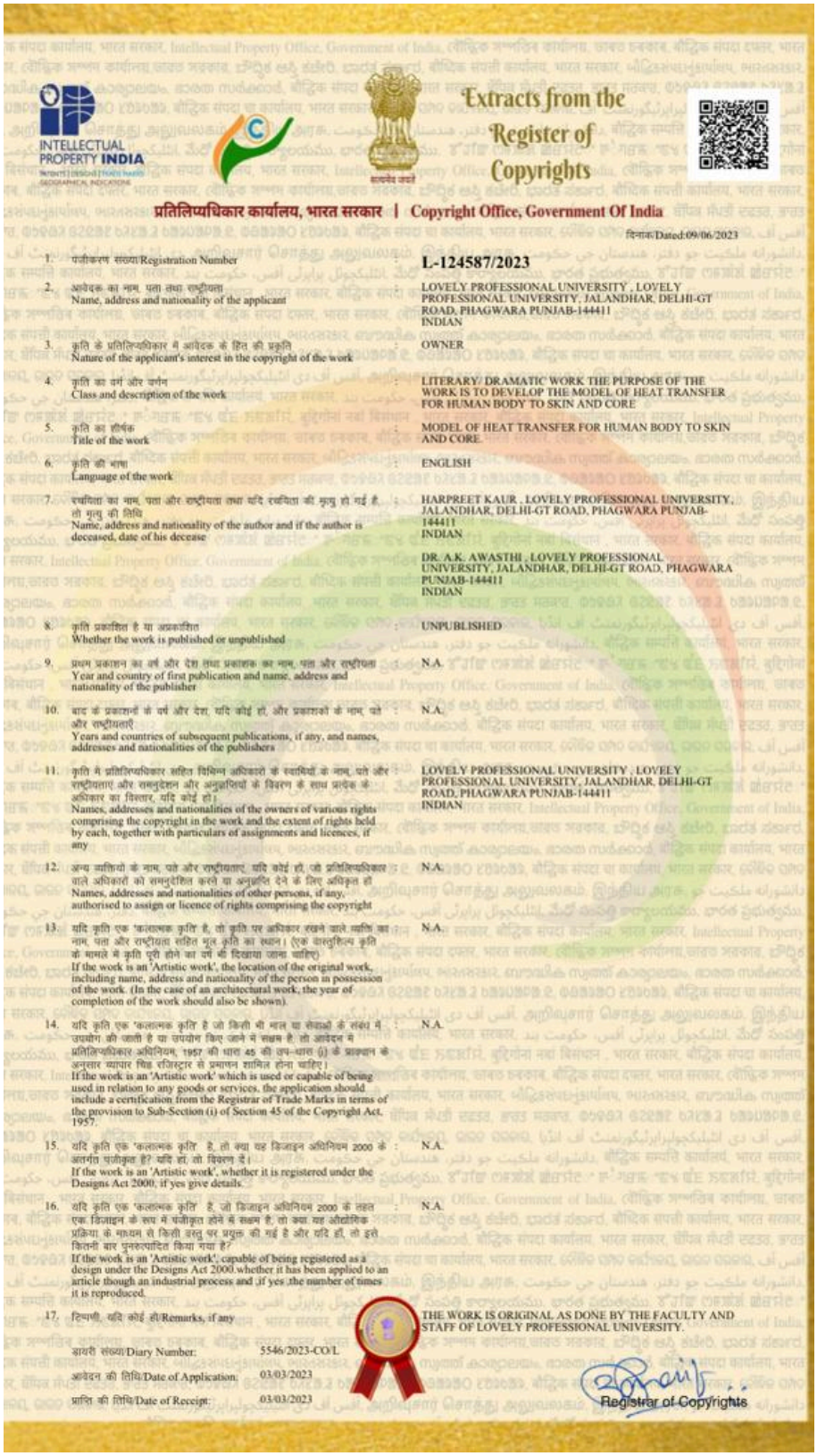

INTELLECTUAL PROPERTY INDIA

PATENTS | DESIGNS | TRADE MARKS | GEOGRAPHICAL INDICATIONS

सत्यमेव जयते

Extracts from the Register of Copyrights

प्रतिलिप्यधिकार कार्यालय, भारत सरकार | Copyright Office, Government Of India

दिनांक/Dated:09/06/2023

1.	पंजीकरण संख्या/Registration Number	:	**L-124587/2023**
2.	आवेदक का नाम, पता तथा राष्ट्रीयता Name, address and nationality of the applicant	:	LOVELY PROFESSIONAL UNIVERSITY , LOVELY PROFESSIONAL UNIVERSITY, JALANDHAR, DELHI-GT ROAD, PHAGWARA PUNJAB-144411 INDIAN
3.	कृति के प्रतिलिप्यधिकार में आवेदक के हित की प्रकृति Nature of the applicant's interest in the copyright of the work	:	OWNER
4.	कृति का वर्ग और उसका Class and description of the work	:	LITERARY/ DRAMATIC WORK THE PURPOSE OF THE WORK IS TO DEVELOP THE MODEL OF HEAT TRANSFER FOR HUMAN BODY TO SKIN AND CORE
5.	कृति का शीर्षक Title of the work	:	MODEL OF HEAT TRANSFER FOR HUMAN BODY TO SKIN AND CORE
6.	कृति की भाषा Language of the work	:	ENGLISH
7.	रचयिता का नाम, पता और राष्ट्रीयता तथा यदि रचयिता की मृत्यु हो गई है तो मृत्यु की तिथि Name, address and nationality of the author and if the author is deceased, date of his decease	:	HARPREET KAUR , LOVELY PROFESSIONAL UNIVERSITY, JALANDHAR, DELHI-GT ROAD, PHAGWARA PUNJAB-144411 INDIAN DR. A.K. AWASTHI , LOVELY PROFESSIONAL UNIVERSITY, JALANDHAR, DELHI-GT ROAD, PHAGWARA PUNJAB-144411 INDIAN
8.	कृति प्रकाशित है या अप्रकाशित Whether the work is published or unpublished	:	UNPUBLISHED
9.	प्रथम प्रकाशन का वर्ष और देश तथा प्रकाशक का नाम, पता और राष्ट्रीयता Year and country of first publication and name, address and nationality of the publisher	:	N.A.
10.	बाद के प्रकाशनों के वर्ष और देश, यदि कोई हो, और प्रकाशकों के नाम, पते और राष्ट्रीयताएँ Years and countries of subsequent publications, if any, and names, addresses and nationalities of the publishers	:	N.A.
11.	कृति में प्रतिलिप्यधिकार सहित विभिन्न अधिकारों के स्वामियों के नाम, पते और राष्ट्रीयताएं और समनुदेशन और अनुज्ञप्तियों के विवरण के साथ प्रत्येक के अधिकार का विस्तार, यदि कोई हो। Names, addresses and nationalities of the owners of various rights comprising the copyright in the work and the extent of rights held by each, together with particulars of assignments and licences, if any	:	LOVELY PROFESSIONAL UNIVERSITY , LOVELY PROFESSIONAL UNIVERSITY, JALANDHAR, DELHI-GT ROAD, PHAGWARA PUNJAB-144411 INDIAN
12.	अन्य व्यक्तियों के नाम, पते और राष्ट्रीयताएं, यदि कोई हो, जो प्रतिलिप्यधिकार वाले अधिकारों को समनुदेशित करने या अनुज्ञप्ति देने के लिए अधिकृत हों Names, addresses and nationalities of other persons, if any, authorised to assign or licence of rights comprising the copyright	:	N.A.
13.	यदि कृति एक 'कलात्मक कृति' है, तो कृति पर अधिकार रखने वाले व्यक्ति का नाम, पता और राष्ट्रीयता सहित मूल कृति का स्थान। (एक वास्तुशिल्प कृति के मामले में कृति पूरी होने का वर्ष भी दिखाया जाना चाहिए) If the work is an 'Artistic work', the location of the original work, including name, address and nationality of the person in possession of the work. (In the case of an architectural work, the year of completion of the work should also be shown).	:	N.A.
14.	यदि कृति एक 'कलात्मक कृति' है जो किसी भी माल या सेवाओं के संबंध में उपयोग की जाती है या उपयोग किए जाने में सक्षम है, तो आवेदन में प्रतिलिप्यधिकार अधिनियम, 1957 की धारा 45 की उप-धारा (i) के प्रावधान के अनुसार व्यापार चिह्न रजिस्ट्रार से प्रमाणन शामिल होना चाहिए। If the work is an 'Artistic work' which is used or capable of being used in relation to any goods or services, the application should include a certification from the Registrar of Trade Marks in terms of the provision to Sub-Section (i) of Section 45 of the Copyright Act, 1957.	:	N.A.
15.	यदि कृति एक 'कलात्मक कृति' है, तो क्या यह डिजाइन अधिनियम 2000 के अंतर्गत पंजीकृत है? यदि हां, तो विवरण दें। If the work is an 'Artistic work', whether it is registered under the Designs Act 2000, if yes give details.	:	N.A.
16.	यदि कृति एक 'कलात्मक कृति' है, जो डिजाइन अधिनियम 2000 के तहत एक डिजाइन के रूप में पंजीकृत होने में सक्षम है, तो क्या यह औद्योगिक प्रक्रिया के माध्यम से किसी वस्तु पर प्रयुक्त की गई है और यदि हाँ, तो इसे कितनी बार पुनरुत्पादित किया गया है? If the work is an 'Artistic work', capable of being registered as a design under the Designs Act 2000,whether it has been applied to an article though an industrial process and ,if yes ,the number of times it is reproduced.	:	N.A.
17.	टिप्पणी, यदि कोई हो/Remarks, if any	:	THE WORK IS ORIGINAL AS DONE BY THE FACULTY AND STAFF OF LOVELY PROFESSIONAL UNIVERSITY.

डायरी संख्या/Diary Number: 5546/2023-CO/L

आवेदन की तिथि/Date of Application: 03/03/2023

प्राप्ति की तिथि/Date of Receipt: 03/03/2023

Registrar of Copyrights

Graphical Abstract

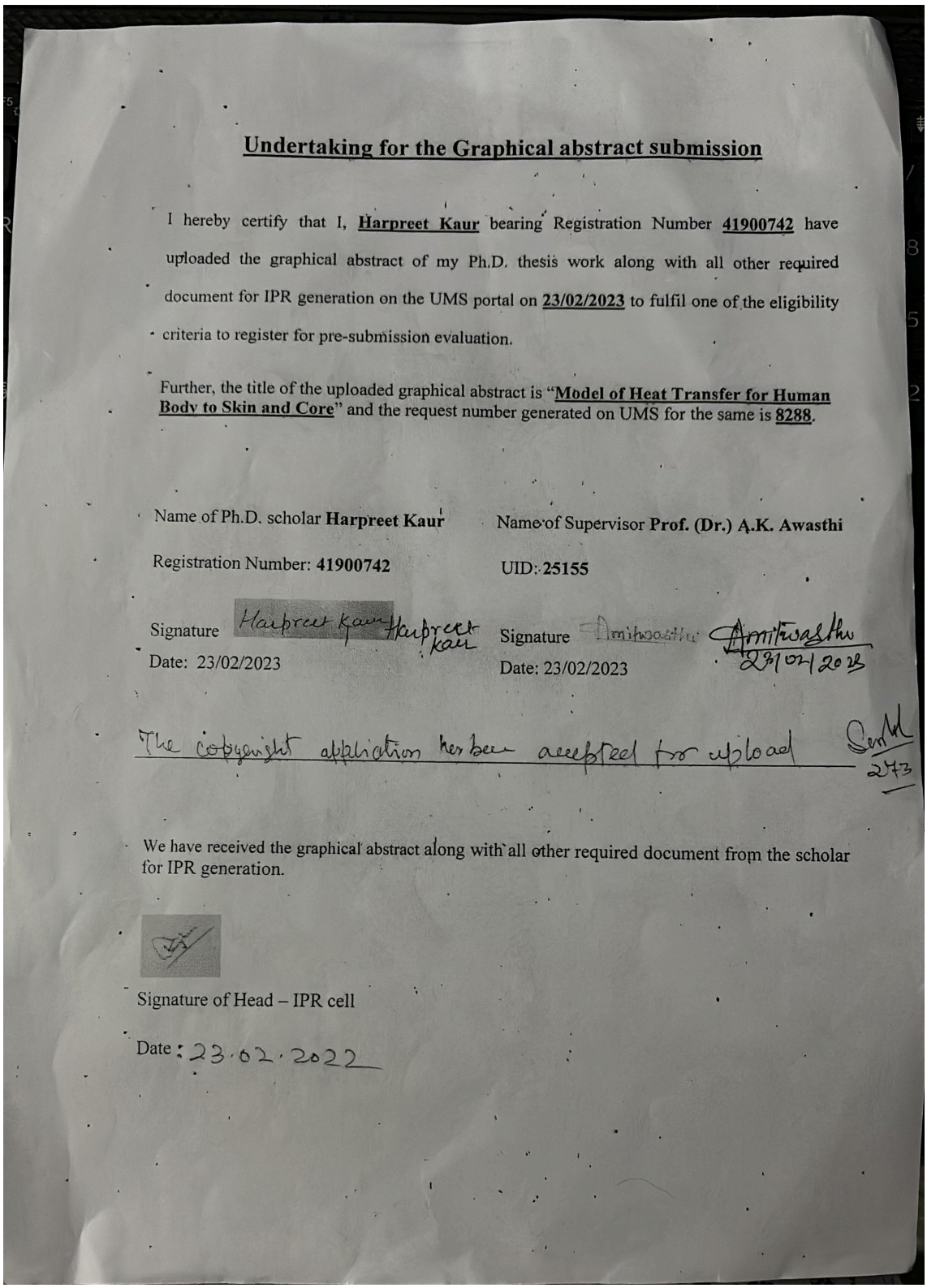

Undertaking for the Graphical abstract submission

I hereby certify that I, **Harpreet Kaur** bearing Registration Number **41900742** have uploaded the graphical abstract of my Ph.D. thesis work along with all other required document for IPR generation on the UMS portal on **23/02/2023** to fulfil one of the eligibility criteria to register for pre-submission evaluation.

Further, the title of the uploaded graphical abstract is "**Model of Heat Transfer for Human Body to Skin and Core**" and the request number generated on UMS for the same is **8288**.

Name of Ph.D. scholar **Harpreet Kaur**

Registration Number: **41900742**

Signature Harpreet Kaur Harpreet Kaur

Date: 23/02/2023

Name of Supervisor **Prof. (Dr.) A.K. Awasthi**

UID: **25155**

Signature Amitawasthi Amit Awasthi 23/02/2023

Date: 23/02/2023

The copyright application has been accepted for upload 273

We have received the graphical abstract along with all other required document from the scholar for IPR generation.

Signature of Head – IPR cell

Date : 23.02.2022

Certificate

International Conference on
"Computational Applied Sciences and its Applications" (ICCASA-2022)
Department of Applied Sciences
University of Engineering and Management, Jaipur

AIP Conference Proceedings
VIRTUAL MODE

ICCASA 2022

CERTIFICATE
OF APPRECIATION

This is to certify that Ms./ Mr./ Dr./ Prof. Harpreet Kaur from Lovely professional university, Phagwara has participated and presented paper entitled A Numerical Study of Transport of O2 and CO2 in a Red Blood Cell in International Conference on "Computational Applied Sciences and its Applications" (ICCASA- 2022) from April 28-29, 2022 conducted by University of Engineering and Management, Jaipur, Rajasthan (India).

Dr. Praphull Chabbra
Convener

Ms. Pallavi Malik
Convener

Prof. Dr. Biswajoy Chatterjee
Vice Chancellor, UEM, Jaipur

Certificate

Certificate No. 225373

LOVELY PROFESSIONAL UNIVERSITY

Transforming Education Transforming India

RAFAS

Certificate of Participation

This is to certify that Ms. Harpreet Kaur

of Lovely Professional University

has given poster presentation on HEAT TRANSFER BETWEEN SKIN AND CORE WITH THE HELP OF MATHEMATICAL MODELLING

in the International Conference on "Recent Advances in Fundamental and Applied Sciences" (RAFAS 2021) held on June 25-26, 2021, organized by School of Chemical Engineering and Physical Sciences, Lovely Faculty of Technology and Sciences, Lovely Professional University, Punjab.

Date of Issue : 15-07-2021
Place of Issue: Phagwara (India)

Prepared by
(Administrative Officer-Records)

Organizing Secretary
(RAFAS 2021)

Convener
(RAFAS 2021

Certificate

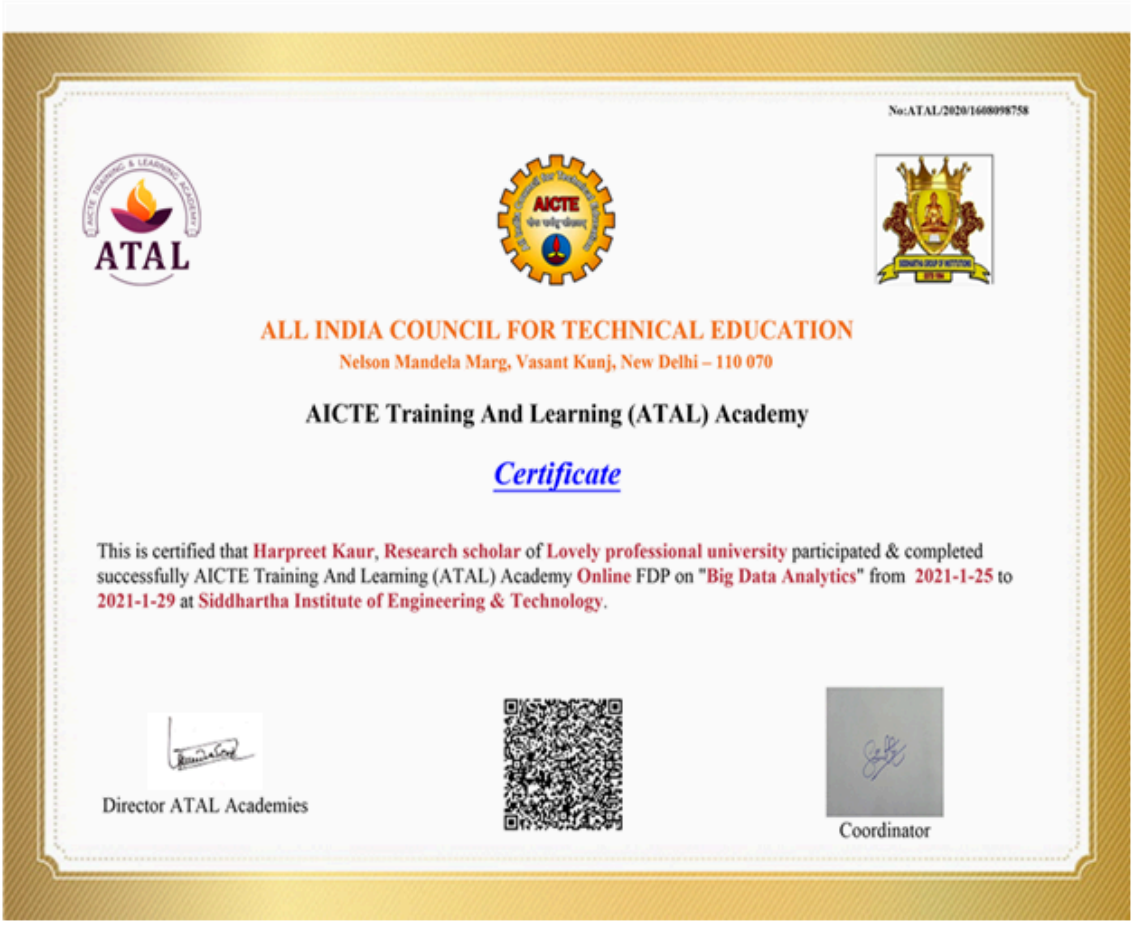

No:ATAL/2020/1608098758

ATAL

ALL INDIA COUNCIL FOR TECHNICAL EDUCATION

Nelson Mandela Marg, Vasant Kunj, New Delhi – 110 070

AICTE Training And Learning (ATAL) Academy

Certificate

This is certified that Harpreet Kaur, Research scholar of Lovely professional university participated & completed successfully AICTE Training And Learning (ATAL) Academy Online FDP on "Big Data Analytics" from 2021-1-25 to 2021-1-29 at Siddhartha Institute of Engineering & Technology.

Director ATAL Academies

Coordinator

Alphabetical Index